

Incentives to Emit in Upstream Oil and Gas: Theory, Evidence, and Policy Implications*

Coly Elhai, *Harvard University*

Toren Fronsdal, *Harvard University*

January 25, 2026

Abstract

We study how market incentives and infrastructure constraints shape oil and gas producers' methane emissions. We develop a model in which producers make drilling and emissions decisions and face transmission costs that depend on pipeline utilization. Leveraging novel emissions data from the Permian Basin, we find that emissions respond to high-frequency price variation. With our estimated model, we show that a \$1,500/metric ton methane tax reduces emissions by up to 7 percent, but effects are attenuated by pipeline congestion and optimistic flaring efficacy assumptions. Expanding gas pipeline infrastructure yields net emission reductions and generates social returns substantially exceeding construction costs.

Keywords: Methane emissions; oil and gas; pipeline capacity; environmental regulation; policy evaluation

JEL Codes: D22, H23, L95, Q35, Q40, Q54, Q58

*Many thanks to Daniel Varon, Lucas Estrada, and Daniel Jacob for providing data and scientific expertise to guide this project. We are grateful to Jesse Shapiro, Jim Stock, Anna Russo, Joe Aldy, Rob Stavins, Nathan Hendren, Ed Glaeser, Ariel Pakes, Myrto Kalouptsi, Gabriel Kreindler, and Ryan Kellogg for their valuable feedback. We also received helpful comments from participants at the US-AEE annual meeting, AERE Summer Conference, and Harvard Graduate Student Workshops in Environmental Economics, Industrial Organization, and Labor/Public Finance. This project is part of the Salata Institute research cluster on reducing global methane emissions. Elhai gratefully acknowledges support from the Chae Family Economics Research Fund and the National Science Foundation Graduate Research Fellowship Program.

1 Introduction

Methane is a potent greenhouse gas, with a social cost per ton over ten times that of carbon dioxide ([EPA 2023](#)). Identifying cost-effective levers in major emitting sectors is therefore a critical policy priority. Roughly a quarter of U.S. methane emissions originate from the oil and natural gas sector. Unlike most pollutants, methane emissions from the oil and gas sector impose not only a social cost, but a private one as well. Because methane is the primary component of natural gas, emissions from this industry represent unsold product and amount to billions of dollars in lost revenue.

This paper examines how market incentives and infrastructure constraints shape methane emissions from the oil and gas sector. Our focus is on the Permian Basin, the largest oil-producing and second largest gas-producing basin in the U.S., accounting for 46 percent and 18 percent respectively of national totals ([Federal Reserve Bank of Dallas n.d.](#)). In the Permian, most gas production is “associated gas,” meaning it is co-produced as a byproduct of more profitable oil extraction. In 2019, Permian methane emissions were estimated at 2.5 teragrams (Tg), roughly 15 percent of total U.S. oil and gas methane emissions, or equivalent to the annual carbon emissions from the electricity used to power 12 million U.S. homes ([Lu et al. 2023](#)). The region has also seen rapid production growth over the past decade, which has frequently strained pipeline capacity, increasing gas transport costs. These infrastructure constraints can exacerbate emissions: when pipeline capacity is limited and transmission costs rise, disposal of gas at well sites becomes more economically attractive than transporting the gas to market. Producers dispose of unmarketed gas either by flaring (combusting) it or venting it directly into the atmosphere, both of which are socially costly due to the release of greenhouse gases.¹

Despite the scale and importance of methane emissions from oil and gas production, measuring them has long been a barrier to research and policy design. Until recently, researchers, regulators, and the public have lacked access to high-frequency, observational data on emissions or flaring, limiting their ability to study how emissions respond to real-time changes in prices, policies, or infrastructure. Even with better data, answering the core economic question—how do market incentives shape emissions behavior?—poses difficult modeling challenges. Methane emissions in the oil and gas sector arise from a series of interrelated choices, including whether to drill new wells (the extensive margin) and, conditional on drilling, what share of the gas produced to market versus emit (the intensive margin). A comprehensive analysis of how policies affect aggregate emissions must account for both margins. The challenge is compounded by equilibrium effects: producers’ collective responses to policy can introduce operational externalities, which in turn feed back into individual abatement decisions.

In this paper, we develop a model of producer behavior in which firms make decisions about drilling and gas disposal. This model allows us to characterize how changes in prices and costs translate into changes in emissions. We draw on newly developed datasets that use advances in atmospheric modeling and satellite

¹Through combustion, flaring converts most of the methane in natural gas into CO₂. Although flaring is preferable to venting in terms of warming potential, even flaring can result in significant methane emissions due to inefficient or unlit flares ([Plant et al. 2022](#); [Evans et al. 2024](#)).

measurement to understand how emissions and gas disposal activities respond to market conditions. Finally, we apply the model to evaluate counterfactual policy interventions—including methane taxes and pipeline expansions—that could reduce emissions from the oil and gas sector.

In our model, oil and gas producers choose in each period (1) how many wells to drill and (2) what share of produced gas to market rather than flare. Drilling decisions are dynamic, reflecting expectations over future prices and production, while gas marketing decisions are static, responding only to contemporaneous gas prices and marketing costs. Because producers cannot adjust output from existing wells, production is exogenous in each period; gas marketing decisions concern only what *share* of gas produced to sell versus emit. Methane emissions arise from three distinct sources: emissions during drilling, baseline leakage from well equipment, and the disposal of unmarketed gas through venting or flaring. A central feature of the model is that marketing costs are endogenously determined and increasing in pipeline utilization. As takeaway pipeline infrastructure approaches capacity, congestion externalities raise the marginal cost of gas transmission, reducing the net profit from marketing gas. This generates a feedback mechanism: individual producers' flaring choices affect aggregate pipeline flows, which in turn influence the marketing costs faced by producers.

To measure methane emissions and flaring in the Permian Basin, we use three complementary data sources. First, we leverage satellite-based imaging spectrometer data that estimates methane emissions by detecting atmospheric methane concentrations and applying inversion models that account for wind and weather patterns. Second, we track flaring activity with satellite images of nighttime light intensity, using the brightness of gas flares as a proxy for flaring volume. Finally, we use lease-level data on drilling, venting, and flaring that oil and gas producers self-report to the Texas Railroad Commission (RRRC), providing a detailed, ground-based record of operator activity. Together, these data sources give us a comprehensive view of the firm-level decisions that lead to emissions (drilling, flaring) as well as the aggregate impacts of these decisions (total emissions). They also allow us to balance the granularity of self-reported data with the objectivity of remote-sensing data.

Reduced-form evidence based on these datasets supports the key predictions of our model. We find that gas flaring is negatively correlated with natural gas prices, but positively correlated with natural gas transport costs, as proxied by the Henry-Waha Hub price spread. This is in line with flaring becoming more appealing when marketing gas is less profitable. Emissions are positively correlated with drilling and with the Henry-Waha price spread, but negatively correlated with gas prices. This pattern is consistent with the model's prediction that total emissions are driven by both flaring and drilling, both of which themselves respond to commodity prices.

We use the estimated model to evaluate several policy counterfactuals. First, we study a methane tax modeled after the Waste Emissions Charge authorized by the Inflation Reduction Act. We predict that a \$1,500/metric ton tax would reduce flaring by as much as 13 percent and methane emissions by up to 7 percent when the pipeline system is congestion-free. Under observed pipeline congestion conditions, the impacts are smaller but the policy would still generate social cost savings between \$570 million and \$4.8 billion annually in the Permian Basin alone. We find that the tax's implementation details matter a great deal: changing the

assumed flaring efficiency alters the effective tax rate enough to change the tax's predicted impacts by a factor of three. Our results indicate that most of the effects of the tax operate through the static margin rather than the dynamic margin; that is, the tax primarily induces producers to flare less of the gas they produce, rather than to drill fewer wells. In a related counterfactual, we find that proposed policies to tax vented and flared gas at the same rate as other gas produced would result in relatively small (around 1 percent) flaring reductions and correspondingly modest social cost savings.

We also evaluate the emissions impacts of alleviating pipeline congestion. While the net emissions impact of infrastructure expansion is theoretically ambiguous—depending on the extent to which congestion relief stimulates new drilling—we find that the reduction in flaring dominates any induced production in the Permian. Specifically, because gas transmission costs have a negligible effect on new well drilling in this region (unlike oil market dynamics), alleviating congestion yields net emissions reductions. We find that fully eliminating congestion would have reduced flaring by 4.7 percent on average during our study period, and by as much as 25 percent during periods of high congestion. Adding a single large pipeline (2 Bcf/day of capacity) would achieve most of the emissions reductions from fully relieving congestion, cutting flaring by 4.3 percent on average. We estimate that the social benefits of such a pipeline would exceed construction costs in just a few years, even under conservative assumptions about the social cost of carbon.

Importantly, our results also indicate that pipeline congestion alleviation and methane taxes are complementary policies. When pipelines are congested, producers' ability to respond to a methane tax is constrained: reducing flaring requires marketing more gas, which exacerbates congestion and raises transmission costs, dampening incentives to market gas. By explicitly capturing this feedback, our model shows that combining a methane tax with pipeline expansion yields emissions reductions greater than the sum of their individual effects.

The primary contribution of this paper is to incorporate a set of empirical facts, some newly documented and others well established, into a unified framework for understanding how methane emissions from oil and gas production respond to market incentives and public policy. These facts include the inelasticity of production from existing wells ([Anderson, Kellogg and Salant 2018](#); [Newell and Prest 2019](#); [Newell, Prest and Vissing 2019](#)), the limited impact of gas prices on drilling behavior in associated gas plays (e.g., [Prest 2025](#)), and the responsiveness of flaring to pipeline congestion ([Agerton et al. 2025](#)). This last paper, which is contemporaneous with our own, is similar in that it provides reduced-form evidence that congestion drives flaring. Our work differs in several ways, including that we study the relationship between emissions and commodity prices, measure emissions due to both drilling and flaring, develop a model of producer behavior, show that the model can help understand the patterns in the data, estimate the parameters of the model, and use the estimated model to study the effect of counterfactual policies.

Another contribution of this paper is to show how emissions depend not just on individual policy levers, but on their interactions. Like [Fowlie, Reguant and Ryan \(2016\)](#) and [Lade and Rudik \(2020\)](#), we demonstrate that emissions taxes alone can underperform relative to policies that account for underlying market structure. Our distinctive contribution is to highlight the role of the transmission system in creating network externalities

that mediate producers' ability to respond to policy. This mechanism is not unique to oil and gas. In many energy systems, such as electricity transmission and renewable integration, the effectiveness of carbon pricing or regulatory interventions similarly hinges on the characteristics of the networks to which producers are connected. Accordingly, we contribute to an emerging literature on the marginal abatement costs of methane (see, e.g., [Marks 2022](#) and [Hausman and Muehlenbachs 2019](#) and reviews by [Aldy, Reinhardt and Stavins 2025](#) and [Agerton, Gilbert and Upton 2023](#)) and the design of effective abatement policies (see, e.g., [Cicala, Hémous and Olsen 2022](#); [Lewis, Wang and Ravikumar 2025](#)).² While previous work has addressed how abatement costs might vary by firm and geography ([Lade and Rudik 2020](#); [Beatty 2022](#)), to our knowledge ours is the first to show how abatement costs also vary with market conditions and to apply this result to policy. A key, previously unexplored implication for policy design is that the emissions impact of a methane tax can be amplified when combined with midstream infrastructure improvements.

The remainder of the paper proceeds as follows. Section 2 provides background on oil and gas production and methane emissions in the Permian Basin. Section 3 describes the data sources and presents key descriptive patterns. Section 4 outlines the economic model we use to analyze emissions and operator behavior. Section 5 presents reduced-form evidence on the relationship between methane emissions, flaring, prices, and marketing costs. Section 6 details the estimation of the model. Section 7 uses the estimated model to simulate counterfactual policy scenarios. Section 8 concludes.

2 Background

2.1 Oil and gas extraction in the Permian Basin

The Permian Basin's geological formations contain a substantial amount of both oil and natural gas. In this region, drilling for oil produces gas as a byproduct because Permian oil can contain significant quantities of dissolved natural gas. Oil is the more lucrative business in the Permian: even the basin's top gas producers earn between 70 percent and 90 percent of their revenues from oil sales (Table C.1). As a result, producers are willing to sustain very low profits (or even losses) from the gas side of their operation if it allows them to continue producing oil.

Oil is the dominant driver of production across the Permian, but gas-to-oil ratios vary significantly throughout the region. Occupying the eastern- and western-most portions of the Permian respectively, the Midland and Delaware sub-basins are the most productive parts of the Permian. The Delaware Basin has higher gas-to-oil ratios (Appendix Figure B.1), and so a large share of the oil produced in the Delaware Basin is produced by wells whose gas-to-oil ratios qualify them as gas wells (Appendix Figure B.2). Nevertheless, these "gas" wells derive over three quarters of their revenues from oil.³

Natural gas is difficult to transport, far more so than oil. Whereas oil can be stored in tanks and carried on trains, natural gas cannot be cost-effectively moved long distances in its gaseous state except via pipeline.

²A related strand of literature focuses on monitoring and enforcement of abatement policies (e.g., [Dunkle Werner and Qiu 2025](#); [Zou 2021](#); [Marks 2022](#)). In this paper, we abstract from issues of enforcement of tax policy.

³This figure was calculated at October 2024 prices.

Aboveground storage of natural gas is cost-prohibitive, and underground storage is constrained by the availability of suitable caverns or depleted reservoirs.⁴ Together, all of these factors imply that gas pipelines are critical to ensuring that producers can bring their gas to market. However, pipeline construction is not always able to keep pace with production growth. In the Permian, for instance, the rapid expansion of production due to the fracking revolution has often outstripped the ability of pipeline operators to build new transmission capacity ([Fleury 2022](#)). This has led to frequent shortfalls in pipeline capacity, which in turn have driven natural gas spot prices at Waha Hub (the main hub serving the Permian Basin) into negative territory. Capacity is a challenge further upstream as well: producers need to use gathering pipelines and processing plants to bring their gas to transmission pipelines in the first place. Construction of this upstream infrastructure in the Permian has also sometimes lagged gas production.

2.2 Methane emissions from the oil and gas industry

Methane emissions from oil and gas production derive from a variety of sources, both intentional and unintentional. On the intentional side, producers often vent natural gas directly into the atmosphere for safety reasons or to maintain proper equipment pressure. Certain steps in the production process require venting, including well completions and workovers, where operators either bring new wells online or fix issues in existing ones to keep oil and gas flowing. Some equipment (e.g., pneumatic devices) vent natural gas as part of normal operations since they rely on gas pressure to control mechanical functions and discharge the gas after each actuation ([Agerton, Gilbert and Upton 2023](#)).

Producers also dispose of natural gas through flaring, the controlled combustion of gas that converts methane into carbon dioxide and water before release. As with venting, flaring can be motivated by operational and safety requirements. For instance, flaring is common during drilling, well testing, and well completion. Flaring can also result from economic decisions. Sometimes, wells enter operation before gathering pipelines—small pipelines that connect individual well sites to the larger transmission network—have been completed. Other times, there is insufficient gathering, processing, or compression capacity to process all of the gas produced in an area. In these circumstances, producers may choose to flare gas rather than incur higher gas marketing costs or temporarily shut in wells and forego oil production. Qualitative evidence suggests a link between frequent capacity issues and flaring activity. A 2019 Dallas Federal Reserve survey asked oil and gas executives why flaring increased in the Permian Basin that year. Nearly three-quarters of respondents attributed flaring increases to insufficient pipeline takeaway capacity, while nearly half cited a lack of gathering and processing capacity ([Federal Reserve Bank of Dallas 2019](#)).

Flaring imposes a significantly lower environmental cost than venting because most of the methane in flared gas is burned off. However, flaring does not entirely prevent methane emissions: [Plant et al. \(2022\)](#) find effective destructive removal efficiency in the Permian to be around 87 percent due to unlit and malfunctioning flares. This statistic implies that about 13 percent of “flared” gas (which is about 80 percent methane) is in

⁴Liquefaction is an alternative to pipelines for long-distance transport in some cases, but is still very expensive and only economical at scale. Even for gas intended for liquefaction, pipelines are needed to move gas from the wellhead to liquefied natural gas (LNG) terminals, which in the U.S. are heavily concentrated on the Gulf Coast and East Coast ([U.S. Department of Energy 2022](#)).

fact released directly to the atmosphere.

Flaring and venting are regulated in all oil- and gas-producing states, including New Mexico and Texas. In Texas, flaring is permitted in the first 10 days after a well is completed. Outside of this window, producers must file an exemption request with the Texas Railroad Commission (RRC) and pay a \$375 fee. In theory, producers must provide justifications for an exemption, such as lack of takeaway capacity or a maintenance event. In practice, the RRC approves nearly all flaring requests. Venting is generally prohibited in Texas, but exceptions are made during and immediately after well completions or for short intervals (16 Tex. Admin. Code § 3.32).⁵ Monitoring and enforcement of venting and flaring regulations is challenging, even assuming that regulators are fully committed to finding violators.

In addition to venting and flaring, methane emissions arise from unintentional leaks, which can occur at many points along the natural gas supply chain, from the wellhead to downstream infrastructure. Although producers are often unaware of leaks on their sites, there is some evidence that emissions from leaks respond to producer oversight effort, which in turn depends on beliefs about leak magnitudes ([Lewis, Wang and Ravikumar 2025](#)).

Because of the large volumes of oil and gas produced and transported in the Permian Basin, methane emissions from the region are substantial. The Permian is not only the largest oil and gas basin by total methane emissions, but also one of the top oil and gas basins by methane intensity of production. [Lu et al. \(2023\)](#) estimate that Permian production had a methane intensity of around 3 percent in 2019, a significant decline since 2014 but still well above most other major oil/gas producing basins in the U.S.

Recent estimates by [Cusworth et al. \(2021\)](#) indicate that about half of Permian methane emissions are from production, which is the segment of the industry that we focus on in this paper.⁶ Other work has shown that there is significant heterogeneity across oil and gas production sites in terms of methane intensity. [Omara et al. \(2018\)](#) finds that low-producing well sites emit a much larger proportion of their production than newer, high-producing well sites. Even controlling for production levels and basin, however, emissions remain highly stochastic across sites. The distribution of emissions has a fat right tail, such that the top 5 percent of high-emitting sites account for 50 percent of total emissions.

3 Data and Descriptive Statistics

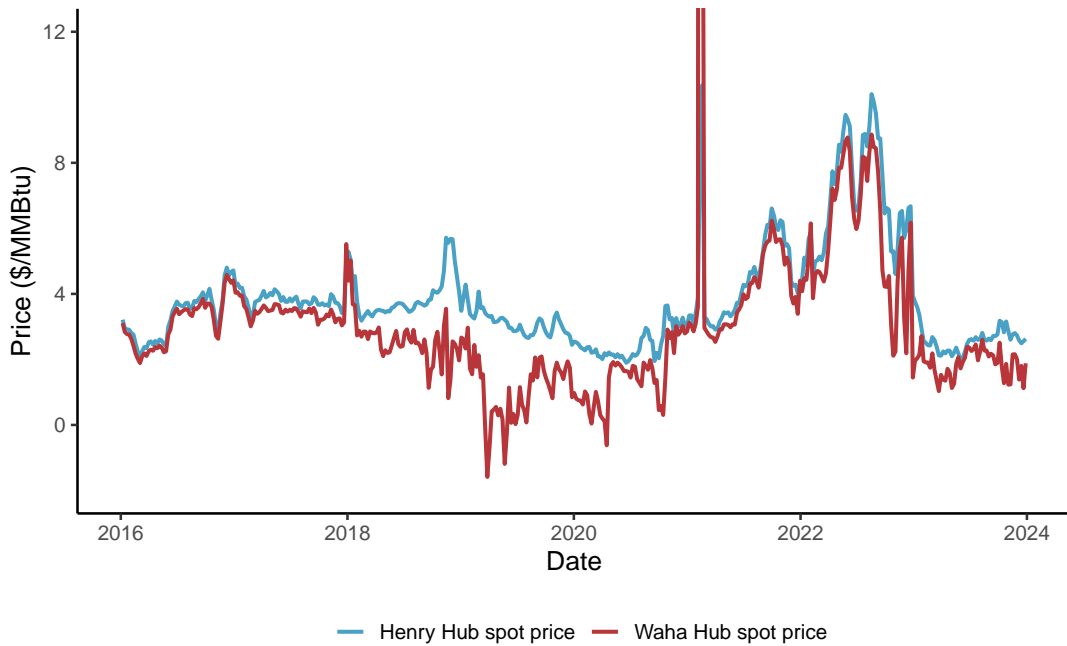
3.1 Prices

We obtain daily natural gas spot price data for Henry Hub and Waha Hub from [S&P Capital IQ \(2024\)](#) (Figure 1). We get futures price data for Henry Hub from the same source. In general, spot prices at both hubs range from \$2 to \$4 per MMBtu. Waha Hub prices tend to lie 10 to 60 cents below Henry Hub prices, though there are periods (such as between 2018 and 2021) during which this gap is much larger.

⁵Texas regulators permit venting up to 10 days after well completion and for up to 24 hours at a time (or up to 72 hours in a month).

⁶The authors estimate that the other half of methane emissions come from gathering and boosting (38 percent) and processing (12 percent). It is worth noting that [Cusworth et al. \(2021\)](#) limit its analysis to persistent point sources, i.e., those detected in at least three overflights. This rules out intermittent sources of methane, such as flares that are only sometimes operating properly.

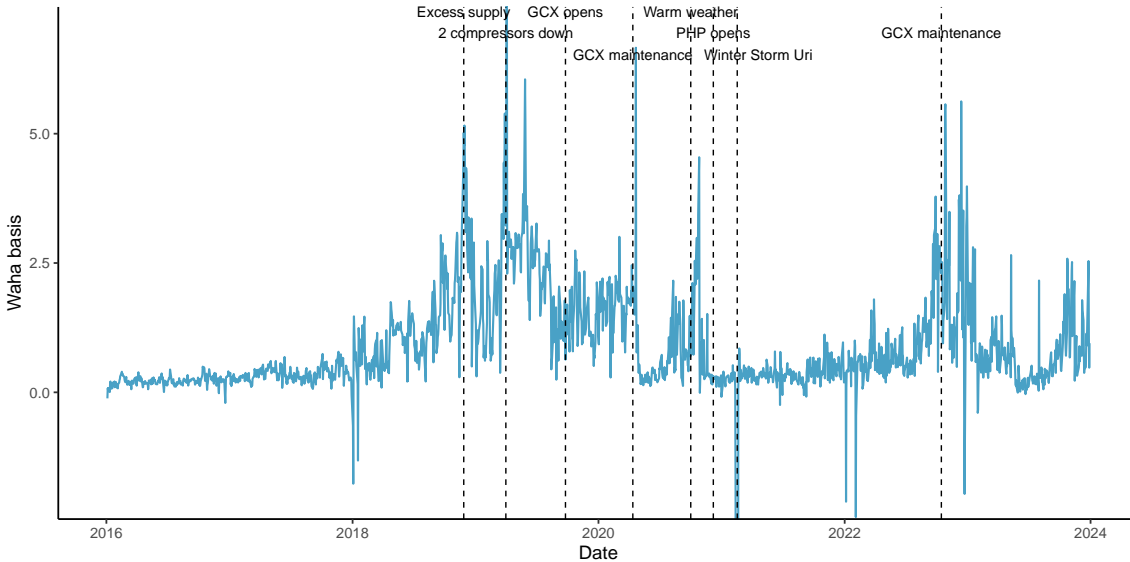
Figure 1: Local and benchmark natural gas spot prices



Notes: Daily gas spot price data from [S&P Capital IQ \(2024\)](#). The large spike in early 2021 corresponds to Winter Storm Uri.

The gap between Henry and Waha Hub spot prices (termed “Waha basis”) is a good proxy for the cost of moving natural gas to market from the Permian Basin. This cost is highly variable, much more so than the commodity value of gas. Commodity values are driven by national and international market dynamics, which are unlikely to be dramatically affected by any single event. Accordingly, Henry Hub spot prices display significant variation, but move relatively slowly (Figure 1). In contrast, Waha basis is quite sensitive to any imbalance of supply and demand (Figure 2). Particularly when pipeline capacity is tight, as it was from 2018 to 2021, maintenance issues or gas oversupply can cause Waha basis to rise dramatically. Even outside of these major disruptions, day-to-day swings in basis can be substantial.

Figure 2: Significant drivers of Waha basis, 2016-2024



Notes: Data from [S&P Capital IQ \(2024\)](#). Annotations added by the authors based on industry reporting. “GCX” is the Gulf Coast Express, a major natural gas pipeline. “PHP” is the Permian Highway Pipeline, another large natural gas pipeline.

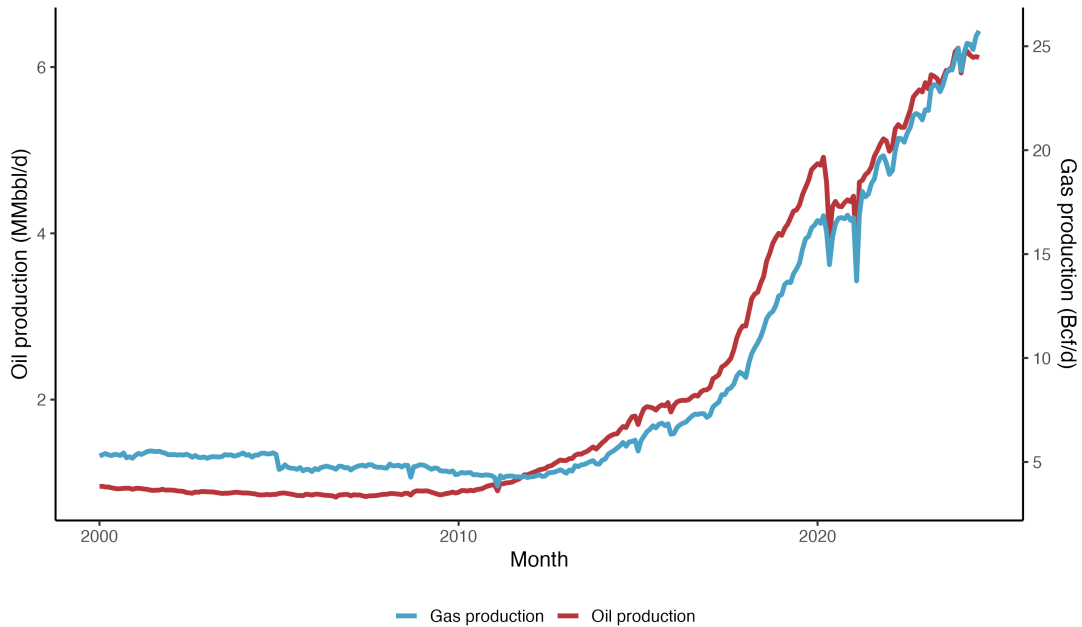
We also obtain oil spot price data from the U.S. Energy Information Administration ([Energy Information Administration 2024a](#)) and oil futures prices from [S&P Capital IQ \(2024\)](#). We use spot prices and future prices for Cushing WTI, the primary U.S. benchmark for oil prices. Prices per barrel ranged from about \$40 to \$100 between 2015 and 2023, dipping briefly below zero during the early months of the COVID-19 pandemic in the U.S. Throughout the analysis, we report energy prices in 2024 dollars, deflating nominal values with the CPI-U.

3.2 Production

Oil and gas production data aggregated to the basin and sub-basin level are from [Enverus \(2024a\)](#). We also use well-month level data from [Enverus \(2024b\)](#) that includes information on drilling dates and monthly production, along with well operator and well type, for wells in the Permian Basin (including both Texas and New Mexico). We use both datasets to demonstrate key facts about oil and gas production in the Permian Basin.

First, as evidenced in Figure 3, innovations in hydraulic fracturing and horizontal drilling have led to an explosion of fossil fuel production in the Permian since 2010. Since oil and gas are produced jointly in this region, the rise in production of these two fossil fuels has been tightly coupled.

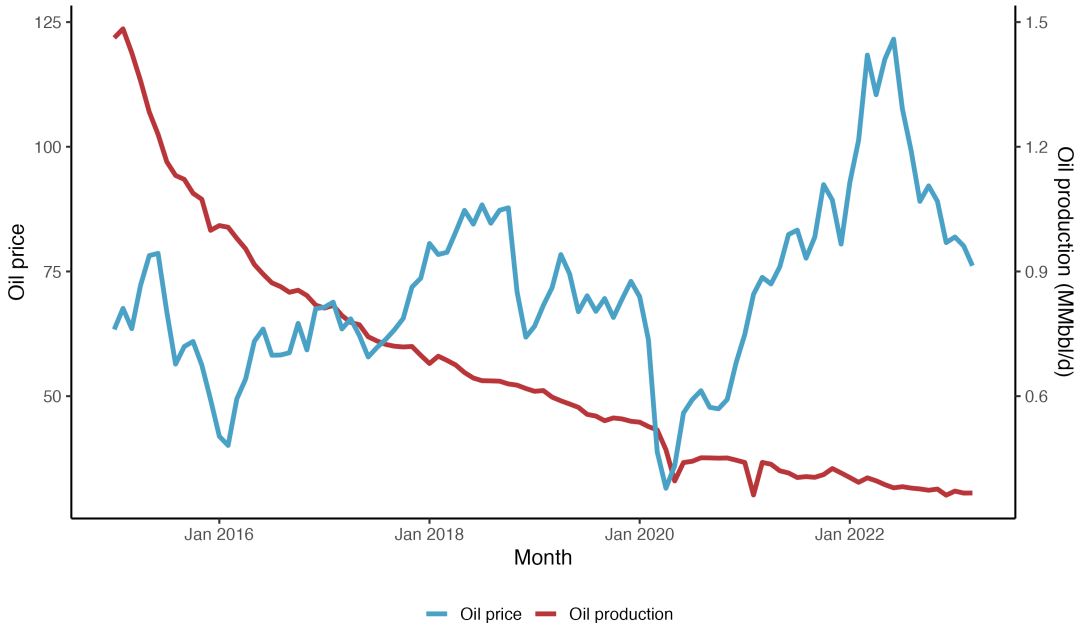
Figure 3: Permian oil and gas production



Notes: The figure plots oil production (left axis) and natural gas production (right axis) in the Permian Basin. Oil production is measured in millions of barrels per day (MMbbl/d). Gas production is measured in billions of cubic feet per day (Bcf/d). Both series are monthly averages. Data from [Enverus \(2024a\)](#).

Second, production from oil and gas wells declines over the life of a well (Figure 4 and Appendix Figure B.3). This pattern is driven by declines in reservoir pressure as more product is extracted, thus slowing the pace at which extraction can occur. It is common to model gas and oil production with decline curves that feature exponential decay, or initial hyperbolic decline followed by slower exponential decay. As demonstrated in [Anderson, Kellogg and Salant \(2018\)](#), these decline curves generally bind: producers do not respond to price shocks by adjusting production from existing wells. In our data as well, we observe that gas and oil production from existing wells is inelastic. We see no correlation between intensive margin production and oil or gas prices (Figure 4 and Appendix Figure B.3). The few periods when production and prices appear to co-move correspond to external events (extreme weather, the COVID-19 pandemic) that affected both demand and production.

Figure 4: Permian oil production from wells drilled before 2015



Notes: We depict production data covering January 2015 through March 2023 for Permian Basin wells that were completed before January 2015. Oil production is measured in millions of barrels per day (MMbbl/d). Oil prices are Cushing spot prices, measured in dollars per barrel. We derive production data from [Enverus \(2024b\)](#). Spot prices are from [Energy Information Administration \(2024a\)](#).

In contrast, well drilling does move with prices. We verify this finding from [Anderson, Kellogg and Salant \(2018\)](#) using data from [Enverus \(2024c\)](#). We find that drilling in the Permian Basin visually tracks oil and gas prices (Appendix Figure B.4). We formalize this observation using a local projections approach in Section 5.2.

3.3 Revenues

We use data from Enverus on lease-month level revenues for Texan producers, including volumes of product sold (both oil and gas), total sales value, and buyer ([Enverus 2024d](#)). This information is originally collected by the Texas Comptroller for tax purposes. By aggregating lease revenues data to the producer level, we find that even the largest gas producers in the Permian derive most of their revenues (70-95 percent) from oil sales (Table C.1).

3.4 Emissions

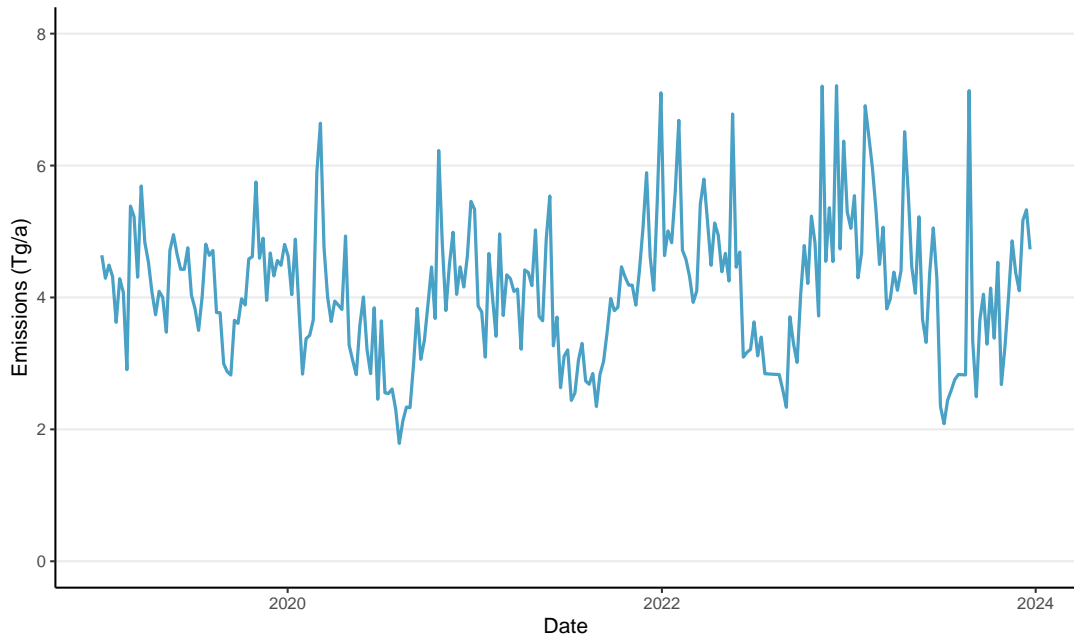
Previous research on the climate costs of oil and gas production has been hampered by the quality of data available on methane emissions. Until recently, large-scale methane measurement has only been possible using firm surveys, bottom-up inventories, and aircraft campaigns. The EPA's Greenhouse Gas Reporting Program is an example of the first: this annual survey is mandatory for large emitters, but relies on firms being honest and accurate regarding their own emissions. The second method, bottom-up inventories, involves measuring the carbon intensity of different activities (e.g., drilling for oil) and multiplying by units of activity

(e.g., wells). This method is not suited to tracking how carbon intensity varies across units or over time. The final method, flying aircraft armed with methane sensors over areas of interest, is accurate but resource intensive. It has not been feasible to use this technique to create panel datasets of an entire region's emissions.

Recent advances in satellite instruments and atmospheric modeling have revolutionized methane measurement. [Varon et al. \(2026\)](#) is an example of this progress. The authors' work is based on satellite observations from the TROPospheric Monitoring Instrument (TROPOMI) aboard the Sentinel-5P satellite, which was developed by the European Space Agency. The TROPOMI instrument can sense methane concentrations at a high spatial resolution, but is unable to determine where the methane originated from. To that end, the authors apply a model of atmospheric transport (GEOS-Chem) combined with prior estimates of emissions from the EDF's 2018 bottom-up inventory. The result is a set of weekly emissions estimates at a $25 \times 25 \text{ km}^2$ resolution, covering the entire Permian Basin. Due to the high frequency and comprehensive nature of this dataset, it is well-suited to our analysis of how emissions respond to prices.

We use weekly estimates of Permian emissions from [Varon et al. \(2026\)](#) covering the period January 2019 through December 2023. We primarily use basin-level and sub-basin-level aggregates of these estimates. Figure 5 plots methane emissions estimates aggregated for the Permian Basin. Methane emissions are highly volatile throughout the study period. There is no apparent trend in emissions, even though gas production increased over the period.

Figure 5: TROPOMI estimates of methane emissions from the Permian Basin



Notes: Weekly methane emissions are estimated using the methodology in [Varon et al. \(2023\)](#) and [Varon et al. \(2026\)](#). Emissions are measured in teragrams per year (Tg/a).

3.5 Flaring and venting

We use two complementary datasets to measure flaring and venting in the Permian Basin. First, we use satellite-based estimates of flaring from [Elvidge et al. \(2013\)](#) and methodology from [Lyon et al. \(2021\)](#). This approach converts radiant heat and light detected by the Visible Infrared Imaging Radiometer Suite (VIIRS) satellite instrument into estimates of the number of flares and volume of gas flared each month. The methodology is unable to detect gas vented either intentionally or via malfunctioning flares. However, it has the advantage of being measured daily and being comparable across jurisdictions despite differences in reporting requirements and definitions across state lines.

The second dataset we use to measure flaring is from the [Railroad Commission of Texas \(2023\)](#), or RRC. These data are collected at the lease-month level when firms fill out their monthly production report (Form PR). Firms must report the total volume of gas they produce, as well as gas volumes in each of several categories of use. One of these categories is flared and vented gas, though firms are not required to include fugitive emissions or gas released during well completion. These data are subject to potential firm misreporting, exist at lower frequency than VIIRS data, and do not cover the part of the Permian Basin that lies in New Mexico. However, they have the advantages of including vented gas and being available for individual wells and leases. This allows us to estimate the parameters of our model at the firm level. Despite the many differences between the VIIRS and RRC datasets, trends in flared volumes generally line up across sources (Appendix Figure B.5).

3.6 Pipelines

We compile data on natural gas pipeline infrastructure serving the Permian Basin using a combination of industry publications and media reports, including [Energy Information Administration \(2024c\)](#). For each Permian egress pipeline, we document its in-service date and its designed takeaway capacity, providing a time series of expansions in regional midstream capacity. A list of Permian pipeline expansions is presented in Appendix Table C.2 and the total Permian takeaway capacity by month from 2010 to 2024 is presented in Appendix Figure B.6.

4 Model

In order to evaluate how market conditions and emissions policies shape producers' decisions, and ultimately to discipline our counterfactual analysis, we present a dynamic model of oil and gas producers' investment and flaring decisions. The model captures two decisions that lead to methane emissions in this industry: (i) the static tradeoff between marketing and flaring associated gas, the latter of which contributes directly to emissions, and (ii) the dynamic investment decision of whether to drill new wells, which governs the long-run scale of production and emissions. Modeling both margins allows us to distinguish how policy affects emissions immediately through flaring choices and over time through drilling incentives and production dy-

namics.

The model has an infinite horizon with discrete decision periods. In each period, firm i 's production from existing wells is predetermined by past drilling decisions, while investment in new wells shapes future production. The firm's state in period t is given by $(\Omega_{it}, \varepsilon_{it})$, where Ω_{it} is the observed state vector and ε_{it} is an i.i.d. shock observed by the firm but not by the econometrician. The observed state is

$$\Omega_{it} = (q_{it}, g_{it}, w_{it}, \mathbf{p}_t, d_t, r_t, \theta_i),$$

where q_{it} and g_{it} denote oil and gas production from existing wells, w_{it} is the firm's active well count, $\mathbf{p}_t = (p_t^o, p_t^g)$ are the net-of-tax oil and gas prices, d_t is the rig dayrate for drilling, r_t is the cost of gas pipeline transmission,⁷ and θ_i summarizes firm-specific productivity parameters, including expected well output and decline rates. Firms are small relative to the market and take p_t , d_t , and r_t as exogenous.

Although firms take the transmission cost r_t as exogenous when making decisions, it is an equilibrium object determined by regional pipeline utilization. Specifically, r_t depends on the interaction between available takeaway capacity and the total quantity of gas marketed from the basin. When aggregate utilization rates rise, transmission costs increase nonlinearly. As a result, policies that lead many firms to change their marketed gas quantities will create feedback loops through equilibrium transmission costs.

Each period, the firm makes two decisions. First, it chooses how much gas to market (i.e., sell), m_{it} . It is constrained above by total gas production, so that $m_{it} \leq g_{it}$. We assume that the remaining gas is flared, generating methane emissions. Marketing gas entails costs $c_i^g(\cdot)$, which depend on transmission conditions and firm characteristics. Because marketing decisions do not affect future states, this is a static choice. Second, the firm decides whether to invest in drilling a new well, which begins production in a subsequent period. Drilling expands future production capacity but entails immediate costs that depend on the drilling rig dayrate d_t . Oil production from existing wells is assumed to have zero marginal cost, and wells remain active until depletion; we therefore abstract from exit decisions.

4.1 Static emissions problem

In each period, firm i decides how much of its associated gas production to market, recognizing that unmarketed gas must be flared and thereby generates methane emissions. The firm chooses $m_{it} \leq g_{it}$ to maximize static payoffs from its existing wells:

$$\bar{\pi}(\Omega_{it}) = \max_{m_{it} \leq g_{it}} \underbrace{p_t^o q_{it} - c_i^o(q_{it})}_{\text{oil profit}} + \underbrace{p_t^g m_{it}}_{\text{gas revenue}} - \underbrace{c_i^g(m_{it}; r_t, \mathbf{X}_{it})}_{\text{gas marketing costs}} - \underbrace{\tau(\ell_f(g_{it} - m_{it}) + \ell_w w_{it})}_{\text{emissions tax}}, \quad (1)$$

⁷We assume that the cost of transmission from the Waha Hub in the Permian basin to the Henry Hub is a sufficient statistic for transmission costs. This relationship is explored in other work, such as [Oliver, Mason and Finnoff \(2014\)](#).

where ℓ_f is the methane emissions factor of flared natural gas, ℓ_w is the per-well baseline methane emissions, and thus $\ell_f(g_{it} - m_{it}) + \ell_w w_{it}$ is total methane released from existing wells.⁸ We assume ℓ_f and ℓ_w are technologically fixed and cannot be altered by the firm.⁹ Producers face an emissions tax $\tau \geq 0$ on each unit of emissions.

Firms face a competitive global market for oil and gas and are therefore price takers. Oil profits are the difference between oil revenues, $p_t^o q_{it}$, and the cost of oil extraction, $c_i^o(q_{it})$. Gas revenues are the product of the gas price p_t^g and the amount of gas sold, $m_{it} \leq g_{it}$. Sending gas to market requires paying marketing costs $c_i^g(\cdot)$, which are convex in marketed volumes and capture the costs of gathering, processing, and transmission to the buyer.

We parameterize gas marketing costs with the Waha basis r_{it} and time-varying producer characteristics \mathbf{X}_{it} . In this way, we capture several key features of this industry. First, producers usually sign long-term contracts for pipeline capacity for some share of their gas production, at rates that vary by firm (depending on volume, bargaining power, etc.). Second, for remaining gas, producers face spot market prices subject to regional congestion, which drives variation in realized marginal costs. Variation in prices arises due to congestion at any point in the natural gas supply chain, from gathering to processing to transmission. As a result, gas marketing costs respond both to firm-level heterogeneity and to system-wide transmission constraints.

Following [Anderson, Kellogg and Salant \(2018\)](#), we assume marginal production costs of 0, i.e., $c_i^o(q_{it}) = 0$. The first-order condition for marketed gas m_{it} when producers are within the feasible set ($m_{it} \in [0, g_{it}]$) is thus:

$$\begin{aligned} p_t^g &= \frac{\partial c_i^g(m_{it}; r_t, \mathbf{X}_{it})}{\partial m_{it}} - \tau \ell_f && \text{if } m_{it} < g_{it}, \\ p_t^g &\geq \frac{\partial c_i^g(m_{it}; r_t, \mathbf{X}_{it})}{\partial m_{it}} - \tau \ell_f && \text{if } m_{it} = g_{it}. \end{aligned} \tag{2}$$

This condition illustrates the basic emissions tradeoff: for an interior solution, the value of selling one more unit of gas must equal its marginal marketing cost, net of the avoided emissions tax from not flaring.

4.2 Endogenous transmission costs

Pipeline transmission costs depend on system-wide utilization: when aggregate marketed gas approaches takeaway capacity, costs rise sharply. Policy changes that shift m_{it} across many firms affect demand for pipeline capacity and therefore affect the equilibrium marginal cost of transmission r_t . While each individual firm takes r_t as given, in counterfactual simulations we must account for this general-equilibrium feedback by re-computing r_t based on aggregate utilization.

⁸Independent of producers' decisions, some baseline emissions arise mechanically from normal operations (e.g., pneumatic devices, separators, dehydrators, compressors). [Omara et al. \(2022\)](#) document that such emissions are relatively invariant to production levels.

⁹In principle, producers may also respond to an emissions policy by investing in technologies that reduce baseline methane emissions from equipment (e.g., replacing pneumatic devices, upgrading compressors, or installing vapor recovery units) or by improving flaring efficiency ([Aldy, Reinhardt and Stavins 2025](#)). Such investments will be more responsive to long-term policy changes than to short-term price variation, since a longer stream of avoided costs is more likely to justify the upfront expense. We shut down this channel in our model for tractability and because detailed data on technology adoption and costs are limited. Exploring the interaction between policy, technology adoption, and emissions outcomes is an important avenue for future research.

To that end, we parameterize the transmission cost as

$$r_t(m_t, k_t) = \delta_1 + \delta_2 \mathbf{1}(m_t/k_t > \nu) (m_t/k_t - \nu)^2, \quad (3)$$

where $m_t \equiv \sum_i m_{it}$ is the total quantity of marketed gas from the basin and k_t is the total pipeline takeaway capacity leaving the basin.

The marginal cost response has two components. First, δ_1 captures the baseline marginal cost of transmission under uncongested conditions. Second, once utilization m_t/k_t exceeds threshold $\nu \in [0, 1]$, marginal costs increase, with δ_2 governing the steepness of the congestion penalty. Following Fowlie, Reguant and Ryan (2016), we assume that above this utilization rate threshold, costs increase with the square of the capacity utilization rate, resulting in a “hockey stick” shape. This specification is consistent with congestion dynamics in other capacity-constrained energy markets, such as electricity transmission. This approach also mirrors those in industry models of gas markets. For example, the ICF Gas Market Model used by the EPA assumes that basis pressure (i.e., sharp increases in transmission costs) typically arises once average monthly pipeline load factors exceed 80 percent (EPA 2024).

4.3 Drilling problem

In each period t , a risk-neutral firm makes a decision about whether to develop a well from its stock of undeveloped opportunities. For simplicity, we assume that a firm can develop at most one well per period. We treat the problem as a sequence of well-level optimal stopping problems. Drilling is an absorbing action: once a well is drilled, it produces according to a deterministic decline curve and exits the choice set.¹⁰

At the start of each period, the state $\Omega_{it} = (q_{it}, g_{it}, w_{it}, p_t, d_t, r_t, \theta_i)$ is realized, summarizing the firm’s current oil and gas production from existing wells, the number of active wells, prevailing oil and gas prices, drilling costs, pipeline transmission costs, and firm-specific productivity. In addition, the firm observes i.i.d. shocks $\varepsilon_{it}(a)$ for each action $a \in \{0, 1\}$ (wait, drill). The firm drills if the expected discounted value of the well’s lifetime revenues net of drilling costs exceeds the continuation value of waiting. We assume expectations about reservoir productivity and decline curves, governed by θ_i , are fixed, so only expectations over prices and costs evolve over time. Prices and costs follow a first-order Markov process with exogenous transition probabilities, which firms take as given. Because marketing costs are convex in the firm’s *total* marketed gas (equation (1)), the net present value of a new well should depend on the firm’s aggregate production across all wells. Thus, for the model to be internally consistent with the per-period profits in Section 4.1, strictly speaking, the firm’s aggregate gas production enters when evaluating the drilling option.

¹⁰We abstract from several features of drilling emphasized in other work in order to focus on the aspects most relevant for emissions. For example, some models incorporate lease terms, where impending lease expiration increases drilling incentives (see, e.g., Herrnstadt, Kellogg and Lewis 2024). Others highlight information spillovers and learning, both within and across firms, about expected production from new wells (e.g., Kellogg 2011, Covert 2015, Agerton 2020, Hodgson 2024). Finally, uncertainty plays an important role in drilling investment, as Kellogg (2014) shows how price uncertainty influences option value and timing, but we abstract from it here for tractability.

Formally, the deterministic components of the choice-specific value functions are given by

$$v_{it}^1(\Omega_{it}) = \text{NPV}_i(g_{it}, p_t^o, p_t^g, r_t, \theta_i) - c_i(d_t) - \tau \ell_a \quad \text{and} \quad v_{it}^0(\Omega_{it}) = \beta \mathbb{E}[V_{i,t+1}(\Omega_{i,t+1})], \quad (4)$$

where $\text{NPV}_i(\cdot)$ is the present value of the new well's lifetime production, $c_i(d_t)$ is the drilling cost determined by the rig dayrate, ℓ_a are the emissions associated with well drilling and completion, and β is the discount factor. If the oil and gas production and marketed gas from the new well drilled in period t implied by θ_i is given by $(\tilde{q}_{is}, \tilde{g}_{is}, \tilde{m}_{is})$ for all $s > t$ and if the marketed gas from all other wells operated by firm i is given by m_{is} , then $\text{NPV}_i = \sum_{s=t}^{\infty} \beta^{s-t} (\tilde{q}_{is} p_s^o + \tilde{g}_{is} p_s^g - [c(m_{is} + \tilde{m}_{is}; \cdot) - c(m_{is}; \cdot)])$. The firm's problem is characterized by the Bellman equation:

$$V_{it}(\Omega_{it}, \varepsilon_{it}) = \max \left\{ v_{it}^1 + \varepsilon_{it}(1), v_{it}^0 + \varepsilon_{it}(0) \right\}. \quad (5)$$

We assume the idiosyncratic shocks $\varepsilon_{it}(a)$ are i.i.d. Type I Extreme Value. This implies logit choice probabilities:

$$P_{it}(a = 1 | \Omega_{it}) = \frac{\exp(v_{it}^1(\Omega_{it}))}{\exp(v_{it}^1(\Omega_{it})) + \exp(v_{it}^0(\Omega_{it}))}, \quad (6)$$

$$P_{it}(a = 0 | \Omega_{it}) = \frac{\exp(v_{it}^0(\Omega_{it}))}{\exp(v_{it}^1(\Omega_{it})) + \exp(v_{it}^0(\Omega_{it}))}. \quad (7)$$

5 Reduced-Form Evidence

In practice, producers can alter emissions in response to economic factors through three channels: (1) allocation of gas between marketable sales and venting or flaring, (2) intensity of well drilling, and (3) investments in maintenance or technology to limit leakage. In our model, and for this analysis, we focus on the first two margins as we believe these represent the primary channels through which short- and medium-term emissions respond to economic incentives and because firm's investments in leak prevention are not observed. In this section, we examine the determinants of producers' emissions abatement and drilling decisions, and the extent to which these decisions explain the intertemporal variability in emissions observed in Figure 5. Our empirical specifications are motivated by the theory laid out in Section 4.

5.1 Flaring

We begin by analyzing how flaring responds to economic conditions. Our model predicts that producers should flare and vent more gas when gas prices are low and when gas marketing costs are high, since both of these conditions reduce the profitability of selling gas. To test this prediction, we focus on flaring and construct basin-week-level measures from VIIRS infrared imaging data, analyzing aggregate patterns across Texas and New Mexico. In our baseline specification, we estimate regressions of the following form:

$$\log(\text{Flared Gas}_{bt}) = \alpha_b^{(1)} + \beta_{1b}^{(1)} p_t^g + \beta_{2b}^{(1)} r_t + \mathbf{X}'_t \theta_b^{(1)} + \varepsilon_{bt}^{(1)}, \quad (8)$$

where b indexes basin (or sub-basin), p_t^g is the gas price at time t , r_t is the Waha basis, and \mathbf{X}_t is a vector of time-varying characteristics that might affect flaring. Within \mathbf{X}_t , we include a linear time trend, to capture secular changes over time in the intensity of flaring, and the log of the number of new wells drilled, since flaring is common during the drilling process and early in a well's lifetime.¹¹ In our baseline specification, the dependent variable, Flared Gas_{bt} , is the total volume of gas flared in teragrams per year, corresponding to the sum across producers in basin b of $g_{it} - m_{it}$ (produced gas minus marketed gas) from our model from Section 4.¹²

A potential concern with this reduced-form specification is endogeneity arising from reverse causality between flaring and the Waha basis. Importantly, such reverse causality would bias estimates toward zero. If exogenous shocks led producers to flare more gas, the resulting reduction in marketed volumes would mechanically ease pipeline congestion and lower the basis, generating a negative correlation that runs counter to the mechanism emphasized in the model. As a result, any reverse-causality bias would attenuate the positive relationship between transport costs and flaring predicted by the model, implying that the reduced-form estimates should be interpreted as a conservative lower bound on the true effect. In addition, to address concerns that basin-level conditions—such as production surges—might simultaneously drive both high basis and flaring, our specification explicitly controls for drilling activity.

In Table 1, we present results from this specification for the Permian Basin (column 1) and its main sub-basins, Midland and Delaware (columns 2 and 3). Across all specifications, we estimate a positive and statistically significant coefficient on new well drilling, suggesting that there is indeed more flaring during periods with more drilling activity. For the Permian as a whole, a 10 percent increase in drilling is associated with a 3.6 percent increase in flared gas. Consistent with the model's predictions, all specifications yield a positive coefficient on the Waha basis—implying higher transmission costs increase flared volumes—and a negative coefficient on the Henry Hub gas price. Across the Permian, a one-dollar increase in transport costs corresponds to a 9.9 percent increase in flared gas and a one-dollar increase in Henry Hub prices implies a 4.5 percent decrease, with both responses statistically significant at the 1 percent level. The former finding is consistent with [Agerton et al. \(2025\)](#), but we believe the latter to be novel.

We also find suggestive evidence that the sensitivity of flaring to these economic factors varies by sub-basin, with Midland flaring showing a stronger response to transport costs and Delaware flaring showing a stronger response to gas prices. In the Midland sub-basin, a one-dollar increase in basis is associated with a 21 percent increase in flared volumes, which is statistically significant at the 1 percent level; the corresponding estimate in Delaware is smaller and not statistically significant. The reverse pattern holds for gas prices. This may be explained by relatively higher gas-to-oil ratios in the Delaware sub-basin (see Appendix Figure B.2). There is anecdotal evidence that producers with higher gas revenues, such as those in the Delaware, are more

¹¹We discuss this point in more depth in Section 5.2.

¹²Flared gas volumes are estimated from satellite infrared imaging data, applying the VIIRS Nightfire algorithm from [Elvidge et al. \(2013\)](#). [Elvidge et al. \(2015\)](#) report that the mean absolute deviation of satellite-based estimates from reported flaring volumes is about 9.5 percent of reported values, though the reported data themselves may be subject to measurement error. Consequently, the detection and quantification algorithm may introduce classical measurement error in the dependent variable, which would not bias coefficients but would reduce the statistical power of our estimates. We discuss measurement error from satellite measurements in greater detail in Section 5.3.

Table 1: Flared gas and economic factors

	Dependent variable:		
	All	log(Flared Gas)	Delaware
	(1)	(2)	(3)
Henry Hub Price	-0.045*** (0.014)	-0.030 (0.019)	-0.067*** (0.013)
Waha Basis	0.099*** (0.036)	0.213*** (0.046)	0.027 (0.035)
log(New Wells)	0.357*** (0.077)	0.374*** (0.100)	0.288*** (0.070)
Year (2018 = 0)	-0.125*** (0.020)	-0.007 (0.026)	-0.266*** (0.020)
Constant	-0.148 (0.323)	-1.272*** (0.348)	0.141 (0.241)
Observations	258	258	258
R ²	0.334	0.189	0.575
Adjusted R ²	0.323	0.177	0.568
Residual Std. Error (df = 253)	0.385	0.510	0.365
F Statistic (df = 4; 253)	31.661***	14.786***	85.518***

Notes: An observation is a week. The sample period is January 2019 to December 2023. The dependent variable is the log of flared gas volume, measured using VIIRS satellite data calibrated to administrative totals, expressed in teragrams per year (Tg/a). Henry Hub natural gas prices and the Waha basis are weekly averages of daily prices (in \$/MMBtu), with daily prices winsorized at the 1 percent level.

* $p < 0.1$, ** $p < 0.05$, *** $p < 0.01$

likely to hedge against Waha price fluctuations by selling gas under contracts tied to Henry Hub prices.¹³ Appendix Table C.3 reports analogous regressions, but using number of flares detected as the outcome rather than flared volume. Results are similar, though the coefficients on Waha basis are smaller.

5.2 Drilling

Our model predicts that drilling decisions respond to expected future prices of oil and gas, introducing additional emissions in two ways. First, drilling new wells is itself emissions-intensive (captured in our model by ℓ_a , the emissions from well drilling and completion). Venting is common during well completion for both operational and safety reasons, especially when flares have not yet been installed.¹⁴ Flaring is also prevalent at new wells, which may not yet be connected to gathering pipelines or may be so productive in their first few months that their production overwhelms gathering or processing capacity (Beatty 2022). Second, because wells release some emissions as part of normal operations (Omara et al. 2022), adding a new well

¹³For instance, Apache Corporation, a major Delaware Basin producer, has used both basis swaps (locking in a fixed Waha basis) and LNG price linkages to reduce exposure to Waha price fluctuations (Mercatus Energy 2019).

¹⁴During well completions, downhole pressures are often high and unpredictable. Venting is used to relieve this pressure and prevent blowouts—uncontrolled releases of oil or gas that can lead to explosions, fires, or equipment failure. In addition, early gas flows are typically unstable and may contain liquids or debris, making flaring unsafe due to the risk of flameouts or ignition hazards.

mechanically raises aggregate emissions over the well's lifespan.

Investment decisions in oil and gas drilling are forward-looking and shaped by firms' expectations about future commodity prices. Specifically, producers assess the anticipated returns from drilling, which depend on the projected prices over the investment horizon. However, even when firms adjust their expectations, their physical responses may be delayed. Operational constraints such as rig availability, permitting requirements, and regulatory frictions can impede the immediate translation of price signals into drilling activity.

To empirically estimate the dynamic response of drilling to changes in expected future prices, we therefore adopt a local projections approach ([Jordà 2005](#)). The estimation equation takes the form:

$$\log(\text{New Wells}_{t+h}) = \beta_o^h \log \tilde{p}_t^o + \beta_g^h \log \tilde{p}_t^g + \mathbf{Z}_t' \theta^h + \varepsilon_{t+h}^h, \quad h = \{0, 1, \dots, 10\}, \quad (9)$$

where \tilde{p}_t^o and \tilde{p}_t^g are the discounted production-weighted average futures prices for oil and gas, respectively.¹⁵ Specifically, we compute

$$\tilde{p}_t^j = \left(\sum_{l=6}^{36} q_l^j \right)^{-1} \sum_{l=6}^{36} \beta^l q_l^j p_{t,l}^j \quad (10)$$

for $j \in \{o, g\}$, where $p_{t,l}^j$ is the futures price for delivery in month $t+l$ observed in month t , q_l^j is the average production l months after spud, and the monthly discount factor β is 0.992.¹⁶ The vector \mathbf{Z}_t includes three lags of both futures prices and drilling activity, capturing short-run dynamics and persistence, and ε_{t+h}^h is an error term. The horizon h ranges from contemporaneous ($h = 0$) to ten months ahead, allowing us to trace out the temporal profile of drilling responses to price expectations.

We assume a well takes six months to complete, which roughly corresponds to the median time between spud and completion we observe in the data.¹⁷ We also assume production intensity follows the hyperbolic decline curve estimated by the EIA for Midland County production in the Permian Basin, with an initial oil production of 1,090 barrels per day and an initial natural gas production of 707 Mcf per day, an initial decline rate of 0.169, and a hyperbolic parameter of 0.351. This decline curve implies 85 percent of a well's total lifetime production occurs in the first two and a half years of the well's operation, which corresponds to month 36 in our estimation.

While using futures prices may help mitigate contemporaneous feedback, a central identification concern is the potential endogeneity of futures prices. In principle, anticipated drilling activity can affect futures prices through market expectations. However, U.S. oil and gas prices (Cushing and Henry Hub prices, respectively) are well-integrated with the global market, making it less likely that individual drilling decisions in the Permian Basin significantly influence futures prices. To the extent that Permian drilling decisions do affect prices, our estimated drilling elasticities would be biased downwards. Given the Permian's greater importance in the U.S. oil market compared to the gas market, this concern is more pronounced for oil than for gas.

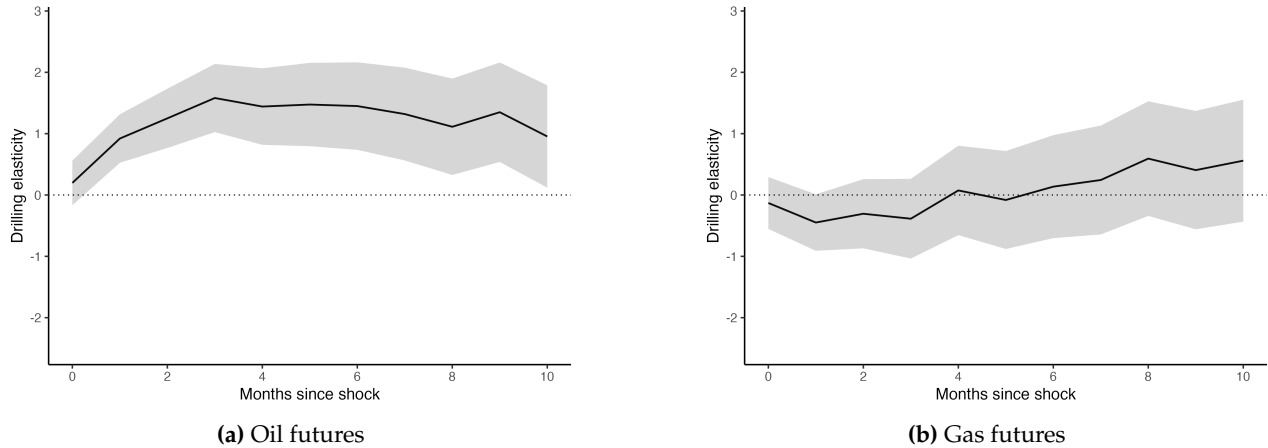
Figure 6 presents the drilling elasticities with respect to oil futures and gas futures, as estimated using

¹⁵An alternative to calculating this production-weighted expected price is simply using the futures price at roughly the midpoint of a well's expected life. This is the approach taken in [Kellogg \(2014\)](#). Our results are qualitatively unchanged using this approach.

¹⁶This corresponds to an annual discount factor of 0.908, approximately an annual hurdle rate of 10 percent.

¹⁷See Appendix Figure B.13 for the distribution of time from spud to completion.

Figure 6: Drilling elasticities, oil and gas futures



Notes: Panels (a) and (b) plot estimated drilling elasticities with respect to oil and gas futures prices, respectively. Each panel shows β_o^h and β_g^h coefficients from equation (9), estimated using weekly data from Enverus covering the Permian Basin, January 2010–December 2023. Shaded regions denote 95 percent confidence intervals. Oil and gas futures prices represent the expected production-weighted average future prices over the 36 months since drilling the well.

equation (9) and Enverus data on drilling activity. Panel (a) reveals a highly elastic response of drilling activity to shocks in the production-weighted average oil futures price. While the contemporaneous oil price elasticity is only slightly positive and not statistically significant, we observe a large and statistically significant drilling response in each of the subsequent nine months. The drilling elasticity climbs to roughly 1.5 within three months, implying that a 10 percent increase in expected oil prices increases well spudding by about 15 percent. This estimate is similar to that calculated by [Newell and Prest \(2019\)](#), who instrument for oil prices with a raw industrials commodities index and estimate an oil price elasticity of 1.6 for unconventional drilling. This drilling responsiveness is consistent with fairly short spud-to-completion cycles and the ready availability of drilling inventories in the Permian; firms appear able to mobilize rigs and crews quickly once price expectations improve.

By contrast, panel (b) of Figure 6 shows that the drilling response to a shock to gas price expectations is statistically indistinguishable from zero. Other studies estimating gas price elasticities often report larger effects when analyzing the U.S. as a whole. For example, [Newell, Prest and Vissing \(2019\)](#) estimates a gas price drilling elasticity of 0.9.¹⁸ However, focusing on the Permian Basin, recent estimates align closely with our findings. In particular, [Prest \(2025\)](#) reports an oil price elasticity of 1.1 but a statistically insignificant gas price elasticity. Even in the Delaware Basin, the most gas-intensive part of the Permian, oil accounts for roughly 90 percent of revenue from “oil” wells and around 75 percent of revenue from wells classified as “gas” wells.¹⁹ The EIA notes that “producers in the Permian region typically respond to changes in the crude oil price when planning their exploration and production activities” ([Energy Information Administration 2023](#)).

¹⁸Though [Newell, Prest and Vissing \(2019\)](#) also focuses on Texas, their sample excludes oil wells and includes several regions that are primarily dry gas plays (the Barnett Shale, Haynesville). Their period of study also predates large increases in associated gas production (i.e., gas that is co-produced with oil), particularly in the Permian Basin.

¹⁹Calculated by the authors using October 2024 price levels.

Public comments by Permian operators corroborate this story.²⁰

As an additional check, we impose the assumption that firms treat oil and gas revenues symmetrically and estimate the elasticity of drilling with respect to expected oil and gas revenues. We construct this futures object by taking the weighted sum of \tilde{p}_t^o and \tilde{p}_t^g , where the weights are the average revenue shares of oil and gas (0.83 and 0.17 respectively). The results are presented in Appendix Figure B.11 and imply a revenue elasticity of 1.4, corresponding to a gas price elasticity of just 0.24. This value falls within the error bounds of the regression in Figure 6b. We interpret this estimate as an upper bound on the true gas price elasticity, since it assumes that oil and gas revenues have equal weight in firms' drilling decisions. Given the industry commentary discussed above, we believe the true gas price elasticity lies below this upper bound.

One potential concern in interpreting our results is that oil and gas prices are collinear. Our main study period falls within the post-2016 period, when the rapid expansion of U.S. LNG exports integrated the domestic gas industry into the global market. This integration led to a significantly tighter link between gas and oil prices ([Stock and Zaragoza-Watkins 2024](#)). To account for the possibility that collinearity between oil and gas prices might confound our results, we conduct a robustness check restricting the sample to the 2010–2015 period, when U.S. natural gas prices were disconnected from oil prices.²¹ The results, shown in Appendix Figure B.7, remain consistent: we continue to observe a large and statistically significant response of drilling to oil futures, and no significant effect for gas futures. These findings are also robust to alternative specifications, including varying the number of lagged price controls and using 18-month-ahead futures prices rather than estimated production-weighted average futures prices.

Although we do not observe a response to gas price expectations in the *number* of wells drilled, changes in price expectations could, in principle, influence the *location* of drilling activity. In particular, when expected gas prices are low but oil prices remain high, producers might shift toward geographic areas with lower gas-to-oil ratios (GORs) to minimize gas output relative to more valuable oil.²² As a result, even if the number of new wells is not sensitive to natural gas prices, the quantity of gas produced from those wells may still vary in response. Using well-level data, we study this empirically by regressing the log GOR on 18-month-ahead log oil and gas futures prices at the time of spudding. The results, shown in Appendix Figure B.8 and Table C.5, indicate that expected gas prices are not statistically significant predictors of well-level GOR. Moreover, the within-operator R^2 values are extremely low—on the order of 0.001 or less—indicating that variation in expected oil and gas prices explains almost none of the within-firm variation in GOR. We conclude that operators cannot easily substitute across formations or adjust well design in response to market signals.

In addition to energy prices, our model implies that expectations about the evolution of gas transmission costs also enter the net present value of drilling a well. However, given the limited influence of gas prices

²⁰For example, in 2024, an Enterprise Products executive noted: “If you look at what drives the economics of the producers in the Permian, it’s not natural gas” ([Enterprise Products Partners L.P. 2024](#)). In 2020, the CFO of Pioneer Natural Resources explained that “natural gas prices do not materially impact the economics of drilling oil wells” ([American Oil and Gas Reporter 2020](#)).

²¹This disconnect arose due to persistent domestic oversupply and limited export infrastructure. See [Stock and Zaragoza-Watkins \(2024\)](#) for details.

²²Spatial variation in GORs across the Permian is primarily driven by geology: deeper zones tend to be more thermally mature and yield higher GORs, while shallower, less mature formations are more oil-prone. Additionally, because deeper wells tend to be gassier, the choice of drilling depth in a given location may also be endogenously linked to price expectations.

on drilling decisions, it is reasonable to expect that the Waha basis exerts even less influence. To assess this formally, we estimate an alternative specification that includes the Waha basis as an explanatory variable.²³ The results are presented in Appendix Figure B.12. We find a precisely estimated null effect, allowing us to reject even modest effects of basis on drilling. Taken together, our results indicate that drilling activity and overall natural gas production in the Permian Basin respond primarily to oil prices rather than gas prices (or gas transmission costs), consistent with statements from both the EIA and industry operators.

5.3 Methane emissions

Having established that emissions-producing decisions respond to prices, we turn now to the question of how methane emissions themselves move with these decisions. Using weekly emissions estimates from the TROPOMI satellite instrument (measured in Tg/a), we estimate the following week-basin-level specification:

$$\log(\text{Emissions}_{bt}) = \alpha_b^{(2)} + \beta_{1b}^{(2)} \log(\text{Flared Gas}_{bt}) + \beta_{2b}^{(2)} \log(\text{New Wells}_{bt}) + \mathbf{X}'_t \boldsymbol{\theta}_b^{(2)} + \varepsilon_{bt}^{(2)}. \quad (11)$$

The \mathbf{X}_t contains time-varying controls that affect emissions independently of producer decision-making. We include heating degree days (HDD) in Texas as measured by [Energy Information Administration \(2024b\)](#), which the scientific literature has shown to be positively correlated with emissions.²⁴ We also include a linear time trend to allow for secular changes in methane intensity over time without absorbing variation from price fluctuations. Furthermore, this time trend captures changes in the stock of existing wells.

The results of this regression are presented in Table 2. We find that drilling is positively and statistically significantly associated with emissions in all regions. A 10 percent increase in spudding (new well drilling) is associated with a 1.7 percent increase in emissions in the Permian as a whole, and a similar increase in both the Midland and Delaware sub-basins. The coefficient on flared gas is not consistently signed and remains fairly close to zero across, though it is positive and statistically significant at the 10 percent level for the Delaware Basin. We postulate three potential explanations for this result. First, methane emissions and flaring are measured using different instruments and methodologies—emissions from spectrometer data and flaring from infrared imaging—introducing orthogonal measurement error in each. This noise reduces precision and attenuates the estimated coefficients toward zero. Second, although greater flaring (and the associated reduction in marketed gas) should mechanically increase methane emissions, any change in flaring efficacy can induce a *negative* correlation between measured emissions and estimated flaring volumes. For instance,

²³Unlike oil and gas futures prices, we do not observe Waha basis futures. We therefore approximate expectations using a first-order Markov process:

$$\log r_{t+1} = \log r_t + \kappa_0 + \kappa_1 r_t + \sigma \nu_{t+1},$$

where volatility σ is assumed to be constant and shocks ν follow an i.i.d. standard normal distribution. We simulate 36-month trajectories, take 100 replications, and use their average to form firms' expectations of the basis path.

²⁴A heating degree day is a measure of how cold a location is relative to 65°F. Each degree that a day's average temperature is below 65°F is counted as one HDD. Work in urban contexts attributes wintertime increases in methane emissions to increased use of natural gas for heating. For instance, [Kariot et al. \(2023\)](#) studies urban methane emissions in Washington, DC, and Baltimore, Maryland, finding that wintertime emissions are about 44 percent higher than summertime emissions. [Sargent et al. \(2021\)](#) finds similar results in Boston, as does [He et al. \(2019\)](#) in Los Angeles. Outside of urban areas, [Varon et al. \(2026\)](#) suggests that higher gas and oilfield emissions in the winter may be due to poorly weatherized gas separators and the physics of gas solubility (which decreases in colder temperatures).

if high winds extinguished large numbers of flares, then measured emissions would increase because more gas would be vented directly into the atmosphere, but measured flaring would decrease because VIIRS only detects flares that are properly lit.²⁵ Finally, new wells often flare more gas, meaning that the two variables are correlated. As a check, we remove new wells from the regression specification in equation (11) and observe a statistically significant positive relationship between flaring and emissions for both the Midland and Delaware sub-basins (see Appendix Table C.4).

Table 2: Methane emissions and producer decisions

	Dependent variable: log(Emissions)		
	All	Midland	Delaware
	(1)	(2)	(3)
log(Flared Gas)	−0.007 (0.037)	0.039 (0.035)	0.073* (0.041)
log(New Wells)	0.167*** (0.043)	0.181*** (0.055)	0.195*** (0.043)
Heating Degree Days (TX)	0.014*** (0.002)	0.012*** (0.003)	0.011*** (0.002)
Year (2018 = 0)	0.002 (0.012)	0.013 (0.014)	−0.012 (0.016)
Constant	0.531*** (0.186)	−0.481** (0.205)	−0.329** (0.158)
Observations	258	258	258
R ²	0.213	0.139	0.199
Adjusted R ²	0.201	0.126	0.186
Residual Std. Error (df = 253)	0.231	0.297	0.248
F Statistic (df = 4; 253)	17.124***	10.232***	15.719***

Notes: An observation is a week. The sample period is January 2019 to December 2023.

The dependent variable is the log of methane emissions, measured in teragrams per year (Tg/a) using satellite spectrometer data following Varon et al. (2026). Flared volumes are measured in Tg/a. New wells are observed monthly and linearly interpolated to the week level.

* $p < 0.1$, ** $p < 0.05$, *** $p < 0.01$

Although it is inherently challenging to measure flaring accurately, it is far easier to measure *incentives* to flare, since these incentives are well captured in observed prices. Therefore, as an additional check on the logic of our model, we directly examine the relationship between prices and emissions. Our model and the empirical results above predict that higher oil prices will lead to higher emissions, as producers drill more wells to increase oil production. We also predict that higher transmission costs (which we proxy for using Waha basis) lead to higher emissions, as producers vent or flare more gas when it is less profitable to sell it. Finally, while the effect of gas price on total emissions is theoretically ambiguous as producers are incentivized to vent and flare less gas but also to drill more wells, we find in Section 5.2 that the drilling

²⁵Lyon et al. (2021) found that 4.9 percent of observed flares were unlit and 11.4 percent of flares were malfunctioning in the Permian in helicopter-based surveys.

response to gas prices is small in the Permian, suggesting the venting and flaring effect will dominate. To test these predictions, we run the following regression:

$$\log(\text{Emissions}_{bt}) = \alpha_b^{(3)} + \beta_{1b}^{(3)} p_t^o + \beta_{2b}^{(3)} p_t^g + \beta_{3b}^{(3)} r_t + \mathbf{X}'_t \theta_b^{(3)} + \varepsilon_{bt}^{(3)}, \quad (12)$$

where p_t^o and p_t^g are the oil and gas prices at time t , respectively, and r_t is the Waha basis. The vector \mathbf{X}_t includes the same time-varying characteristics as in equation (11): heating degree days and a linear time trend.

Table 3 reports the results of this regression. Across all geographies, we find that the Waha basis is positively and statistically significantly associated with emissions. For the Permian as a whole, a one-dollar increase in Waha basis is associated with a 8.2 percent increase in methane emissions. Oil prices also enter positively and significantly, though with a much smaller magnitude: a one-dollar increase in the oil price is associated with a 0.3 percent increase in Permian methane emissions. In contrast, there is a consistent negative relationship between emissions and Henry Hub price, but the coefficient is largest in magnitude and significant at the 5 percent level only for the Delaware. In the Delaware, a one-dollar increase in the Henry Hub price is associated with a 5.3 percent decline in emissions. This pattern mirrors the flaring results in Table 1 and further suggests that, given Delaware is the sub-basin with the highest gas-to-oil ratio, producers there are more responsive to gas price movements than elsewhere in the Permian.

Across all regions and specifications, we observe a seasonal pattern in emissions. Colder temperatures, as measured by Texas heating degree days, are associated with higher levels of emissions. For the Permian as a whole, a one-standard deviation increase in HDD (6.6 HDD) is associated with a 10.0 percent increase in emissions. This is consistent with the scientific literature documenting seasonal variation in methane emissions. Notably, however, colder weather does not coincide with increased well completions or flaring (Appendix Figures B.9 and B.10), suggesting that the effect arises from operating conditions rather than producer activity.

In total, these economic variables and covariates explain only about a quarter of the observed variation in methane emissions in the Permian. Part of the unexplained variation likely reflects measurement noise in satellite-based emissions estimates, but it may also arise from large unintentional methane releases. Scientific research on oil and gas emissions suggests that the distribution of methane emissions exhibits a strong right tail, such that the top emitting sites account for a large share of total emissions ([Cusworth et al. 2021](#); [Omara et al. 2018](#)). These “superemitters” (which include unlit flares, leaky equipment, and other malfunctions) may not respond to economic variables, thus limiting their explanatory power.

Overall, the reduced-form results align closely with the predictions of our model. Higher oil prices stimulate drilling activity, which translates into higher emissions. Rising costs of transporting gas to market, as captured by the Waha basis, increase both flaring and aggregate emissions. The effect of gas prices is theoretically ambiguous, since higher prices reduce emissions at existing wells but encourage new well development, which raises emissions. In the Permian, however, we estimate little to no drilling response to gas prices and

Table 3: Methane emissions and prices

	Dependent variable:		
	log(Emissions)		
	All	Midland	Delaware
	(1)	(2)	(3)
Henry Hub Price	-0.021* (0.011)	-0.010 (0.014)	-0.053*** (0.012)
Waha Basis	0.082*** (0.019)	0.107*** (0.025)	0.093*** (0.020)
Cushing Spot Oil Price	0.003*** (0.001)	0.004** (0.002)	0.006*** (0.001)
Heating Degree Days (TX)	0.016*** (0.002)	0.014*** (0.003)	0.013*** (0.002)
Year (2018 = 0)	0.013 (0.013)	0.022 (0.017)	-0.026* (0.014)
Constant	1.008*** (0.066)	-0.166** (0.084)	0.122* (0.070)
Observations	258	258	258
R ²	0.249	0.185	0.256
Adjusted R ²	0.234	0.169	0.241
Residual Std. Error (df = 252)	0.226	0.289	0.239
F Statistic (df = 5; 252)	16.678***	11.468***	17.310***

Notes: An observation is a week. Sample covers January 2019 through December 2023. Emissions are in log teragrams per year (Tg/a). Prices reflect the average of daily prices over the week, where daily prices are winsorized at the 1 percent level.

* $p < 0.1$, ** $p < 0.05$, *** $p < 0.01$

instead find that aggregate emissions decline when prices rise, suggesting that the intensive margin at existing wells dominates the extensive margin from new drilling.

6 Estimation

While our empirical analysis in Section 5 provides suggestive evidence of the forces highlighted by our model, we now turn to estimating the structural model to discipline these mechanisms and evaluate the equilibrium implications of counterfactual policies. Estimation proceeds in three stages. First, we estimate the parameters of the per-period profit function. This includes the parameters governing how marketed gas quantity, transmission rates, and gas prices affect emissions decisions. Next, we estimate parameters of the transmission cost curve. Finally, for counterfactuals of interest, we employ an iterative convergence procedure to re-compute equilibria based on the endogenous transmission cost response.

For our estimation, we use lease-level data from the Texas Railroad Commission ([Railroad Commission of Texas 2023](#)). We limit our sample to Texan leases located within the Permian Basin (Texas Railroad Commission districts 7C, 8, and 8A) during the period from January 2016 through December 2023. To be included,

a lease must report disposition data for at least 12 months during the sample period. Additionally, after its first appearance in the dataset, the lease must report disposition data for at least 90 percent of the subsequent months. These restrictions ensure that our analysis is based on leases that are observed at length and continuously, reducing the risk of bias from irregular or incomplete reporting.

6.1 Flaring response

The firm's choice of marketed gas m_{it} is characterized by the first-order condition in equation (2).²⁶ Let θ denote the parameters governing the gas marketing cost curve. In principle, one could estimate θ directly from the first-order condition by specifying a parametric functional form for the marginal cost function $\partial c_i^g(m_{it}; \theta) / \partial m_{it}$. In practice, however, (i) the cost function is not the object of direct interest, and (ii) strong parametric assumptions on $\partial c_i^g(\cdot; \theta) / \partial m_{it}$ may be restrictive given limited knowledge of production technology and constraints.

Instead, our empirical objective is to quantify how flaring responds to variation in natural gas prices and transmission costs. Define flaring as the difference between gas produced and gas marketed:

$$F_{it} = g_{it} - m_{it}. \quad (13)$$

By the Implicit Function Theorem, provided the gas marketing cost function is strictly convex ($\partial^2 c_i^g(\cdot) / \partial m_{it}^2 > 0$), the first-order condition defines a unique, smooth inverse mapping from prices and covariates to marketed gas, $m_{it} = f(p_t, r_t, \mathbf{X}_{it}; \theta)$. It follows that flaring can also be expressed as a smooth function of $(p_t, r_t, \mathbf{X}_{it})$:

$$F_{it} = g_{it} - f(p_t, r_t, \mathbf{X}_{it}; \theta). \quad (14)$$

Motivated by this structure, we estimate a reduced-form flaring response function of the form:

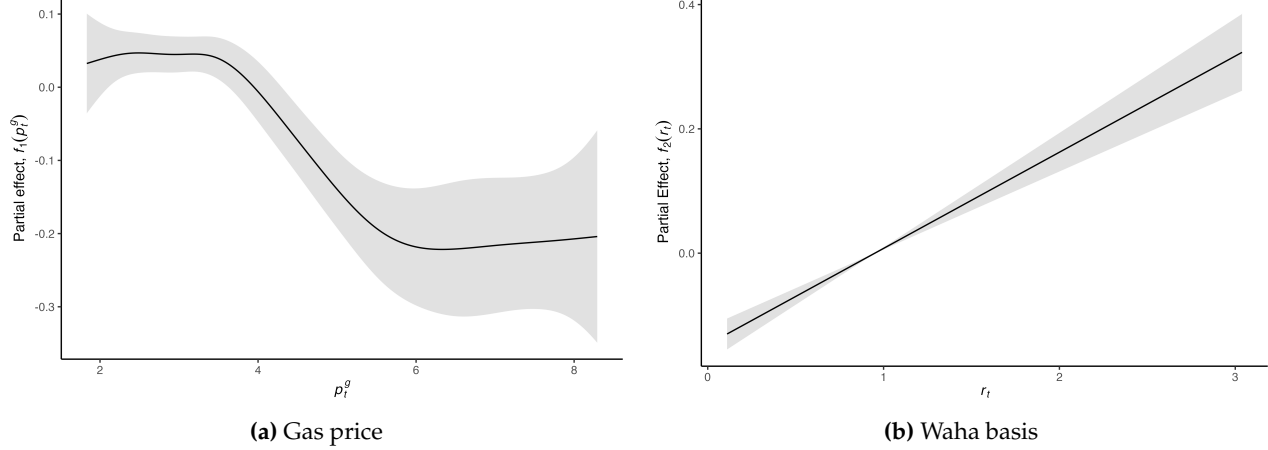
$$\log F_{it} = \alpha_i + f_1(p_t) + f_2(r_t) + \mathbf{X}'_{it}\gamma + \varepsilon_{it}, \quad (15)$$

where $f_1(\cdot)$ and $f_2(\cdot)$ are unknown smooth functions capturing the potentially nonlinear effects of gas prices and transmission conditions, respectively, while time-varying firm characteristics \mathbf{X}_{it} enter linearly. The functions f_1 and f_2 are estimated using penalized spline bases, with smoothing parameters selected by restricted maximum likelihood (REML) to balance flexibility and overfitting. Firm fixed effects, α_i , absorb time-invariant heterogeneity in production potential and baseline flaring intensity. Within firm characteristics, we include logged oil and gas production, new wells, lagged new wells, and the firm's gas-to-oil ratio in each period. To estimate the parameters in equation (15), we use data that producers report to the Texas Railroad Commission on monthly production, drilling, and venting and flaring. We exclude producer-months in which producers report that they marketed over 99 percent of gas produced. With this restriction, we exclude cases where the

²⁶Note that although the model includes τ to represent a potential methane tax, in the data we observe $\tau = 0$ since no such tax is in place; introducing $\tau > 0$ is therefore one of our counterfactual exercises.

first-order condition does not hold with equality (i.e., $m_{it} \approx g_{it}$), allowing for some margin of error due to unavoidable venting and flaring. The results reported below are robust to other capture rate thresholds (e.g., 98 percent and 99.5 percent).

Figure 7: Partial effects, gas price and Waha basis



Notes: Estimated partial effects of gas prices and transmission costs on log flaring from equation (15). Smooth functions are estimated with penalized splines and are centered at zero; shaded regions show 95 percent confidence intervals with firm-clustered standard errors. Gas price and basis are measured in dollars per MMBtu (2024 dollars). Firm fixed effects and linear controls are included.

Figure 7 presents the estimated partial effects of gas prices and transmission costs (Waha basis) on log flaring from equation (15). Panel (a) shows a monotonic, nearly linear negative relationship between the gas price and flaring, consistent with the model's prediction that higher prices raise the incentive to market gas rather than flare it. Panel (b) shows that higher Waha basis costs increase flaring, reflecting the disincentive created by more expensive access to transmission. The magnitudes of these effects imply that at the sample mean gas price of \$2.91/MMBtu, the price elasticity of flaring is -0.17 . At the sample mean Waha basis of \$0.71/MMBtu, the transmission cost elasticity of flaring is 0.21 . These results corroborate the basin-wide aggregate estimates reported in Section 5.1. In particular, Table 1, which uses VIIRS satellite-derived measures, yields a basin-wide price elasticity of flaring of -0.17 at the same mean gas price. Taken together, the evidence indicates that producers' emissions decisions are responsive to economic conditions: flaring decreases as gas prices rise and increases as transmission costs rise.

6.2 Transmission cost response

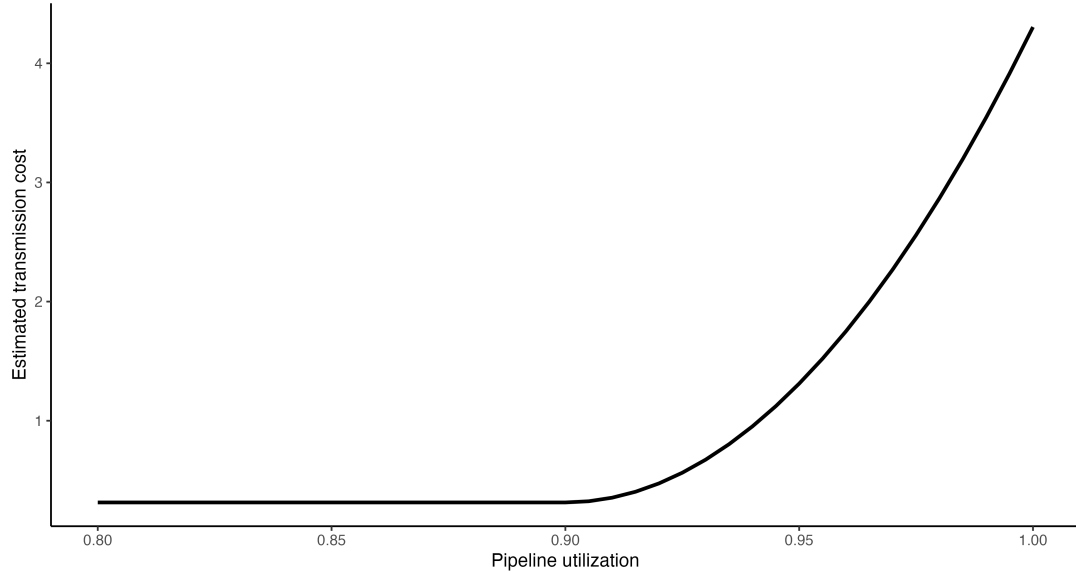
Because pipeline utilization, m_t/k_t , is determined simultaneously with transmission costs, estimating the relationship in equation (3) directly via OLS would yield biased estimates. In particular, this simultaneity would lead us to underestimate the sensitivity of utilization rates to transmission costs: higher transmission costs incentivize producers to vent or flare gas, thereby reducing pipeline utilization and bringing down transmission costs.

To address this endogeneity, we instrument using two sources of plausibly exogenous variation in the

pipeline utilization rate: oil production and the timing of new pipeline entry. Our identifying assumption for the pipeline entry instrument is that, while the development of new pipelines is endogenous, the exact timing of completion is not. The completion of a new pipeline induces a discontinuous change in utilization as k_t increases while m_t is slow to adjust to the new capacity level. To form this instrument, we determine the timing of completion and calculate the percentage increase in pipeline capacity from new entry based on industry reports.

Our oil production instrument exploits the co-production of oil and gas: although *marketed* gas production is endogenous to transmission costs, total production is not. There is effectively no intensive margin response to prices for oil and gas production (see Section 3.2 and [Anderson, Kellogg and Salant 2018](#)). Further, on the extensive margin, as shown in Section 5.2, drilling in the Permian is driven primarily by oil revenues rather than movement in the gas markets.²⁷

Figure 8: Estimated transmission cost curve



Notes: Results from equation (3) estimated via two-stage least squares.

We set the utilization threshold at $\nu = 0.9$ and estimate parameters δ_1 and δ_2 of the transmission cost function using two-stage least squares. The F-statistic in the first stage is 19.1, indicating that the instruments are sufficiently strong to address concerns about weak identification. The resulting estimated transmission cost curve is presented in Figure 8. When pipeline utilization is below 90 percent, the estimated transmission cost from the Waha Hub to the Henry Hub is \$0.18. The cost increases to \$1.31 at 95 percent utilization, to \$2.56 at 97.5 percent utilization, and to \$3.55 at 99 percent utilization.

²⁷We rely on oil production as our instrument rather than total gas production because of concerns that producers may not correctly report the total gas produced. The results are qualitatively indistinguishable when we use total (marketed and non-marketed) gas production. As shown in Figure 3, total oil and gas production co-move closely over time.

6.3 Drilling response

The dynamic model in Section 4.3 yields equation (6), which characterizes the probability that a firm drills a new well in a given period as a function of the expected net present value of drilling relative to the continuation value of waiting.

Empirically, we incorporate the finding that expectations of the Waha basis r_t have no discernible effect on drilling activity in the Permian (Appendix Figure B.12). Given this precisely estimated null effect, we assume that gas marketing costs do not enter the drilling decision. While this departs from full internal consistency between the static marketing problem and the dynamic drilling problem, it delivers two advantages. First, r_t and the firm's aggregate production need not be included in the drilling state space. Second, drilling decisions can be treated as independent across wells, since the payoff to drilling is independent of contemporaneous production from other wells. We assume that potential wells are identical (i.e., $\theta = \theta_i$ for all i) and that the value function is the same across producers.

Under these simplifications, the deterministic component of the drilling value function reduces to

$$v_t^1(\Omega_{it}) = \text{NPV}(p_t^o, p_t^g, \theta) - c(d_t) - \tau\ell_a.$$

Aggregating over wells, the expected drilling response function is

$$D(\tilde{p}_t^g; \tilde{p}_t^o, d_t) = N_t P_t = N_t \frac{1}{\exp(v_t^0 - v_t^1) + 1}.$$

We further assume that the primary source of variation in drilling costs is captured by movements in oil and gas prices. When prices rise, drilling activity expands, creating tightness in the services market and driving up rig dayrates and other input costs. By omitting $c_i(d_t)$ explicitly, we treat these cost pressures as part of the equilibrium adjustment to prices, so that our estimates recover a reduced-form drilling response that already incorporates feedback through drilling costs. Define \tilde{p}_t^g and \tilde{p}_t^o as the discounted, production-weighted futures prices for gas and oil, specified in equation (10). Assuming linear value functions,

$$\begin{aligned} v_t^0 &= \beta_o^0 \tilde{p}_t^o + \beta_g^0 \tilde{p}_t^g + \epsilon_t^0, \\ v_t^1 &= \beta_o^1 \tilde{p}_t^o + \beta_g^1 \tilde{p}_t^g + \epsilon_t^1. \end{aligned}$$

The aggregate drilling function then becomes

$$D(\tilde{p}_t^g; \tilde{p}_t^o, d_t) = N_t \frac{1}{\exp\left([\beta_o^0 - \beta_o^1] \tilde{p}_t^o + [\beta_g^0 - \beta_g^1] \tilde{p}_t^g + (\epsilon_t^0 - \epsilon_t^1)\right) + 1}. \quad (16)$$

Equation (16) highlights that, by not separately estimating continuation values, the coefficients on \tilde{p}_t^o and \tilde{p}_t^g capture the combined influence of prices on both current and continuation values, averaged over the observed data. This feature introduces bias when the estimates are used in counterfactuals.

In particular, consider our reduced-form estimates of the drilling response in Section 5.2, which estimate the relationship between prices ($\tilde{p}_t^g, \tilde{p}_t^o$) and drilling activity using a local projections framework.²⁸ These estimates will tend to overstate the effect of a permanent policy such as a methane tax. Our estimates are based on the average behavior of prices in the data, in which price changes today do not perfectly predict price changes tomorrow. Therefore, our regression assumes a larger change in the relative attractiveness of drilling today versus waiting than would truly be realized if policy changed permanently. We view this bias as informative rather than problematic: our reduced-form estimates from Section 5.2 provide an empirical upper bound on how strongly drilling might respond to a permanent tax. We treat zero response as a lower bound.

In this way, rather than directly estimating a fully structural dynamic model, we discipline our counterfactual analysis by bounding the drilling response $D(\tilde{p}_t^g; \cdot)$ between zero and the reduced-form estimates observed in the data. In the former case, we assume that policies only have static effects, i.e., that they only change flaring decisions at existing wells. In the latter case, we assume that drilling responds to policy changes in proportion to our estimated drilling elasticity and the policies' effects on the expected returns to new wells.

6.4 Equilibrium

To estimate the equilibrium effect of the counterfactual policies we consider, we must account for feedback between producer behavior and transmission costs. Policies such as a methane tax or a pipeline expansion influence marketed gas m_t through two channels: (i) on the static margin, by shifting firms' flaring versus marketing decisions for existing wells, and (ii) on the dynamic margin, by altering drilling incentives and thereby the number of producing wells in future periods. Both channels affect aggregate marketed gas, which determines transmission costs, which in turn feed back into producers' gas marketing decisions.

Formally, an equilibrium is a pair (m_t^*, r_t^*) such that

$$m_t^* = \sum_i m_{it}(q_{it}, g_{it}, w_{it}; p_t^o, p_t^g, r_t^*, \tau), \quad r_t^* = r(m_t^*, k_t),$$

where $m_{it}(\cdot)$ reflects both the static marketing choice and the dynamic evolution of production via drilling.

We solve for this fixed point using an iterative procedure. The algorithm proceeds as follows: (1) compute the direct effect of the policy on marketed quantities by aggregating firm-level responses, taking into account both flaring and drilling behavior; (2) update transmission costs r_t based on the new aggregate marketed gas m_t using equation (3); (3) recalculate marketed quantities given the updated r_t ; and (4) repeat steps (2) and (3) until convergence.²⁹

Although we do not prove existence and uniqueness analytically, the algorithm consistently converges

²⁸Work by [Rambachan and Shephard \(2025\)](#) and [Kolesár and Plagborg-Møller \(2025\)](#) shows that, under certain assumptions, local projections can recover a weighted average of marginal average treatment effects. The price shocks we construct satisfy the required conditions that shocks be randomly assigned and independent over time, if we assume (as is standard) that prices follow a random walk.

²⁹We declare convergence when successive iterations satisfy $\|m^{(k+1)} - m^{(k)}\| < \epsilon$ for tolerance $\epsilon = 10^{-4}$. In practice, the procedure typically converges within fewer than 15 iterations.

to the same fixed point from multiple initializations. Furthermore, equilibrium represents the intersection of the upward-sloping transmission cost function $r(m)$ and the empirically estimated marketed gas response function $m(r)$, which is monotonically decreasing in our spline estimates. We conclude that uniqueness is plausible in our setting.

We implement the iterative procedure separately for each counterfactual policy scenario in Section 7. In each counterfactual, exogenous state variables such as oil and gas prices are held fixed at their observed values, while policy-relevant parameters (the emissions tax τ and pipeline capacity k_t) are varied according to the scenario. Because drilling is a dynamic decision, the effect of each policy on equilibrium outcomes unfolds over time. We therefore simulate the impact of each counterfactual at different horizons following policy implementation. In the first periods after a tax is introduced, flaring reductions entirely reflect the static margin: existing wells adjust marketed gas upward in response to the higher cost of flaring. Over time, the dynamic drilling response amplifies the tax's effect. As production from pre-tax wells declines, a growing share of output comes from wells drilled under the new regime, which were selected based on lower expected emissions costs. In contrast, the effect of infrastructure expansion is front-loaded: congestion relief immediately lowers flaring from existing wells, but as drilling expands and aggregate output rises, the emissions benefit diminishes. Thus, the relative importance of the two policy levers shifts with the horizon, with taxes becoming more effective in steady state and infrastructure improvements less effective.

7 Counterfactuals

With our estimated model, we evaluate a series of policy counterfactuals aimed at reducing flaring and methane emissions. We consider two policies that would directly change the cost of flaring: a methane tax and equalization of the tax treatment for flared and marketed gas. We also consider policies that would alleviate pipeline congestion, indirectly affecting the benefits of flaring. We evaluate counterfactuals over the period January 2019 through December 2023, as this is the date range for which we have emissions data.

To quantify emissions reductions under each counterfactual, we rely on estimates from the scientific literature of the methane content of natural gas, the methane emissions factor of flared natural gas, and typical per-well methane emissions. We assume that the methane content of natural gas is 80 percent.³⁰ In line with analysis by [Plant et al. \(2022\)](#) based on airborne sampling, we assume that flaring has a destructive efficiency of 91.1 percent, meaning that 8.9 percent of flared gas is emitted as methane rather than fully combusted. However, in some of our analyses, we assume that methane taxes are imposed *as if* flaring were 98 percent effective, which is the upper bound that the EPA assumes in implementing the Inflation Reduction Act's methane fee. This higher efficiency value assumes that flares are all functioning properly, whereas the [Plant et al. \(2022\)](#) number reflects unlit flares and other malfunctions that affect flaring efficacy in practice.³¹ Lastly,

³⁰ Although this value varies across basins, the 80 percent methane content assumption is standard in work focusing on the Permian, such as [Varon et al. \(2023\)](#). We assume the other components of gas are ethane (15 percent) and propane (5 percent).

³¹ In fact, [Plant et al. \(2022\)](#) finds that flaring efficacy in the Permian is 86.8 percent, even lower than is observed in other major U.S. gas-producing basins. Experimental work by [Evans et al. \(2024\)](#) shows that variation in flaring efficacy can be explained by factors including gas composition, flow rate, and wind velocity.

we assume that drilling and completing a new well emits 5.9 metric tons (309 Mcf) of methane (EPA 2015) ($\ell_a = 309$). After completion, wells emit baseline methane emissions of 900 kg per month, or about 48 Mcf ($\ell_w = 48$).³²

In all counterfactuals, we assume that the social cost of flaring is equal to the value of the lost gas plus the climate cost of the greenhouse gases emitted, including both carbon dioxide (produced when gas is combusted) and methane released due to incomplete combustion. This assumption implies that the displacement rate of flared gas is one, i.e., when gas is flared instead of consumed, an equal amount of gas from some other source is consumed instead.³³ We assume a social cost of methane (SCM) of either \$2,024 or \$6,880 per metric ton. We assume a social cost of carbon (SCC) of \$67 or \$293 per metric ton. We take these figures from work by the [Interagency Working Group on the Social Cost of Greenhouse Gases \(2021\)](#) and [Azar et al. \(2023\)](#), respectively, and adjust to 2024 USD. While the ranges of estimates for the SCC and SCM in the literature extend beyond these figures, we believe that the values we choose provide reasonable bounds for policy analysis.

For the two tax policies, we present both static and dynamic results. The static results assume a drilling response of zero, meaning that policies impact emissions only through changes in the share of gas that is flared. The dynamic results incorporate drilling responses based on our drilling elasticity estimates from Section 5.2 and our calculations of how each policy would affect the net present value of drilling a well. We assume that any resulting reductions in drilling reduce total emissions by the amount of methane that would have been released from (1) the drilling of new wells, (2) the normal operations of these wells, and (3) the flaring of gas that would have been produced by these wells. On point (3), we assume that the wells would have flared gas at the average rate observed in the data. For the reasons discussed in Section 6.3, we consider the dynamic results we present here to be an upper bound and the static results to be a lower bound. Refer to Appendix A for more details on how we calculate the dynamic counterfactuals. We assume there are no dynamic responses for the pipeline expansion counterfactual, as our results indicate a precise zero effect of transmission costs on drilling (Appendix Figure B.12).

7.1 Imposing a methane tax

7.1.1 Background

First, we consider a methane tax modeled after the Waste Emissions Charge (WEC) mandated by the Inflation Reduction Act (IRA) and implemented by the EPA. The EPA's rule, finalized in November 2024, imposed a fee per unit of methane emitted by oil and gas facilities, where emissions are assessed based on self-reported

³²To derive this number, we first scale the 1.7 kg/hr/site estimate from [Omara et al. \(2018\)](#) up to the month level. Notably, this paper finds that site-specific emissions are largely invariant to the volume of gas produced at each site. Then, we multiply by 0.75 to difference out emissions from flaring. This factor is based on work by [Cusworth et al. \(2021\)](#) showing that 12 percent of detected plume emissions in the Permian Basin were from flares, as compared with 50 percent total from production. This is of course a rough approximation, as the degree and sources of methane leakage from oil and gas sites have been shown to vary significantly within and across production sites.

³³Other researchers, including [The World Bank \(n.d.\)](#), also use this assumption. We believe this is reasonable: other work finds that natural gas price elasticities are fairly small ([Labandeira, Labeaga and López-Otero 2017](#)), and each unit of gas flared is unlikely to significantly impact gas prices. If the true displacement rate for flared gas is less than one, then our estimates of the social costs of flaring should be scaled down by roughly the true displacement rate.

measures of activity (e.g., number of hours of operation for a pneumatic pump or amount of flared gas).³⁴ The proposed methane fee started at \$900 per metric ton for 2024 and increased to \$1,500 per metric ton by 2026.³⁵ In 2025, however, Congress repealed the EPA's implementing rule and then prohibited the EPA from collecting the fee until 2034. As a result, the WEC is not currently being enforced, and any future implementation would require new regulations ([Environmental and Energy Law Program at Harvard Law School 2025](#)). Nevertheless, the WEC is a useful benchmark for understanding how a methane tax could impact producer behavior and emissions.

We abstract from the particularities of the WEC to consider a general methane tax τ of comparable magnitude. We assume that the tax applies at the level of a producer, and that all producers are subject to the tax. Our estimates do not account for tax-induced investments in emissions-reducing technologies, such as flares with automatic shut-offs and real-time monitoring, since the 2024 implementation of the WEC primarily estimates taxable emissions by applying emission factors uniformly based on engineering calculations. However, the agency is increasingly shifting toward frameworks that reward direct measurement and equipment upgrades, which may better incentivize operators to adopt more effective mitigation technologies.³⁶

7.1.2 Estimation and Results

Producers are price takers in both commodity and transmission markets, but in equilibrium a methane tax can indirectly affect prices and costs by shifting aggregate marketed gas. The total effect of a tax on emissions can therefore be decomposed into three channels: a direct response to the tax, an indirect response through commodity prices, and an indirect response through transmission costs. We define emissions E_{it} to be producer i 's period t emissions from flaring, drilling, and normal well operations: $E_{it} \equiv \ell_f F_{it} + \ell_a a_{it} + \ell_w w_{it}$. The equilibrium impact of tax τ on emissions is given by:

$$\frac{dE_{it}}{d\tau} = \underbrace{\frac{\partial E_{it}}{\partial \tau}}_{\text{direct effect}} + \underbrace{\frac{\partial E_{it}}{\partial p_t^g} \frac{dp_t^g}{d\tau}}_{\text{price response}} + \underbrace{\frac{\partial E_{it}}{\partial r_t} \frac{dr_t}{d\tau}}_{\text{transmission cost response}}. \quad (17)$$

The direct effect term, $\frac{\partial E_{it}}{\partial \tau} = \ell_f \frac{\partial F_{it}}{\partial \tau} + \ell_a \frac{\partial a_{it}}{\partial \tau} + \ell_w \frac{\partial w_{it}}{\partial \tau}$, captures the partial-equilibrium response of producer i 's emissions to the methane tax, holding the gas price and transmission costs fixed. Although the stock of producing wells w_{it} is predetermined in period t , it is endogenous over time; if the tax was active in prior periods, then w_{it} reflects the tax's impact on historical drilling decisions. Accordingly, $\frac{\partial w_{it}}{\partial \tau} = 0$ for contemporaneous

³⁴Environmental advocates have raised concerns about relying on self-reported data. Even assuming that producers do not misreport, they can still choose among different reporting methods to minimize reported emissions. In an attempt to address compliance challenges, the EPA has introduced measures to incorporate third-party verification and advanced measurement technologies to track methane emissions. The IRA provided over \$1 billion in financial and technical assistance to help monitor, measure, quantify, and reduce methane emissions from the oil and gas sector. Further, as part of the EPA's Methane Super-Emitter Program, third-party notifiers can use EPA-approved remote-sensing technologies to detect super-emitter events. The future of these programs is unclear under the Trump administration.

³⁵The rule included additional details that may change in future implementations: it only applies to facilities above a certain emissions threshold (25,000 metric tons of CO₂ equivalent annually), and only on emissions exceeding 0.2 percent of gas sold.

³⁶For instance, in 2024, the EPA introduced revisions to Subpart W of the Greenhouse Gas Reporting Program that make assumed flare efficiency a function of the particular flare technology used by each producer. Producers that invest in flare equipment that meets the highest standards can claim a flare efficiency of 98 percent rather than the default 92 percent (40 CFR 98.233(n)).

changes in the tax, while the effect grows over time as the stock of wells evolves, converging to a steady state once all active wells reflect post-tax drilling decisions. Our main results focus on this long-run steady state (the “dynamic” result), although we also present the immediate response (the “static” result) that excludes the drilling margin for comparison. Finally, the price and transmission cost terms capture indirect general-equilibrium effects. Through these channels, the tax shifts aggregate marketed gas m_t , altering equilibrium prices and transmission costs, which feedback into the producer’s flaring and drilling decisions.

Because oil and gas are globally traded commodities, and the effect of a methane tax on total global marketed quantities is small, we assume that $\frac{dp_t^g}{d\tau} = \frac{\partial p_t^g}{\partial m_t} \frac{dm_t}{d\tau} = 0$, so the price effect drops out of our decomposition. By contrast, the transmission effect may matter, but only under conditions of congestion. As specified in equation (3), transmission costs are flat when aggregate utilization is below the threshold $v = 0.9$, so that $\frac{dr_t}{d\tau} = 0$ in uncongested periods. When utilization is high, however, transmission costs rise steeply with additional marketed gas, and the responsiveness of r_t to a tax is positive: $\frac{dr_t}{d\tau} = \frac{\partial r_t}{\partial m_t} \frac{dm_t}{d\tau} \geq 0$. In congested conditions, therefore, the transmission effect dampens the equilibrium impact of the tax: additional gas marketing induced by the tax raises transmission costs, which reduces the incentive to market gas and offsets some of the emissions reductions that would otherwise occur.

Our identification of the effect of a tax relies on the assumption that producers’ emissions decisions (flaring and drilling) respond to changes in commodity prices in the same way that they would to an equivalent tax change, i.e., $\frac{\partial E_{it}}{\partial p_t^g} \approx \frac{\partial E_{it}}{\partial \tau}$. This assumption is necessary in the absence of direct observations of a methane tax. In reality, a persistent tax may induce long-run adjustments that producers would not make in response to temporary price shocks. To the extent such adjustments occur, our estimates likely underestimate the impact of an emissions tax.

We convert τ , the tax per metric ton of methane emitted, into an equivalent tax τ' per MMBtu of flared gas. We consider tax rates that embed two different assumptions on the destruction efficiency of flaring: 98 percent from the EPA versus 91 percent from [Plant et al. \(2022\)](#). Under these assumptions, a \$900 per metric ton fee converts to \$0.31 (EPA) or \$1.39 ([Plant et al. 2022](#)) per MMBtu of gas flared. Regardless of the flaring efficiency assumed by the tax, we calculate methane emissions based on the 91 percent efficacy found in [Plant et al. \(2022\)](#).

[Table 4](#) displays the equilibrium effects of the tax, including both dynamic drilling effects and endogenous transmission cost responses. We estimate that a tax of \$900 per metric ton of methane that assumes a flaring efficacy of 98 percent would reduce flaring by 2.1 percent, reduce methane emissions by 1.5 percent, and reduce social costs by between \$340 million and \$980 million annually, depending on the social cost of methane used. If the tax instead assumes the observed flaring efficacy of 91 percent, the effects are over three times larger: the same tax reduces flaring by 6.7 percent and methane emissions by 3.9 percent, resulting in social cost reductions between \$1.0 billion and \$3.0 billion annually. The effects of a \$1,500 per metric ton tax are larger than those of the \$900 tax, but this increase is less than that of changing the flaring efficacy assumption. These results demonstrate that choices in the implementation of a tax can result in large differences in its magnitude and potency.

Table 4: Annualized effects of methane fee and severance tax counterfactuals

	Methane fee, \$900/mt ^a		Methane fee, \$1500/mt ^b		Severance tax ^c
	98% efficacy	91% efficacy	98% efficacy	91% efficacy	
Percent change in flaring	-2.113%	-6.749%	-3.499%	-10.99%	-1.22%
Percent change in methane emissions	-1.452%	-3.872%	-2.409%	-6.319%	-0.638%
Value of abated gas	\$123.3M	\$403.0M	\$204.2M	\$656.0M	\$89.2M
IWG social costs					
Carbon cost reduction	\$114.5M	\$365.7M	\$189.6M	\$595.4M	\$66.1M
Methane cost reduction	\$104.9M	\$279.7M	\$174.1M	\$456.5M	\$46.1M
Social cost reduction	\$342.7M	\$1.05B	\$567.8M	\$1.71B	\$201.4M
Azar et al. social costs					
Carbon cost reduction	\$501.0M	\$1.60B	\$829.8M	\$2.61B	\$289.2M
Methane cost reduction	\$356.7M	\$950.8M	\$591.6M	\$1.55B	\$156.7M
Social cost reduction	\$981.0M	\$2.95B	\$1.63B	\$4.81B	\$535.1M

Note: Values report the model-implied percentage change in flaring and methane emissions, as well as the annual reduction in monetized damages from emissions and lost gas, under counterfactual policies in equilibrium. Results incorporate both the static intensive-margin flaring adjustment and the dynamic extensive-margin response in drilling. Counterfactuals are computed in general equilibrium, with transmission costs adjusting endogenously to pipeline congestion, so reported effects capture indirect equilibrium responses in addition to the direct effects of the counterfactual policies. Negative percentages indicate reductions relative to the baseline (no-fee) scenario. Monetary values represent annual changes in damages valued using the social costs of carbon and methane from the [Interagency Working Group on the Social Cost of Greenhouse Gases \(2021\)](#) (\$67/mt and \$2,024/mt, respectively), and [Azar et al. \(2023\)](#) (\$293/mt and \$6,880/mt, respectively), expressed in 2024 dollars.

^a Proposed 2024 IRA methane fee (\$900/mt).

^b Proposed 2026 IRA methane fee (\$1,500/mt).

^c Tax flared gas at the same rate as the Texas natural gas severance tax (7.5% of market value).

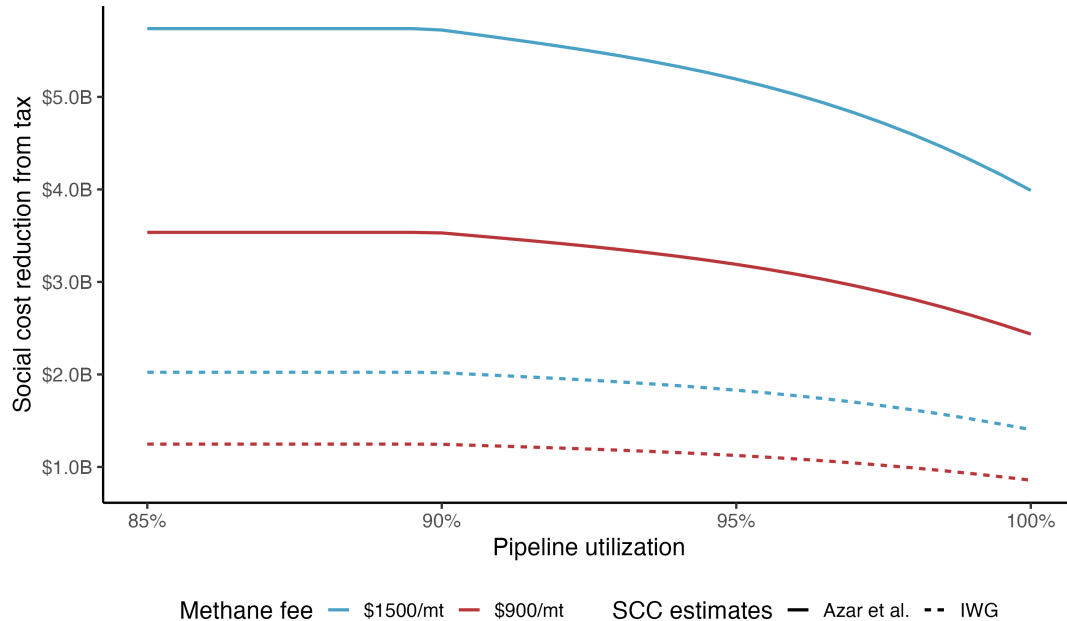
Dynamic drilling effects account for about a percentage point of flaring reductions at all tax levels (Table C.6).³⁷ This amplification occurs because the tax not only makes emitting from existing wells less attractive, but also reduces the incentive to drill new wells that would emit methane over their entire lifetimes. Quantitatively, however, the dynamic margin is relatively small: for a tax assuming 91 percent flaring efficacy, 80 percent of emissions reductions arise from the static reallocation of gas away from flaring at existing wells. Accordingly, our main policy conclusions do not hinge on the precise modeling of drilling dynamics.

Our equilibrium results also reflect transmission cost responses that reduce the equilibrium effect of the tax on flaring and methane emissions relative to the direct effect (Table C.7). Under congested conditions, reductions in flaring increase the volume of marketed gas, which in turn increases the marginal cost of transmission and reducing the net returns from selling gas. For a \$1,500 per metric ton tax that assumes 91% flaring efficacy, the transmission cost response reduces the impact of the tax on flaring by 13 percent (1.7 percentage points) and on emissions by 12 percent (0.9 percentage points) on average over our sample period. While these results reflect the equilibrium effect under observed pipeline congestion during our sample period, the

³⁷ Dynamic effects are largely invariant to assumptions of flaring efficacy because the tax's main effect on drilling costs is via drilling and baseline emissions, not emissions from flaring. By contrast, static effects capture only the flaring decision margin, for which flaring efficacy assumptions are crucial. Because static effects are larger than dynamic effects in this context, the tax's aggregate impact is highly sensitive to flaring efficacy assumptions.

attenuation effect can be larger as congestion grows. Figure 9 presents our estimates of the effects of a methane fee at varying levels of pipeline congestion. When the pipeline system operates at 99.5 percent of its maximum capacity, the reduction in venting and flaring attributable to the tax is 25 to 35 percent smaller than it would be under uncongested conditions. We return to the interaction between congestion and tax efficacy in Section 7.4.

Figure 9: Effect of methane fee counterfactuals by baseline pipeline utilization



Notes: This figure reports equilibrium reductions in social costs (in 2024 dollars) under counterfactual policies for given levels of baseline pipeline utilization. In all counterfactuals presented here, the fee is calculated assuming a flaring efficacy of 91 percent. Emissions are valued using social cost parameters from the [Interagency Working Group on the Social Cost of Greenhouse Gases \(2021\)](#) (SCC: \$67/mt; SCM: \$2,024/mt) and [Azar et al. \(2023\)](#) (SCC: \$293/mt; SCM: \$6,880/mt). Results incorporate both the static intensive-margin flaring adjustment and the dynamic extensive-margin response in drilling. Counterfactuals are computed in general equilibrium, with transmission costs adjusting endogenously to pipeline congestion, so reported effects capture indirect equilibrium responses in addition to the direct effects of the counterfactual policies.

7.2 Eliminating the severance tax exemption for flared gas

Second, we examine the impact of taxing flared gas at rates comparable to marketed gas. In Texas and New Mexico, natural gas is subject to severance taxes of 7.5 percent and 3.75 percent, respectively, of the value of the sold gas. However, in both states, gas that is lawfully flared is exempt from this tax. In this counterfactual, we consider a policy that would impose a 7.5 percent severance tax on all flared gas based on the market value of that gas, as measured by each month's average Henry Hub spot price. For simplicity, we assume that the same severance tax rate applies to flared gas in both Texas and New Mexico, making the tax more burdensome for New Mexico producers than tax equalization alone would imply. This tax change is theoretically distinct from the methane fee because the cost it imposes on producers scales with the market value of natural gas and because it does not apply to methane emitted from non-flaring activities.

Although similar policies have been considered in these states, none have yet been enacted.³⁸ In other settings, efforts to tax flared gas have met with mixed results. In North Dakota, laws aimed at reducing flaring include a provision that after the first year of a well's production, continued flaring incurs the same taxes and royalties as if the gas were marketed, unless an exemption is granted due to economic infeasibility (North Dakota Century Code Section 38-08-06.4). However, a rule proposed by the Bureau of Land Management that would have (among other things) charged royalties on gas vented or flared by oil and gas producers on public lands has been blocked pending litigation.

We present results in the fifth column of Table 4. We estimate that, in equilibrium, removing the implicit subsidy for flaring would decrease the quantity of flared gas by 1.2 percent and methane emissions by 0.6 percent. This value is essentially unaffected by eliminating the dynamic drilling response (Table C.6), since the tax change has a relatively small effect on the overall profitability of drilling new wells. Our estimate is also nearly unchanged when we take out transmission cost responses (Table C.7). The social benefit of this policy ranges from \$201 million to \$535 million annually, well below the benefits from the methane fee analyzed in Section 7.1.

7.3 Relieving pipeline congestion

In the absence of pipeline congestion, transmission costs between the Waha Hub and the Henry Hub remain relatively steady at around 18 cents per MMBtu. However, as Figure 10 illustrates, pipeline congestion has sometimes led to significantly higher transmission costs. In some cases, the Waha basis has risen to well over \$2, occasionally higher than the Henry Hub spot price itself. Given recent and expected pipeline congestion in the Permian, it is crucial to evaluate the impact of relieving congestion on emissions, as well as the interaction between congestion alleviation and tax policies.³⁹

To evaluate the implications of elevated transmission costs due to congestion, we compare actual flaring levels to those under two counterfactuals in which takeaway capacity is increased. In the first counterfactual, we assume that transmission costs are exogenously reduced to the congestion-free level. We are agnostic about the specific policies that could achieve this outcome.⁴⁰ In our second counterfactual, we assume that pipeline capacity increases by either 1,000 or 2,000 MMcf/d, comparable to the capacity of recently constructed long-distance pipelines from the Permian Basin to the Gulf Coast.

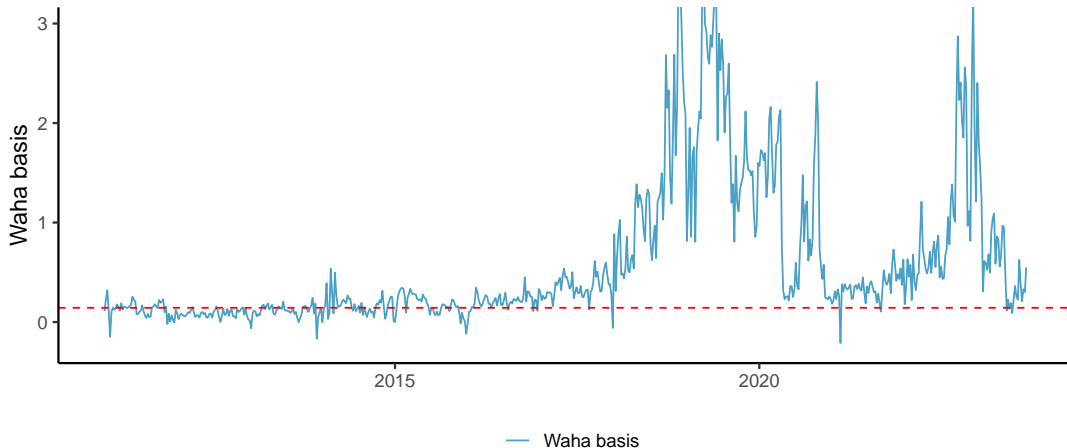
To evaluate the first counterfactual, we use our estimate of the sensitivity of flaring to transmission costs, $\partial F_{it} / \partial r_t$, to calculate what flaring levels would be under a fixed, low r_{it} . We assume that with no congestion, r_{it} is equal to the first decile value of Waha basis, or about 18 cents. The results are presented in Figure 11

³⁸Texas House Bill 228 from the 88th Legislature proposed making flared or vented gas subject to the gas production tax at a *higher* rate than the severance tax, but this bill was not enacted. The bill would have taxed vented or flared gas at 25 percent of its market value, based on the average price for gas sold in the month it was vented or flared.

³⁹Analyses such as [Newman \(2025\)](#) suggest that congestion is expected to continue in the coming years, despite the recent addition of new pipeline capacity.

⁴⁰One way this might be achieved in practice is through changes to regulation around pipeline development and expansion. Natural gas pipelines are heavily regulated because they tend to function as natural monopolies. The Federal Energy Regulatory Commission (FERC) oversees interstate pipeline construction approvals, transportation rates, and environmental reviews. Historically, FERC has capped the return on equity for new pipelines at 14 percent. Increasing this cap or streamlining the approval process could accelerate the development of takeaway capacity, though of course any change may incur other costs.

Figure 10: Waha basis



Notes: The dashed line represents our estimate of the Waha basis at the congestion-free level and is calculated as the first decile of the Waha basis, which is approximately \$0.18 per MMBtu.

and column 1 of Table 5. We find that from 2019 to 2023, reducing transmission costs to congestion-free levels would have reduced flaring by 4.7 percent on average. In periods with the most severe transmission bottlenecks—such as the spring of 2019—eliminating pipeline capacity constraints would have resulted in around a 20-25 percent reduction in flaring. In total, our estimates imply that fully alleviating transmission constraints would have reduced methane emissions by 2.4 percent. The combined value of this emissions abatement, including both the environmental benefits and the market value of the recovered gas, ranges from \$712 million to \$2.0 billion annually depending on assumptions regarding the social cost of carbon.

We next model the addition of a 1,000 or 2,000 MMcf/d in pipeline capacity for the duration of our sample period. Between January 2019 and December 2023, we estimate that adding this incremental egress capacity from the Permian Basin would have reduced Permian flaring by 3.3 percent and 4.3 percent for the 1,000 and 2,000 MMcf/d pipelines respectively (columns 2 and 3 of Table 5). Either pipeline would achieve the majority of the social cost reductions we predict from fully relieving pipeline congestion. The social value of emissions abatement, including both the environmental benefits and the market value of the recovered gas, ranges from \$523 million to \$1.8 billion annually during our study period.

To place the social costs of insufficient pipeline capacity in context, we compare them to the estimated costs of expanding pipeline infrastructure. Using historical reported cost estimates, we calculate a back-of-the-envelope estimate of the cost of building long-distance natural gas pipelines to alleviate Permian egress constraints. This rough calculation is intended only to provide an indicative benchmark and does not account for regulatory and political frictions or other non-pecuniary costs. From the EIA, we obtain data on major U.S. natural gas pipeline projects from 1996 to 2024 ([Energy Information Administration 2024c](#)). The data includes miles, additional capacity (MMcf/d), and—for a subset of projects—cost estimates from companies’ press releases and regulatory filings. The sample includes new pipeline construction and expansions of infrastructure, typically carried out through “looping,” where a parallel pipe is added alongside an existing line. For each of

Table 5: Annualized effects of pipeline expansion counterfactuals

	Fully relieve congestion	1 Bcf/d expansion	2 Bcf/d expansion
Percent change in flaring	-4.668%	-3.255%	-4.3%
Percent change in methane emissions	-2.414%	-1.683%	-2.224%
Value of abated gas	\$285.2M	\$225.4M	\$264.3M
IWG social costs			
Carbon cost reduction	\$252.9M	\$176.3M	\$233.0M
Methane cost reduction	\$174.4M	\$121.6M	\$160.7M
Social cost reduction	\$712.4M	\$523.3M	\$657.9M
Azar et al. social costs			
Carbon cost reduction	\$1.11B	\$771.7M	\$1.02B
Methane cost reduction	\$592.8M	\$413.3M	\$546.1M
Social cost reduction	\$1.98B	\$1.41B	\$1.83B

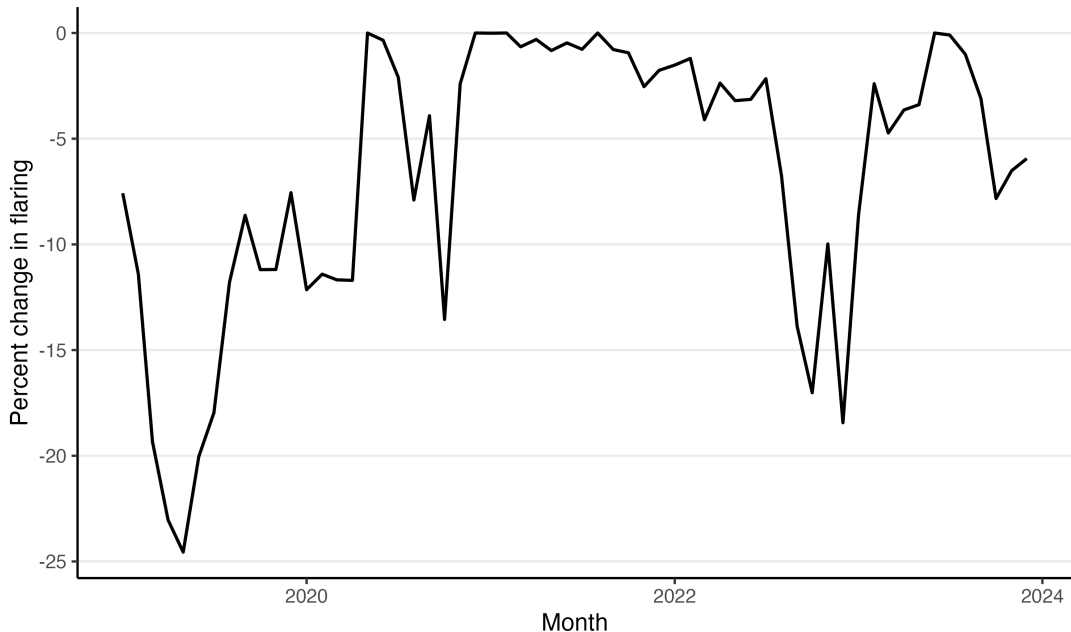
Note: Values report the model-implied percentage change in flaring and methane emissions, as well as the annual reduction in monetized damages from emissions and lost gas, under counterfactual policies. The first two columns present the impact of the expanding Permian takeaway pipeline capacity by 1 Bcf/d and 2 Bcf/d, respectively, and the third column presents the results under a counterfactual in which congestion is fully relieved (i.e., marginal transmission costs are not affected by incremental production). Counterfactuals are computed in general equilibrium, with transmission costs adjusting endogenously to pipeline congestion, so reported effects capture indirect equilibrium responses in addition to the direct effects of the counterfactual policies. Negative percentages indicate reductions relative to the baseline (no-fee) scenario. Monetary values represent annual changes in damages valued using the social costs of carbon and methane from the [Interagency Working Group on the Social Cost of Greenhouse Gases \(2021\)](#) (\$67/mt and \$2,024/mt, respectively), and [Azar et al. \(2023\)](#) (\$293/mt and \$6,880/mt, respectively), expressed in 2024 dollars.

these project types, we estimate a regression of log project cost on log pipeline length and log capacity. The results are presented in Appendix Table C.10.

Since new pipelines serving the Permian Basin have primarily been built to transport natural gas to the Gulf Coast, we focus on the cost of a representative 500-mile pipeline project (the distance between the Permian and the Gulf). Our regressions indicate that a new 500-mile pipeline with capacity of 1,000 MMcf/d would cost around \$1.3 billion, while an expansion project of the same capacity would cost approximately \$1.1 billion in 2024 dollars (Appendix Figure B.14). The equivalent costs for a pipeline with capacity of 2,000 MMcf/d would be \$1.9 billion and \$1.6 billion. These figures are broadly consistent with reported costs for recent real-world projects.⁴¹ Assuming this upfront cost captures both social and private costs, a pipeline of this scale would generate social benefits sufficient to pay for itself in just a few years, even fully ignoring economic benefits of the pipeline outside of the value of transported gas and assuming a low value of the social

⁴¹The Gulf Coast Express Pipeline, completed in 2019, added 1,980 MMcf/d at a cost of \$1.75 billion, while the Permian Highway Pipeline, completed in 2019, added 2,100 MMcf/d at a cost of \$2 billion ([Kinder Morgan, Inc. 2019 2021](#)). A subsequent expansion of the Permian Highway Pipeline in 2023, which added 550 MMcf/d through compression and looping, cost an estimated \$573 million ([Kinder Morgan, Inc. 2024](#)).

Figure 11: Change in flared gas from relieving pipeline congestion



Notes: This figure plots the model-implied monthly percentage change in flaring under the counterfactual of easing pipeline congestion, defined as pipeline utilization at or below 90 percent. Magnitudes can be interpreted as the share of flaring emissions attributable to pipeline congestion. Negative values indicate reductions in flaring relative to observed outcomes.

cost of carbon. Thus, even under conservative assumptions, our results indicate that investment in pipeline infrastructure can yield substantial social returns.

These findings underscore the significant role of infrastructure limitations in shaping emissions outcomes. Importantly, upstream producers do not fully internalize the costs of venting and flaring when making pipeline capacity purchase decisions, and neither do midstream operators in their pipeline investment decisions.

7.4 Combining tax and congestion relief policies

Congestion alleviation and methane tax policies are complementary: the combination of the two policies reduces flaring by more than the product of their individual effects. Table 6 demonstrates this. With the \$1,500 tax, for instance, the combined effect is a 16.8 percent reduction in flaring (column 5) versus the 15.1 percent reduction predicted by multiplying the individual effects (columns 2 and 3). This superadditivity arises because congestion relief eliminates the transmission cost response from equation (17), amplifying the flaring reductions induced by the tax.

In Figure 12, we illustrate this effect in terms of social cost reduction. Using the IWG SCC estimate, with a \$1,500/mt tax assuming 91 percent flaring efficacy, the tax alone reduces social costs by \$1.71 billion annually, while congestion relief alone reduces social costs by \$0.71 billion annually. However, when combined, the two policies reduce social costs by \$2.57 billion annually, which is modestly greater than the sum of their individual effects (\$2.32 billion). This pattern holds across all tax levels and flaring efficacy assumptions. In the sample period for which these effects are computed, 58 percent of months exhibited binding congestion (de-

Table 6: Annualized effects of combining methane fee (91% flaring efficacy) and pipeline congestion relief counterfactuals

	Observed congestion		Fully relieving congestion		
	\$900/mt methane fee	\$1500/mt methane fee	No methane fee	\$900/mt methane fee	\$1500/mt methane fee
Percent change in flaring	-6.749%	-10.99%	-4.668%	-11.959%	-16.762%
Percent change in methane emissions	-3.872%	-6.319%	-2.414%	-6.566%	-9.304%
Value of abated gas	\$403.0M	\$656.0M	\$285.2M	\$707.0M	\$985.1M
IWG social costs					
Carbon cost reduction	\$365.7M	\$595.4M	\$252.9M	\$647.9M	\$908.1M
Methane cost reduction	\$279.7M	\$456.5M	\$174.4M	\$474.4M	\$672.2M
Social cost reduction	\$1.05B	\$1.71B	\$712.4M	\$1.83B	\$2.57B
Azar et al. social costs					
Carbon cost reduction	\$1.60B	\$2.61B	\$1.11B	\$2.84B	\$3.97B
Methane cost reduction	\$950.8M	\$1.55B	\$592.8M	\$1.61B	\$2.28B
Social cost reduction	\$2.95B	\$4.81B	\$1.98B	\$5.16B	\$7.24B

Note: Values report the model-implied percentage change in flaring and methane emissions, as well as the annual reduction in monetized damages from emissions and lost gas, under counterfactual policies. The first two columns present the impact of the tax under the observed pipeline congestion and the remaining columns present the results under a counterfactual regime with no pipeline congestion (i.e., marginal transmission costs are not affected by incremental production). Counterfactuals under observed congestion are computed in general equilibrium, with transmission costs adjusting endogenously to pipeline congestion, so reported effects capture indirect equilibrium responses in addition to the direct effects of the counterfactual policies. Negative percentages indicate reductions relative to the baseline (no-fee) scenario. Monetary values represent annual changes in damages valued using the social costs of carbon and methane from the [Interagency Working Group on the Social Cost of Greenhouse Gases \(2021\)](#) (\$67/mt and \$2,024/mt, respectively), and [Azar et al. \(2023\)](#) (\$293/mt and \$6,880/mt, respectively), expressed in 2024 dollars.

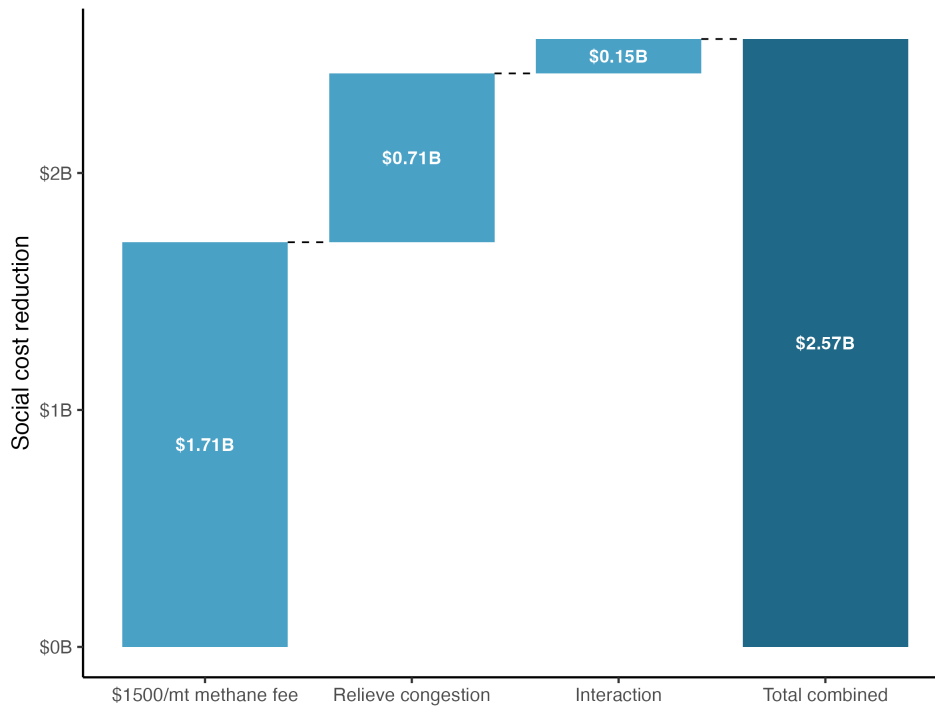
fined as utilization exceeding 90 percent), while only one-quarter of months experienced utilization above 95 percent. If pipeline utilization rates increase in the future, the effectiveness of the tax will not only diminish—as illustrated in Figure 9—but this superadditivity effect will also grow, both in absolute magnitude and as a share of the total impact. We conclude that addressing infrastructure constraints can increase the effectiveness of price-based emissions reduction policies.

8 Conclusion

Reducing methane emissions rapidly will be essential as the world attempts to rein in climate change. Although prior work has explored different methods to regulate methane emissions coming from the oil and gas sector, emissions regulation may not be stringent enough, nor politically palatable enough, to make the necessary impact. In this paper, we explore the market forces driving methane emissions from oil and gas production to better understand policy and non-policy options for emissions abatement.

We find that emissions are strongly increasing in natural gas transport costs, but not significantly corre-

Figure 12: Decomposition of the impact of combining methane fee and pipeline congestion relief counterfactuals



Notes: This figure decomposes the annual social cost reductions (in 2024 dollars) resulting from a \$1,500/mt methane tax and full pipeline congestion relief. Estimates assume the [Interagency Working Group on the Social Cost of Greenhouse Gases \(2021\)](#) social cost valuations and that the tax is implemented with an assumed flaring efficacy of 91 percent. The first two bars display the reductions from each policy implemented in isolation. The “Interaction” bar captures the superadditive effect of combining the policies, which arises because congestion relief eliminates the countervailing transmission cost response to the tax. The “Total combined” bar represents the simultaneous implementation of both policies.

lated with natural gas prices. We explain this pattern using a model of producer behavior in which firms make dynamic drilling decisions and static gas disposal choices, both of which contribute to aggregate emissions. Our empirical work shows that in the Permian Basin, new well drilling is not significantly responsive to natural gas prices but is closely linked with oil prices. Natural gas flaring is responsive to natural gas prices and transport costs. Our results allow us to evaluate a range of counterfactual policies, including tax changes and investments that alleviate pipeline congestion. A central conclusion is that congestion alleviation and emissions taxation are complementary policies: when implemented together, they generate emissions reductions that exceed the effects of the policies in isolation.

Although the Permian Basin is by no means representative of oil and gas production in the U.S. or globally, we believe that our findings based on the Permian are important for U.S. emissions as a whole. First, the Permian is not only the largest oil-producing basin and second largest gas-producing region in the U.S., but it is also the region with among the highest methane leak rates ([Sherwin et al. 2024](#)). Second, since the Permian has a smaller gas price elasticity than other basins, any tax targeting either gas production or methane emissions directly would likely make Permian methane emissions a larger share of U.S. emissions.⁴² More broadly,

⁴²See [Prest \(2025\)](#) for a more in-depth discussion of oil and gas price elasticities across basins and implications for emissions responses to shocks.

our findings regarding the role of transmission congestion are relevant beyond the Permian. In recent years, several other U.S. basins have faced constraints on natural gas takeaway capacity, and some are projected to encounter increasingly tight infrastructure bottlenecks in the near future. This is particularly true in other oil-dominated regions such as the Bakken region ([McDonough 2025](#); [Dwan 2024](#)), but also applies in some gas-focused regions like Appalachia ([Carr 2025](#)). The modeling framework we present is flexible enough to be applied even in contexts like Appalachia, where gas price drilling elasticities are likely to be larger.

Overall, our work results highlight the substantial potential for policies aimed at methane emissions reductions that are designed with an understanding of producer incentives. Though these incentives may differ across regions, our framework provides a roadmap for measuring these differences and designing effective policies accordingly.

9 Appendix

A Estimating counterfactuals

In this section, we detail many of the assumptions necessary to translate our empirical estimates into the counterfactual policy impacts presented in Section 7.

A.1 Static effects

Venting and flaring are not the only sources of methane emissions in the Permian, so a key challenge in determining the static effects of a policy is determining what share of total emissions come from sources that are price-sensitive in the short run. [Williams et al. \(2025\)](#) estimates that 68 percent of methane emissions from the U.S. oil and gas sector originate at production well sites. In the Permian, this share is slightly higher—over three quarters of total methane emissions are attributable to well sites. However, not all well-site emissions are responsive to prices: baseline operational emissions from equipment and leaks also contribute to emissions (e.g., [Omara et al. 2018](#)). To gauge the aggregate implications, we compare the basin-wide price elasticity of methane emissions, estimated from [Varon et al. \(2026\)](#) data as -0.07 (Table 3), with the elasticity of venting and flaring, -0.17 (Table 1). The ratio of these elasticities implies that slightly more than half of total emissions are not responsive to price, leading us to scale the effect of counterfactual policies on venting and flaring by 45 percent when translating to aggregate methane emissions. Given the analysis in [Williams et al. \(2025\)](#), we view this adjustment as a reasonable approximation, while acknowledging uncertainty in the precise share of price-insensitive emissions.

A.2 Dynamic effects

Our approach to modeling counterfactuals with drilling responses consists of two basic steps. First, we estimate how much the policy would change the number of wells drilled each month. We do this by scaling the revenue elasticity of drilling (Section 5.2) by the policy's impact on the net present value (NPV) of drilling a new well. Second, we estimate the emissions impact of the change in drilling activity by multiplying the change in wells drilled by expected emissions per well. We describe each of these steps in more detail below.

Throughout, we assume certain standard parameters for a well in this region. We assume that a well begins producing six months after drilling begins. Once producing, we assume that initial oil and gas production are equal to the median observed peak production for Permian wells (27,271.5 bbl and 42,727 Mcf, respectively). Production declines following a hyperbolic decline curve with parameters (hyperbolic parameter of 0.550, initial decline rate of 0.194) from the [Energy Information Administration \(2021\)](#). We assume that the well operates for 20 years. Finally, we assume that flaring is 91 percent effective and remains constant at a rate of 1.5 percent of total production throughout the well's lifetime, the average of the observed flaring rate for our sample.

A.2.1 Calculating the change in wells drilled

For the methane tax, we assume that the tax applies to all methane emissions from a well, including emissions from drilling, normal operations, and flaring. We calculate the tax burden from each of these sources, summing recurring tax payments (for emissions from operations and flaring) across the lifetime of the well assuming that the producer's monthly discount factor is 0.992. The result is a well-level estimate of the present value of the tax burden. The tax burden from imposing a severance tax on vented and flared gas is calculated similarly, except that we only apply this tax to the volume of gas flared and vented over the well's lifetime.

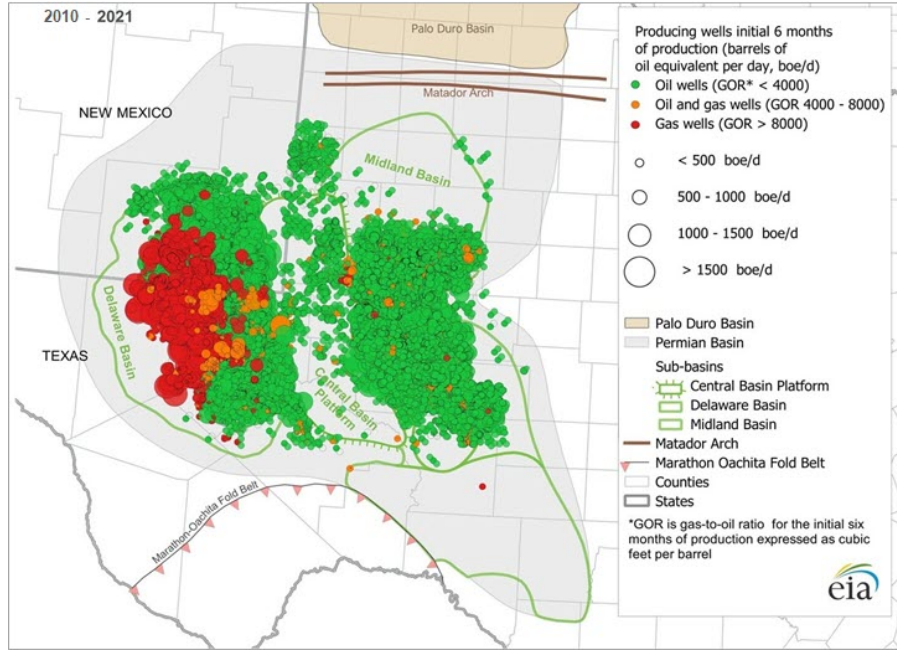
To estimate the NPV of a new well without a new tax, we multiply expected production in each month of the well's life with realized oil and gas prices over the period 2022-2023. We calculate revenues over the lifetime of the well and discount them back to present value using the same discount rate.

Finally, we calculate the percentage change in NPV as a result of the tax by dividing the tax burden by the NPV of a new well without the tax. We then use the result to scale the revenue elasticity of drilling to get the percentage change in wells drilled.

A.2.2 Calculating emissions impacts per well not drilled

As above, we assume that wells produce emissions from drilling, normal operations, and flaring. We assume that each well avoided would have had emissions from drilling of 308.68 Mcf ([EPA 2015](#)). For normal operations, we assume constant monthly emissions of 48 Mcf ([Omara et al. 2018](#)) over the well's lifetime. For flaring emissions, we make the same assumptions as above: wells flare gas at a constant rate of 1.5 percent across their lifetime. We assume that the social cost of these emissions depends on the period in which the emissions occur, using monthly social cost of methane estimates from [Interagency Working Group on the Social Cost of Greenhouse Gases \(2021\)](#) and [Azar et al. \(2023\)](#).

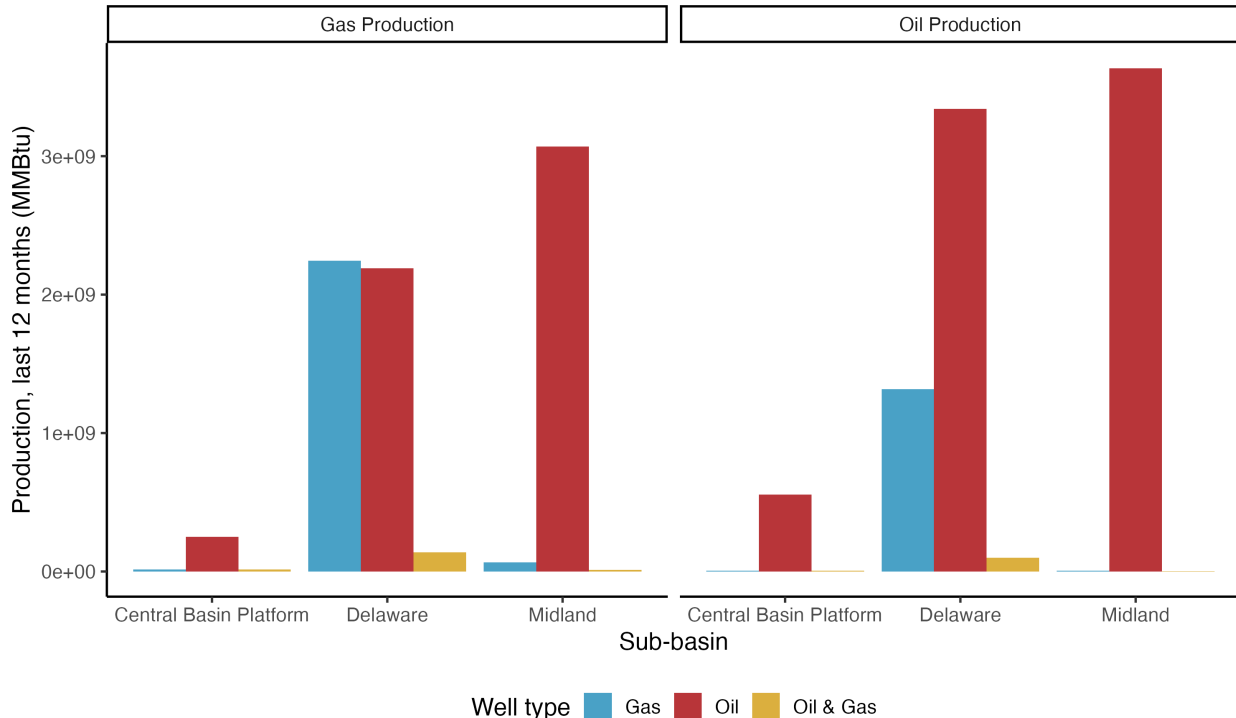
Figure B.1: Oil and gas production



Notes: This figure was produced by the [Energy Information Administration](#) (EIA) and summarizes first 6 months production from wells drilled in the Permian between 2010 and 2021.

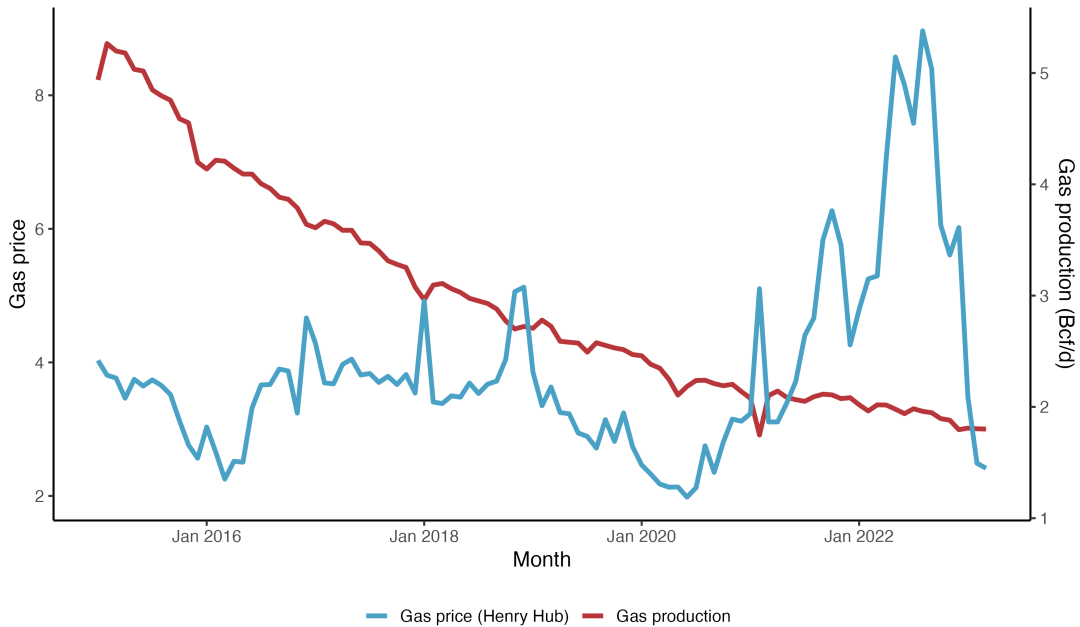
B Figures

Figure B.2: Oil and gas production by basin



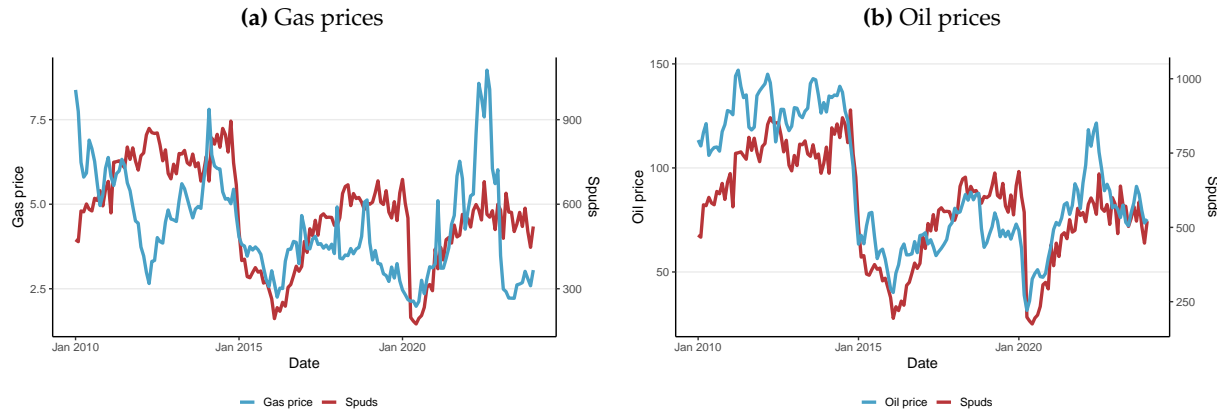
Notes: Production data from [Enverus \(2024b\)](#). We aggregate the last 12 months of oil and gas production as of the last reported month of operation in 2023. Wells types are categorized based on gas-to-oil ratios, as defined by the operator on the filing.

Figure B.3: Permian gas production from wells drilled before 2015



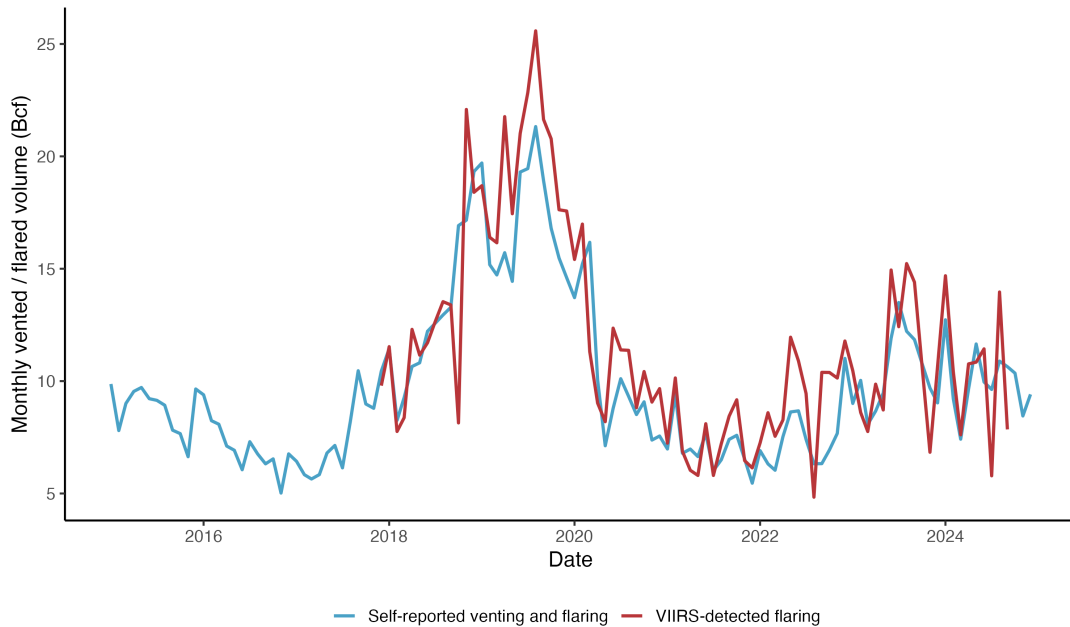
Notes: We depict production data covering January 2015 through March 2023 for Permian Basin wells that were completed before January 2015. Gas production is measured in billions of cubic feet per day (Bcf/d). Waha natural gas spot prices are measured in dollars per MMBtu. We derive production data from [Enverus \(2024b\)](#). Spot prices are from [S&P Capital IQ \(2024\)](#).

Figure B.4: Well drilling and prices



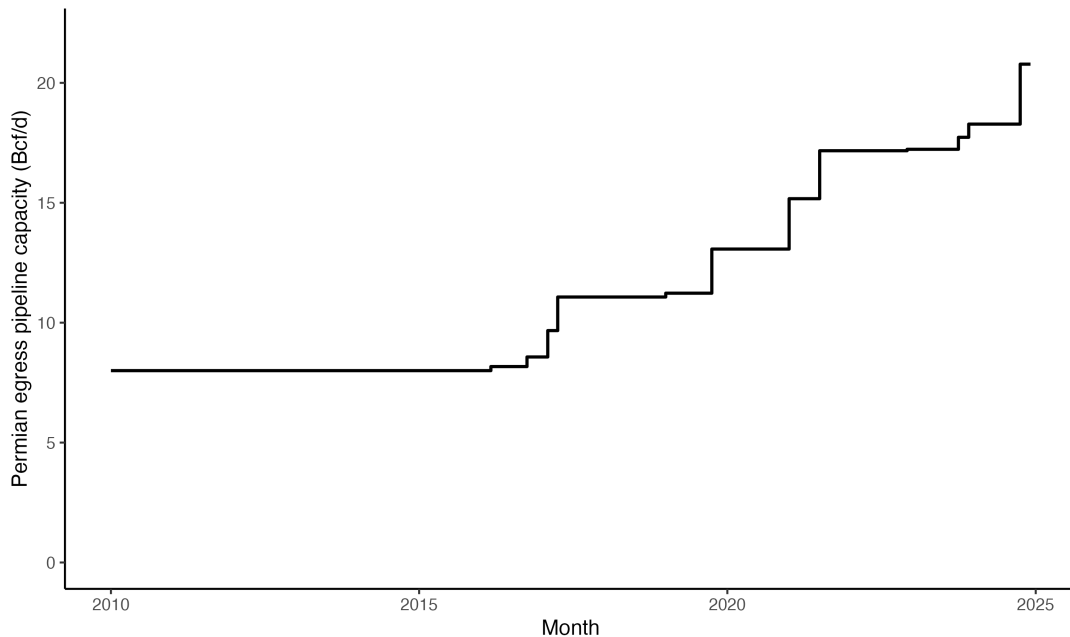
Notes: In both panels, we depict number of spuds (the beginning of drilling operations) by sub-basin of the Permian Basin between 2010 and 2023. We plot this against Cushing WTI spot oil prices and Henry spot prices. Spud data are from [Enverus \(2024c\)](#). Spot prices are from [S&P Capital IQ \(2024\)](#).

Figure B.5: Self-reported and remote-sensed venting and flaring volumes



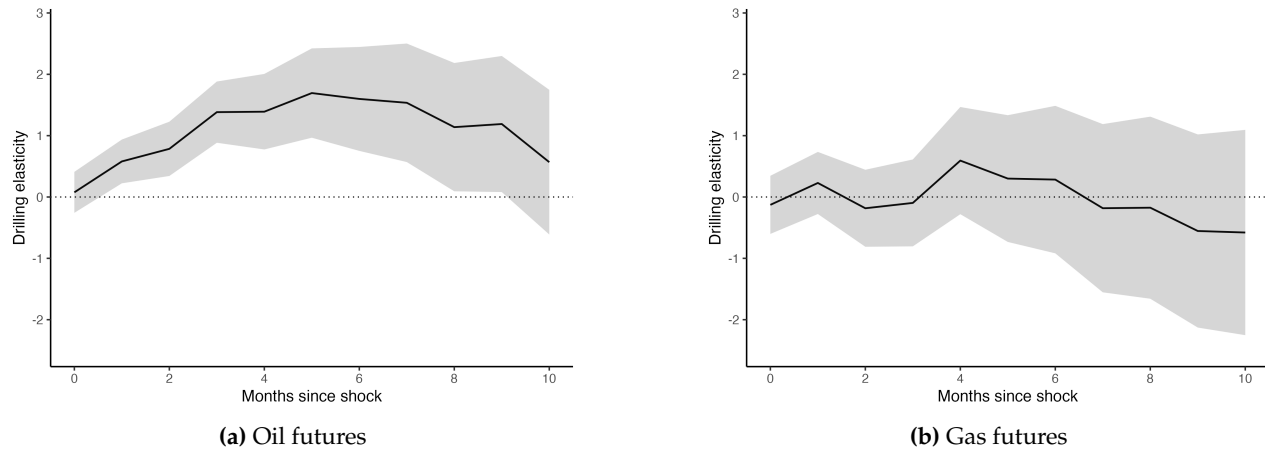
Notes: VIIRS series represents estimates of flared gas calculated by the authors using data from [Elvidge et al. \(2013\)](#) and methodology from [Lyon et al. \(2021\)](#). Self-reported series represents data reported by producers to the Texas Railroad Commission ([Railroad Commission of Texas 2023](#)) and includes both flared and vented gas. Both series capture totals for the Texas Permian Basin.

Figure B.6: Permian natural gas egress pipeline capacity, 2010-2024



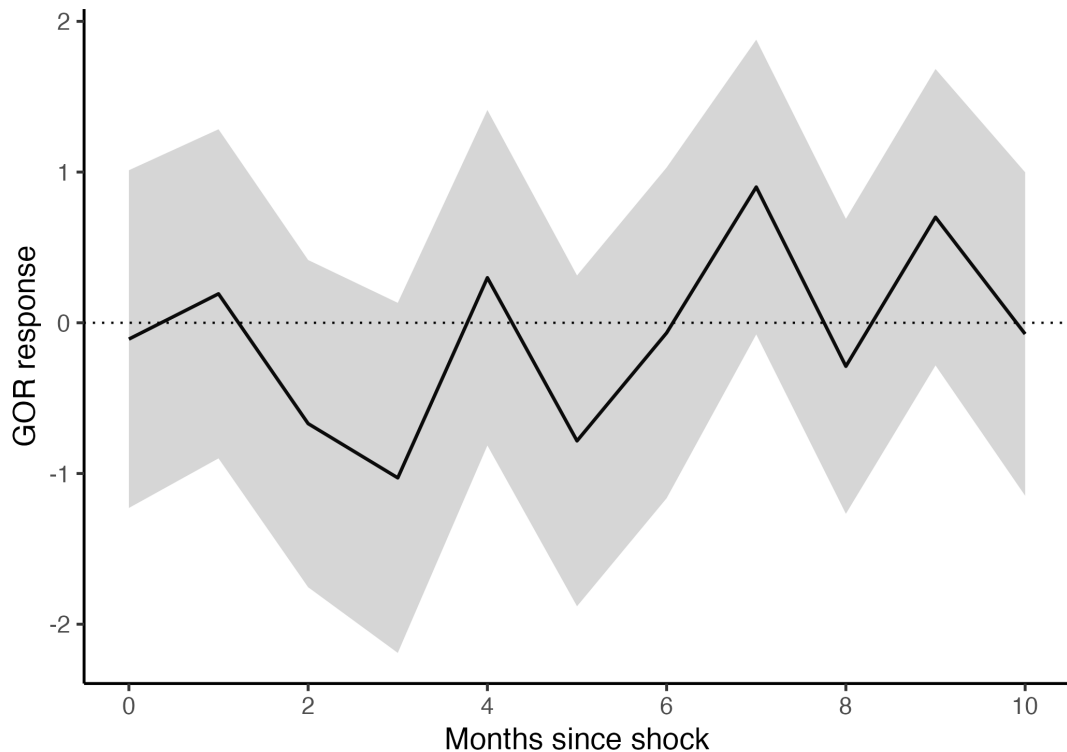
Notes: Permian gas takeaway capacity collected by authors from industry reports and press releases on pipeline completions.

Figure B.7: Drilling elasticities, oil and gas futures, 2010-2015



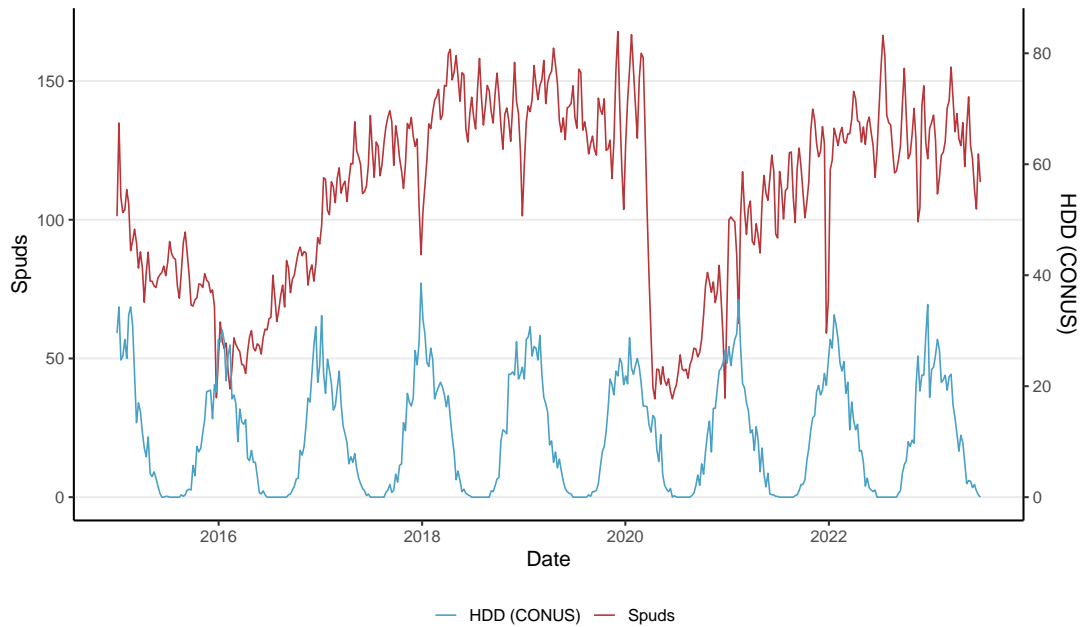
Notes: We present β_o^h and β_g^h estimates from estimating equation (9) using data from Enverus. Data span the entire Permian Basin between January 2010 and December 2015, before the U.S. natural gas market became integrated with the global market.

Figure B.8: Gas-to-oil ratio (GOR) response to gas futures



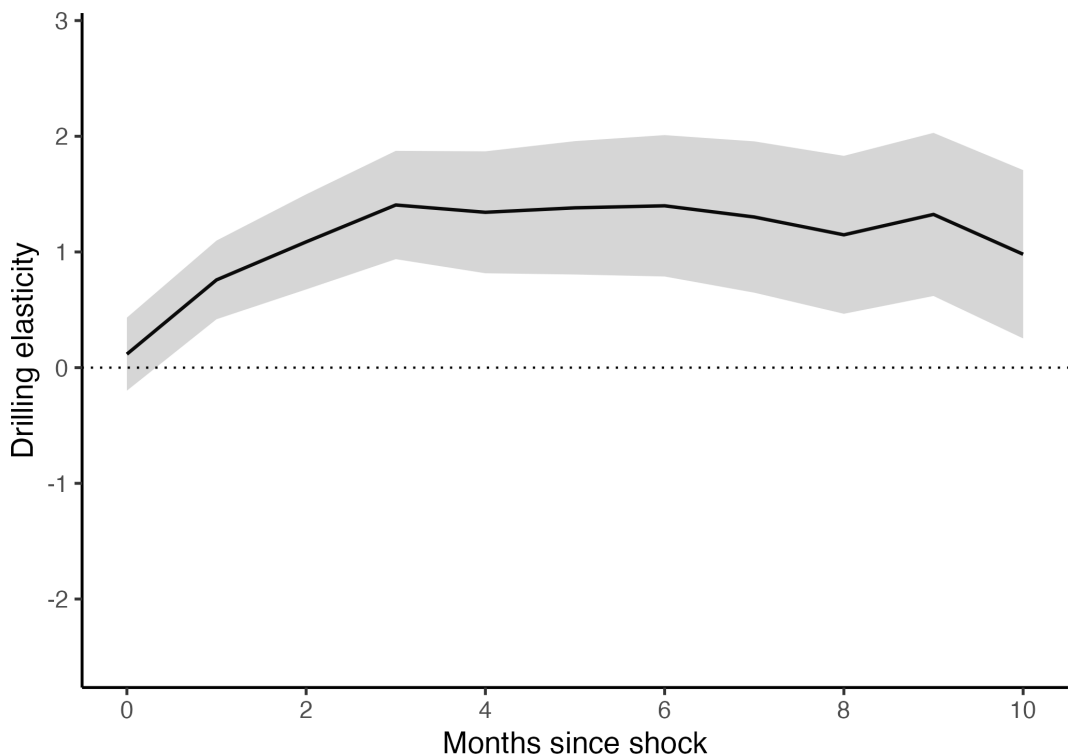
Notes: Local projection results from equation (9), where the outcome is the gas-to-oil ratio for first six months of production.

Figure B.9: Well Drilling and Heating Degree Days



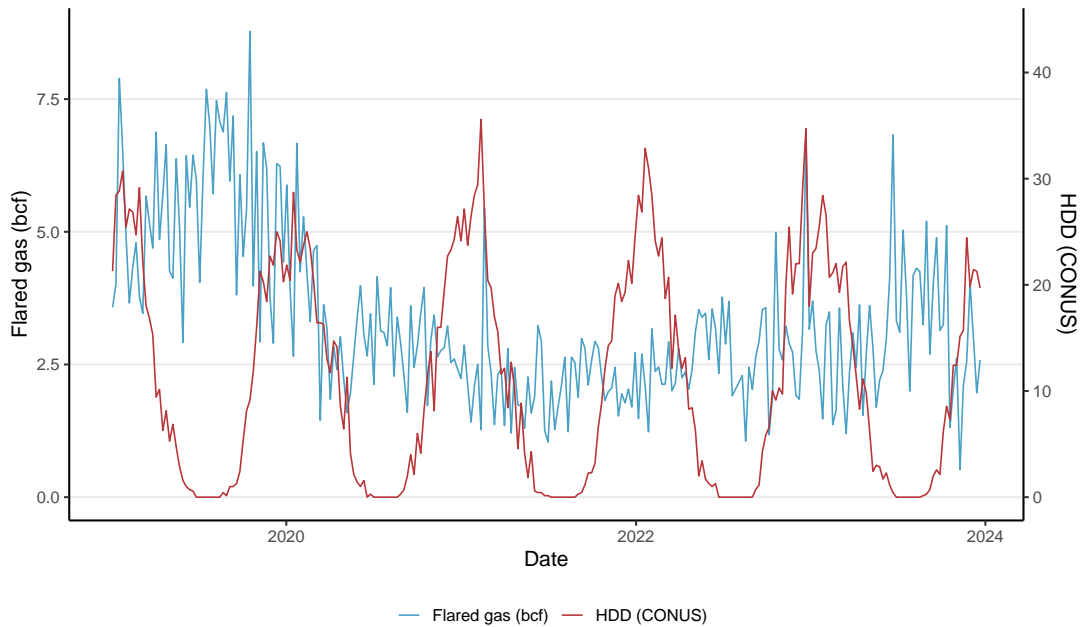
Notes: We plot heating degree days for the continental U.S. alongside the number of spuds in the Permian.

Figure B.11: Drilling elasticities, composite futures price index



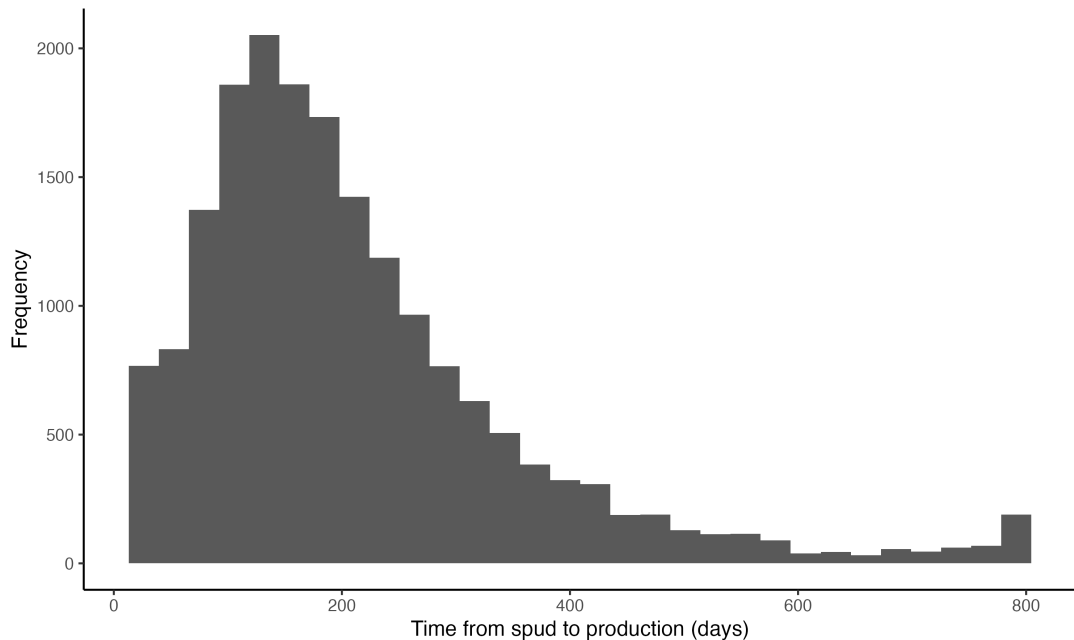
Notes: Local projection results from equation (9), replacing the separate oil and gas price variables with the composite energy futures price index.

Figure B.10: Flaring and Heating Degree Days



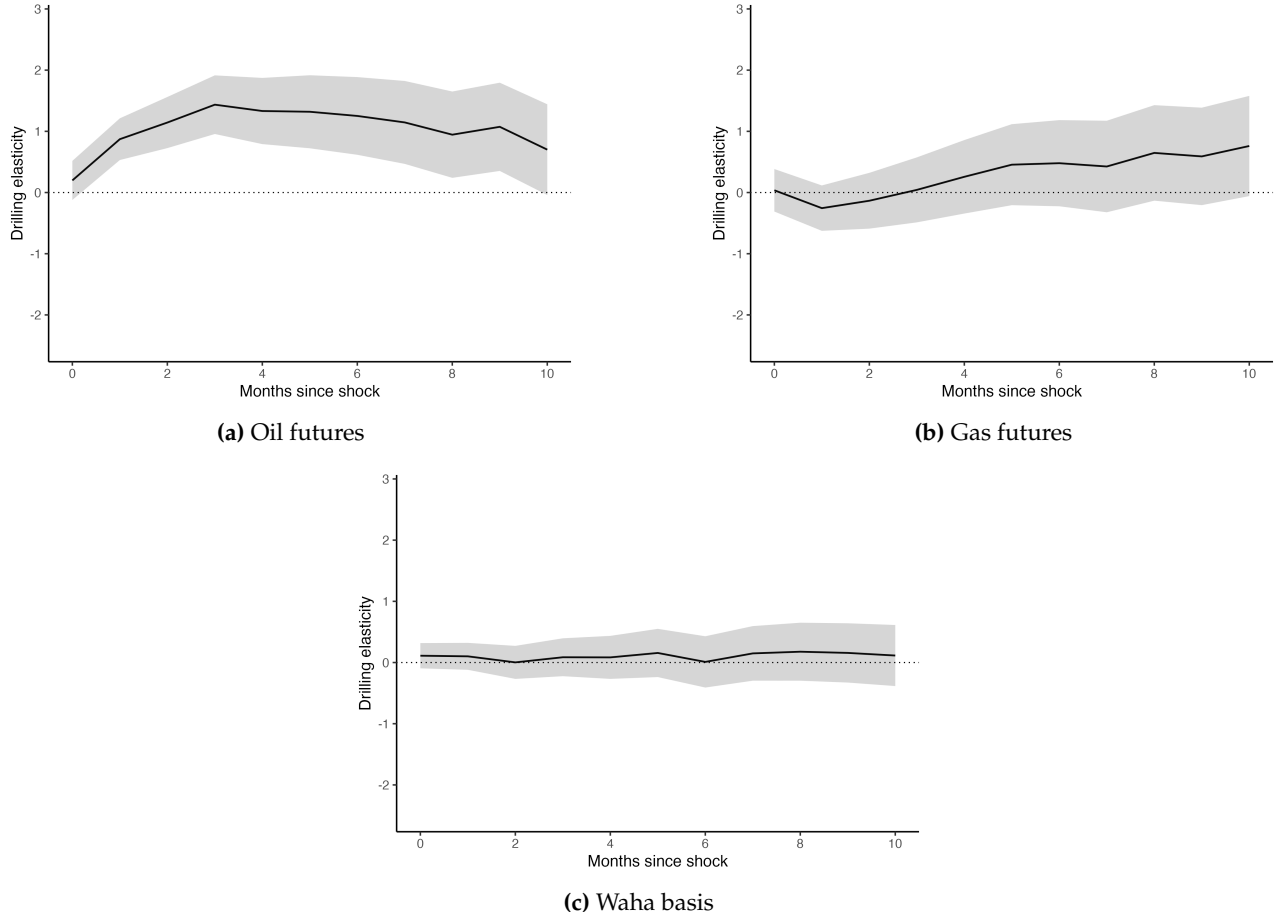
Notes: We plot heating degree days for the continental U.S. alongside VIIRS-based estimates of flared gas volumes for the Permian.

Figure B.13: Time between drilling and first production



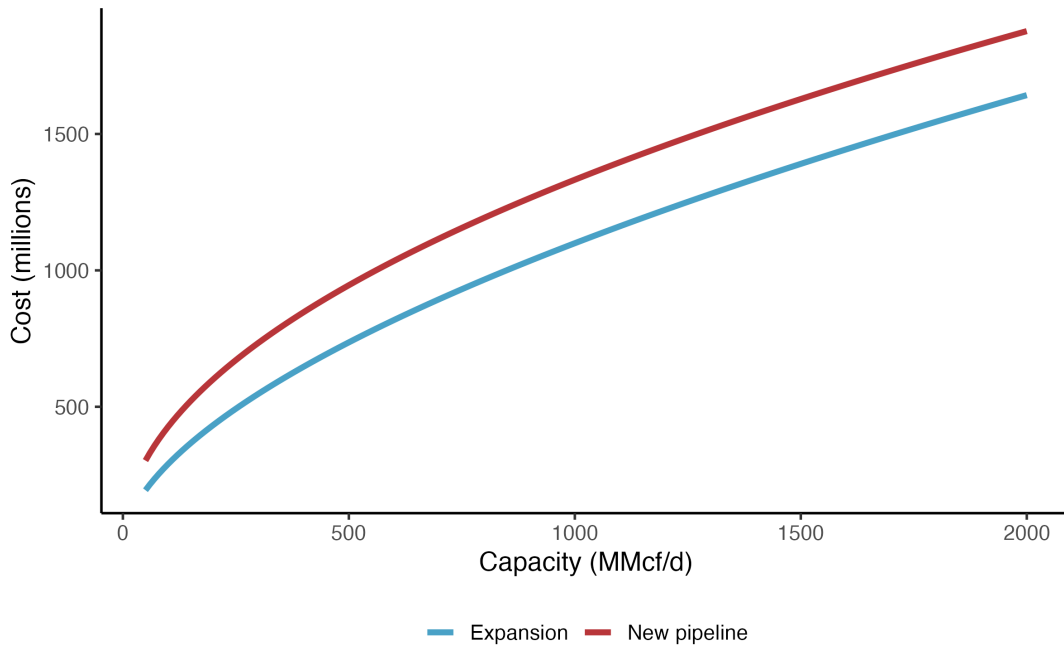
Notes: Using data from [Enverus \(2024b\)](#), we present the time between a well's spudding (when drilling begins) and its first production. The sample is limited to Permian gas and oil wells drilled in or after 2018 that have been productive at least as recently as 2023. We winsorize at the 1 percent level.

Figure B.12: Drilling elasticities, including Waha basis



Notes: We present estimates of a variant of equation (9) that includes simulated expected production-weighted Waha basis as a dependent variable using data from Enverus. Data span the entire Permian Basin between January 2010 and December 2023.

Figure B.14: Estimated cost of a representative 500-mile pipeline project



Notes: This figure presents predicted costs of a representative 500-mile pipeline project of varying capacity, based on the regression estimates in Appendix Table C.10. The figure compares predicted costs for new pipeline construction and expansion projects. Dollar values are expressed in 2024 dollars.

C Tables

Table C.1: Oil revenue shares for top gas producers, 2018

Producer	Gas Volume (BCF)	Oil Volume (MMBbl)	Oil Revenue Share
PIONEER NATURAL RESOURCES USA, INC.	270.41	74.45	0.8612
APACHE CORPORATION	226.77	30.34	0.7048
CHEVRON U.S.A. INC.	141.39	29.08	0.7083
XTO ENERGY INC.	124.38	52.29	0.8738
ANADARKO E&P ONSHORE LLC	107.23	25.68	0.8083
COG OPERATING LLC	106.42	26.26	0.7743
PARSLEY ENERGY OPERATIONS, LLC	71.43	22.77	0.8365
ENERGEN RESOURCES CORPORATION	71.05	27.73	0.8715
OCCIDENTAL PERMIAN LTD.	64.04	33.82	0.9434
LAREDO PETROLEUM, INC.	59.35	12.35	0.7793

Notes: Lease-level sales data from [Enverus \(2024d\)](#). We aggregate sales volumes and values by reported seller name for all Texan lease-months in 2018. We present here the data for the top 10 gas producers by volume in 2018. We calculate the oil value share to be the ratio of oil sales value to the sum of oil and gas value for each producer.

Table C.2: Permian Basin natural gas egress pipeline expansions

Date	Pipeline Name	Operator	Capacity Increase (Bcf/d)	Total Capacity (Bcf/d)
2016-03-10	Roadrunner	ONEOK Partners	0.17	8.17
2016-10-01	Roadrunner	ONEOK Partners	0.40	8.57
2017-01-30	Comanche Trail	ETP	1.10	9.67
2017-03-31	Trans-Pecos	ETP	1.40	11.07
2019-01-01	Old Ocean Pipeline	Enterprise/ETP	0.16	11.23
2019-09-25	Gulf Coast Express (GCX)	Kinder Morgan	2.00	13.07
2021-01-01	Permian Highway Pipeline (PHP)	Kinder Morgan	2.10	15.17
2021-07-01	Whistler Pipeline	WhiteWater, MPLX	2.00	17.17
2022-12-01	Oasis	Energy Transfer	0.06	17.23
2023-09-30	Whistler Pipeline	WhiteWater, MPLX	0.50	17.73
2023-12-12	Permian Highway Pipeline (PHP)	Kinder Morgan	0.55	18.28
2024-10-01	Matterhorn	WhiteWater, EnLink Midstream, Devon Energy Corp, and MPLX	2.50	20.78

Table C.3: Determinants of flare counts

	Dependent variable: log(Number of Flares)		
	All	Midland	Delaware
	(1)	(2)	(3)
Henry Hub Price	-0.037*** (0.011)	-0.018 (0.015)	-0.057*** (0.011)
Waha Basis	0.040 (0.029)	0.098*** (0.036)	0.020 (0.030)
log(New Wells)	0.269*** (0.062)	0.378*** (0.077)	0.175*** (0.060)
Year (2018 = 0)	-0.104*** (0.016)	0.025 (0.021)	-0.208*** (0.017)
Constant	5.839*** (0.259)	4.000*** (0.270)	6.176*** (0.207)
Observations	258	258	258
R ²	0.293	0.160	0.534
Adjusted R ²	0.281	0.146	0.527
Residual Std. Error (df = 253)	0.308	0.396	0.313
F Statistic (df = 4; 253)	26.153***	12.008***	72.569***

Notes: An observation is a week. The sample period is January 2019 to December 2023. The dependent variable is the log number of clustered flaring object detections, measured using VIIRS satellite data. Henry Hub natural gas prices and the Waha basis are weekly averages of daily prices (in \$/MMBtu), with daily prices winsorized at the 1 percent level.

* $p < 0.1$, ** $p < 0.05$, *** $p < 0.01$

Table C.4: Methane emissions and flaring

	Dependent variable:			
	All	log(Emissions)		
	(1)	Midland	Delaware	
	(2)	(3)		
log(Flared Gas)	0.042 (0.035)	0.076** (0.034)	0.119*** (0.041)	
Heating Degree Days (TX)	0.016*** (0.002)	0.014*** (0.003)	0.012*** (0.002)	
Year (2018 = 0)	0.017 (0.012)	0.025* (0.013)	0.013 (0.016)	
Constant	1.212*** (0.065)	0.170*** (0.049)	0.346*** (0.058)	
Observations	258	258	258	
R ²	0.166	0.103	0.133	
Adjusted R ²	0.156	0.092	0.123	
Residual Std. Error (df = 254)	0.238	0.302	0.257	
F Statistic (df = 3; 254)	16.854***	9.727***	13.023***	

Notes: An observation is a week. The sample period is January 2019 to December 2023. The dependent variable is the log of methane emissions, measured in teragrams per year (Tg/a) using satellite spectrometer data following [Varon et al. \(2026\)](#). Flared volumes are measured in Tg/a.

* $p < 0.1$, ** $p < 0.05$, *** $p < 0.01$

Table C.5: Gas-to-oil ratio and futures prices

Model:	Sample	Dependent Variable: log(GOR at t+3)			
		Full sample		2010-2015	
		6-mo GOR	12-mo GOR	6-mo GOR	12-mo GOR
<i>Variables</i>					
log(18-month Henry Hub gas futures)		0.1545** (0.0632)	0.1545** (0.0632)	0.2562* (0.1505)	0.2562* (0.1505)
log(18-month WTI oil futures)		0.0167 (0.0711)	0.0167 (0.0711)	-0.2309** (0.1108)	-0.2309** (0.1108)
<i>Fixed-effects</i>					
Firm		Yes	Yes	Yes	Yes
<i>Fit statistics</i>					
Observations		65,583	65,583	22,010	22,010
R ²		0.75468	0.75468	0.71185	0.71185
Within R ²		0.00261	0.00261	0.00161	0.00161

Clustered (Firm) standard-errors in parentheses

Signif. Codes: ***: 0.01, **: 0.05, *: 0.1

Notes: Unit of observation is a spudded well. Gas-to-oil ratios are winsorized at the 1st and 99th percentiles. All specifications include operator fixed effects. The full sample comprises wells spudded between January 2010 and January 2023. The 2010–2015 subsample includes only wells spudded before January 2016.

Table C.6: Annualized effects of methane fee and severance tax counterfactuals

	Methane fee, \$900/mt ^a				Methane fee, \$1500/mt ^b				Severance tax ^c	
	98% flaring efficacy		91% flaring efficacy		98% flaring efficacy		91% flaring efficacy		Static response	With dynamics
	Static response	With dynamics	Static response	With dynamics	Static response	With dynamics	Static response	With dynamics		
Percent change in flaring	-1.386%	-2.113%	-6.014%	-6.749%	-2.298%	-3.499%	-9.814%	-10.99%	-1.204%	-1.22%
Percent change in methane emissions	-0.717%	-1.452%	-3.11%	-3.872%	-1.188%	-2.409%	-5.075%	-6.319%	-0.623%	-0.638%
Value of abated gas	\$83.7M	\$123.3M	\$363.1M	\$403.0M	\$138.8M	\$204.2M	\$592.1M	\$656.0M	\$88.3M	\$89.2M
IWG social costs										
Carbon cost reduction	\$75.1M	\$114.5M	\$325.8M	\$365.7M	\$124.5M	\$189.6M	\$531.7M	\$595.4M	\$65.2M	\$66.1M
Methane cost reduction	\$51.8M	\$104.9M	\$224.7M	\$279.7M	\$85.9M	\$174.1M	\$366.7M	\$456.5M	\$45.0M	\$46.1M
Social cost reduction	\$210.5M	\$342.7M	\$913.6M	\$1.05B	\$349.2M	\$567.8M	\$1.49B	\$1.71B	\$198.5M	\$201.4M
Azar et al. social costs										
Carbon cost reduction	\$328.6M	\$501.0M	\$1.43B	\$1.60B	\$544.9M	\$829.8M	\$2.33B	\$2.61B	\$285.6M	\$289.2M
Methane cost reduction	\$176.0M	\$356.7M	\$763.8M	\$950.8M	\$291.9M	\$591.6M	\$1.25B	\$1.55B	\$153.0M	\$156.7M
Social cost reduction	\$588.2M	\$981.0M	\$2.55B	\$2.95B	\$975.6M	\$1.63B	\$4.17B	\$4.81B	\$526.8M	\$535.1M

Note: Values report the model-implied percentage change in flaring and methane emissions, as well as the annual reduction in monetized damages from emissions and lost gas, under counterfactual policies. *Static response* reflects only the intensive-margin adjustment in flaring behavior at existing producing wells; drilling decisions and well counts are held fixed. *With dynamics* incorporates both the intensive-margin flaring adjustment and the extensive-margin drilling response to the fee in *steady state*, assuming the policy has been in place long enough that all producing wells were drilled under the tax regime. Counterfactuals are computed in general equilibrium, with transmission costs adjusting endogenously to pipeline congestion, so reported effects capture indirect equilibrium responses in addition to the direct effects of the counterfactual policies. Negative percentages indicate reductions relative to the baseline (no-fee) scenario. Monetary values represent annual changes in damages valued using the social costs of carbon and methane from the [Interagency Working Group on the Social Cost of Greenhouse Gases \(2021\)](#) (\$67/mt and \$2,024/mt, respectively), and [Azar et al. \(2023\)](#) (\$293/mt and \$6,880/mt, respectively), expressed in 2024 dollars.

^a Proposed 2024 IRA methane fee (\$900/mt).

^b Proposed 2026 IRA methane fee (\$1,500/mt).

^c Tax flared gas at the same rate as the Texas natural gas severance tax (7.5% of market value).

Table C.7: Annualized direct effects of methane fee and severance tax counterfactuals

	Methane fee, \$900/mt ^a				Methane fee, \$1500/mt ^b				Severance tax ^c	
	98% flaring efficacy		91% flaring efficacy		98% flaring efficacy		91% flaring efficacy		Static response	With dynamics
	Static response	With dynamics	Static response	With dynamics	Static response	With dynamics	Static response	With dynamics		
Percent change in flaring	-1.555%	-2.282%	-6.922%	-7.65%	-2.592%	-3.79%	-11.536%	-12.689%	-1.304%	-1.319%
Percent change in methane emissions	-0.804%	-1.54%	-3.579%	-4.337%	-1.341%	-2.559%	-5.965%	-7.197%	-0.674%	-0.69%
Value of abated gas	\$90.8M	\$130.3M	\$403.9M	\$443.6M	\$151.3M	\$216.5M	\$673.2M	\$736.0M	\$76.1M	\$77.0M
IWG social costs										
Carbon cost reduction	\$84.3M	\$123.6M	\$375.0M	\$414.4M	\$140.4M	\$205.3M	\$625.0M	\$687.5M	\$70.6M	\$71.5M
Methane cost reduction	\$58.1M	\$111.2M	\$258.6M	\$313.4M	\$96.9M	\$184.9M	\$431.0M	\$520.0M	\$48.7M	\$49.8M
Social cost reduction	\$233.1M	\$365.2M	\$1.04B	\$1.17B	\$388.6M	\$606.8M	\$1.73B	\$1.94B	\$195.4M	\$198.3M
Azar et al. social costs										
Carbon cost reduction	\$368.8M	\$541.0M	\$1.64B	\$1.81B	\$614.7M	\$898.7M	\$2.74B	\$3.01B	\$309.1M	\$312.8M
Methane cost reduction	\$197.5M	\$378.1M	\$879.0M	\$1.07B	\$329.2M	\$628.5M	\$1.47B	\$1.77B	\$165.6M	\$169.4M
Social cost reduction	\$657.1M	\$1.05B	\$2.92B	\$3.32B	\$1.10B	\$1.74B	\$4.87B	\$5.51B	\$550.8M	\$559.1M

Note: Values report the model-implied percentage change in flaring and methane emissions, as well as the annual reduction in monetized damages from emissions and lost gas, under counterfactual policies. *Static response* reflects only the intensive-margin adjustment in flaring behavior at existing producing wells; drilling decisions and well counts are held fixed. *With dynamics* incorporates both the intensive-margin flaring adjustment and the extensive-margin drilling response to the fee in *steady state*, assuming the policy has been in place long enough that all producing wells were drilled under the tax regime. Reported effects reflect direct policy impacts only, holding transmission costs fixed. Negative percentages indicate reductions relative to the baseline (no-fee) scenario. Monetary values represent annual changes in damages valued using the social costs of carbon and methane from the [Interagency Working Group on the Social Cost of Greenhouse Gases \(2021\)](#) (\$67/mt and \$2,024/mt, respectively), and [Azar et al. \(2023\)](#) (\$293/mt and \$6,880/mt, respectively), expressed in 2024 dollars.

^a Proposed 2024 IRA methane fee (\$900/mt).

^b Proposed 2026 IRA methane fee (\$1,500/mt).

^c Tax flared gas at the same rate as the Texas natural gas severance tax (7.5% of market value).

Table C.8: Annualized effects of methane fee counterfactuals under observed pipeline congestion and no congestion

	Under observed congestion		Under no congestion	
	\$900/mt methane fee	\$1500/mt methane fee	\$900/mt methane fee	\$1500/mt methane fee
Percent change in flaring	-6.749%	-10.99%	-7.65%	-12.689%
Percent change in methane emissions	-3.872%	-6.319%	-4.337%	-7.197%
Value of abated gas	\$403.0M	\$656.0M	\$443.6M	\$736.0M
IWG social costs				
Carbon cost reduction	\$365.7M	\$595.4M	\$414.4M	\$687.5M
Methane cost reduction	\$279.7M	\$456.5M	\$313.4M	\$520.0M
Social cost reduction	\$1.05B	\$1.71B	\$1.17B	\$1.94B
Azar et al. social costs				
Carbon cost reduction	\$1.60B	\$2.61B	\$1.81B	\$3.01B
Methane cost reduction	\$950.8M	\$1.55B	\$1.07B	\$1.77B
Social cost reduction	\$2.95B	\$4.81B	\$3.32B	\$5.51B

Note: Values report the model-implied percentage change in flaring and methane emissions, as well as the annual reduction in monetized damages from emissions and lost gas, under counterfactual policies. The first two columns present the impact of the tax under the observed pipeline congestion and the second two columns present the results under a counterfactual regime with no pipeline congestion (i.e., marginal transmission costs are not affected by incremental production). Counterfactuals under observed congestion are computed in general equilibrium, with transmission costs adjusting endogenously to pipeline congestion, so reported effects capture indirect equilibrium responses in addition to the direct effects of the counterfactual policies. Negative percentages indicate reductions relative to the baseline (no-fee) scenario. Monetary values represent annual changes in damages valued using the social costs of carbon and methane from the [Interagency Working Group on the Social Cost of Greenhouse Gases \(2021\)](#) (\$67/mt and \$2,024/mt, respectively), and [Azar et al. \(2023\)](#) (\$293/mt and \$6,880/mt, respectively), expressed in 2024 dollars.

Table C.9: Annualized effects of combining methane fee (98% flaring efficacy) and pipeline congestion relief counterfactuals

	Observed congestion		Fully relieving congestion		
	\$900/mt methane fee	\$1500/mt methane fee	No methane fee	\$900/mt methane fee	\$1500/mt methane fee
Percent change in flaring	-2.113%	-3.499%	-4.668%	-6.841%	-8.278%
Percent change in methane emissions	-1.452%	-2.409%	-2.414%	-3.897%	-4.88%
Value of abated gas	\$123.3M	\$204.2M	\$285.2M	\$409.1M	\$491.0M
IWG social costs					
Carbon cost reduction	\$114.5M	\$189.6M	\$252.9M	\$370.6M	\$448.5M
Methane cost reduction	\$104.9M	\$174.1M	\$174.4M	\$281.6M	\$352.6M
Social cost reduction	\$342.7M	\$567.8M	\$712.4M	\$1.06B	\$1.29B
Azar et al. social costs					
Carbon cost reduction	\$501.0M	\$829.8M	\$1.11B	\$1.62B	\$1.96B
Methane cost reduction	\$356.7M	\$591.6M	\$592.8M	\$957.2M	\$1.20B
Social cost reduction	\$981.0M	\$1.63B	\$1.98B	\$2.99B	\$3.65B

Note: Values report the model-implied percentage change in flaring and methane emissions, as well as the annual reduction in monetized damages from emissions and lost gas, under counterfactual policies. The first two columns present the impact of the tax under the observed pipeline congestion and the remaining columns present the results under a counterfactual regime with no pipeline congestion (i.e., marginal transmission costs are not affected by incremental production). Counterfactuals under observed congestion are computed in general equilibrium, with transmission costs adjusting endogenously to pipeline congestion, so reported effects capture indirect equilibrium responses in addition to the direct effects of the counterfactual policies. Negative percentages indicate reductions relative to the baseline (no-fee) scenario. Monetary values represent annual changes in damages valued using the social costs of carbon and methane from the [Interagency Working Group on the Social Cost of Greenhouse Gases \(2021\)](#) (\$67/mt and \$2,024/mt, respectively), and [Azar et al. \(2023\)](#) (\$293/mt and \$6,880/mt, respectively), expressed in 2024 dollars.

Table C.10: Estimated pipeline costs

	<i>Dependent variable:</i>	
	Log cost (millions)	
	New pipeline (1)	Expansion (2)
Log length (miles)	0.761*** (0.068)	0.480*** (0.040)
Log capacity (MMcf/d)	0.495*** (0.067)	0.579*** (0.046)
Constant	-0.949** (0.394)	0.023 (0.222)
Observations	133	338
R ²	0.690	0.565
Adjusted R ²	0.685	0.562
Residual Std. Error	0.959 (df = 130)	1.103 (df = 335)
F Statistic	144.580*** (df = 2; 130)	217.402*** (df = 2; 335)

Notes: This table reports OLS regressions of log project cost on log pipeline length and log capacity for major U.S. natural gas pipeline projects between 1996 and 2023. A unit of observation is a pipeline project. Data are from the U.S. Energy Information Administration (EIA) and based on cost estimates from company press releases and regulatory filings. The sample includes both new pipeline construction and expansion projects (typically carried out through "looping"). Reported coefficients measure elasticities of project costs with respect to pipeline length and capacity. All dollar values are expressed in 2024 dollars.

* $p < 0.1$, ** $p < 0.05$, *** $p < 0.01$

References

- Agerton, Mark.** 2020. "Learning Where to Drill: Drilling Decisions and Geological Quality in the Haynesville Shale." *SSRN Electronic Journal*. Available at: <https://www.ssrn.com/abstract=3583149>.
- Agerton, Mark, Ben Gilbert, and Gregory B. Upton.** 2023. "The Economics of Natural Gas Flaring and Methane Emissions in US Shale: An Agenda for Research and Policy." *Review of Environmental Economics and Policy*, 17(2): 251–273. Publisher: The University of Chicago Press.
- Agerton, Mark, Wesley Blundell, Ben Gilbert, and Gregory Upton.** 2025. "Midstream Infrastructure and Environmental Externalities in Oil and Gas: Permian Basin Flaring and Methane Emissions." USAEE Working Paper 24-627. <https://papers.ssrn.com/abstract=4890180>.
- Aldy, Joseph, Forest Reinhardt, and Robert Stavins.** 2025. "Methane Abatement Costs in the Oil and Gas Industry: Survey and Synthesis." *NBER Working Paper Series*. <http://www.nber.org/papers/w33564.pdf>.
- American Oil and Gas Reporter.** 2020. "Permian Basin Companies Getting Back To Work." <https://www.aogr.com/magazine/cover-story/Permian-Basin-Getting-Back-To-Work>, Accessed: 2025-06-12.
- Anderson, Soren T., Ryan Kellogg, and Stephen W. Salant.** 2018. "Hotelling under Pressure." *Journal of Political Economy*, 126(3): 984–1026. Publisher: The University of Chicago Press.
- Azar, Christian, Jorge García Martín, Daniel JA Johansson, and Thomas Sterner.** 2023. "The social cost of methane." *Climatic Change*, 176(6).
- Beatty, Lauren.** 2022. "How Do Natural Gas Pipeline Networks Affect Emissions From Drilling and Flaring?" *Working paper*. Available at: https://lbeatty1.github.io/files/Beatty_JMP.pdf.
- Carr, Housley.** 2025. "Don't Stop Believin' - Appalachia Gas Production Growth Tied to Takeaway Adds, In-Basin Power Needs." <https://rbnenergy.com/daily-posts/blog/appalachia-gas-production-growth-tied-takeaway-adds-basin-power-needs>, Accessed: 2026-01-12.
- Cicala, Steve, David Hémous, and Morten G Olsen.** 2022. "Adverse Selection as a Policy Instrument: Unraveling Climate Change." *NBER Working Paper Series*. <https://www.nber.org/papers/w30283>.
- Covert, Thomas R.** 2015. "Experiential and Social Learning in Firms: The Case of Hydraulic Fracturing in the Bakken Shale." *SSRN Electronic Journal*. Available at: <https://www.ssrn.com/abstract=2481321>.
- Cusworth, Daniel H., Riley M. Duren, Andrew K. Thorpe, Winston Olson-Duvall, Joseph Heckler, John W. Chapman, Michael L. Eastwood, Mark C. Helmlinger, Robert O. Green, Gregory P. Asner, Philip E. Dennison, and Charles E. Miller.** 2021. "Intermittency of Large Methane Emitters in the Permian Basin." *Environmental Science & Technology Letters*, 8(7): 567–573.
- Dunkle Werner, Karl, and Wenfeng Qiu.** 2025. "Information Matters: Feasible Policies for Reducing Methane Emissions." *Journal of the Association of Environmental and Resource Economists*, 12(5): 1389–1429.
- Dwan, Gage.** 2024. "Gas Constraints Could Limit Bakken Oil Growth." <https://www.eastdaley.com/media-and-news/gas-constraints-could-limit-bakken-oil-growth>, Accessed: 2025-06-12.
- Elvidge, Christopher D., Mikhail Zhizhin, Feng-Chi Hsu, and Kimberly E. Baugh.** 2013. "VIIRS Nightfire: Satellite Pyrometry at Night." *Remote Sensing*, 5(9): 4423–4449. Number: 9 Publisher: Multidisciplinary Digital Publishing Institute.
- Elvidge, Christopher D, Mikhail Zhizhin, Kimberly Baugh, Feng-Chi Hsu, and Tilottama Ghosh.** 2015. "Methods for global survey of natural gas flaring from visible infrared imaging radiometer suite data." *Energies*, 9(1): 14.
- Energy Information Administration.** 2021. "Production Decline Curve Analysis in the Annual Energy Outlook 2021." Available at: https://www.eia.gov/analysis/drilling/curve_analysis/archive/2021/, Accessed: 2025-12-03.

- Energy Information Administration.** 2023. "High Permian well productivity, crude oil prices drive U.S. natural gas production growth." <https://www.eia.gov/todayinenergy/detail.php?id=60702>, Accessed: 2025-06-12.
- Energy Information Administration.** 2024a. "Cushing, OK WTI Spot Price FOB." Available at: <https://www.eia.gov/dnav/pet/hist/rwtd.htm>, Accessed: 2024-08-30.
- Energy Information Administration.** 2024b. "Heating Degree-Days by Census Division." Available at: <https://www.eia.gov/totalenergy/data/monthly/>, Accessed: 2024-03-12.
- Energy Information Administration.** 2024c. "Natural Gas Pipeline Projects." Available at: <https://www.eia.gov/naturalgas/data.php#pipelines>, Accessed: 2024-10-24.
- Enterprise Products Partners L.P.** 2024. "First Quarter 2024 Earnings Call Transcript." Conference call transcript, S&P Global Market Intelligence, Accessed: 2025-06-12.
- Enverus.** 2024a. "DrillingInfo Monthly Production: Grouped by DI Basin." Available at: <https://www.enverus.com/>, Accessed: 2024-03-08.
- Enverus.** 2024b. "DrillingInfo Wells Table." Available at: <https://www.enverus.com/>, Accessed: 2023-04-21.
- Enverus.** 2024c. "Prism Distinct API/UWI Count by Spud Date." Available at: <https://www.enverus.com/>, Accessed: 2024-05-02.
- Enverus.** 2024d. "Prism Revenues (beta)." Available at: <https://www.enverus.com/>, Accessed: 2024-02-04.
- Environmental and Energy Law Program at Harvard Law School.** 2025. "EPA VOC and Methane Standards for Oil and Gas Facilities." <https://eelp.law.harvard.edu/tracker/epa-voc-and-methane-standards-for-oil-and-gas-facilities-2/>, Accessed: 2026-01-25.
- EPA.** 2015. "Inventory of U.S. Greenhouse Gas Emissions and Sinks 1990-2013: Revision to Hydraulically Fractured Gas Well Completions and Workovers Estimate." <https://web.archive.org/web/20170304084814/https://www3.epa.gov/climatechange/pdfs/HF-Gas-well-completion-workover-update-memo-4-10-2015.pdf>, Accessed: 2025-07-01.
- EPA.** 2023. "Report on the Social Cost of Greenhouse Gases: Estimates Incorporating Recent Scientific Advances." Available at: https://www.epa.gov/system/files/documents/2023-12/epa_scghg_2023_report_final.pdf, Accessed: 2025-09-04.
- EPA.** 2024. "Chapter 8: Natural Gas." <https://www.epa.gov/system/files/documents/2024-04/chapter-8-natural-gas.pdf>, Accessed: 2025-08-20.
- Evans, Peter, David Newman, Raj Venuturumilli, Johan Liekens, Jon Lowe, Chong Tao, Jon Chow, Anan Wang, Lei Sui, and Gerard Bottino.** 2024. "Full-Size Experimental Measurement of Combustion and Destruction Efficiency in Upstream Flares and the Implications for Control of Methane Emissions from Oil and Gas Production." *Atmosphere*, 15(3): 333. Number: 3 Publisher: Multidisciplinary Digital Publishing Institute.
- Federal Reserve Bank of Dallas.** 2019. "Dallas Fed Energy Survey." Available at: <https://www.dallasfed.org/research/surveys/des/2019/1904/>, Accessed: 2024-06-05.
- Federal Reserve Bank of Dallas.** n.d.. "Permian Basin." Available at: <https://www.dallasfed.org/research/energy11/permian>, Accessed: 2025-12-18.
- Fleury, Katy.** 2022. "The Waha Hub natural gas price continues to fall below the Henry Hub price." <https://www.eia.gov/todayinenergy/detail.php?id=53919>, Accessed: 2025-08-04.
- Fowlie, Meredith, Mar Reguant, and Stephen P. Ryan.** 2016. "Market-Based Emissions Regulation and Industry Dynamics." *Journal of Political Economy*, 124(1): 249–302. Publisher: The University of Chicago Press.
- Hausman, Catherine, and Lucija Muehlenbachs.** 2019. "Price Regulation and Environmental Externalities: Evidence from Methane Leaks." *Journal of the Association of Environmental and Resource Economists*, 6(1): 73–109.

- He, Liyin, Zhao-Cheng Zeng, Thomas J. Pongetti, Clare Wong, Jianming Liang, Kevin R. Gurney, Sally Newman, Vineet Yadav, Kristal Verhulst, Charles E. Miller, Riley Duren, Christian Frankenberg, Paul O. Wennberg, Run-Lie Shia, Yuk L. Yung, and Stanley P. Sander.** 2019. "Atmospheric Methane Emissions Correlate With Natural Gas Consumption From Residential and Commercial Sectors in Los Angeles." *Geophysical Research Letters*, 46(14): 8563–8571. <https://onlinelibrary.wiley.com/doi/pdf/10.1029/2019GL083400>.
- Herrnstadt, Evan, Ryan Kellogg, and Eric Lewis.** 2024. "Drilling Deadlines and Oil and Gas Development." *Econometrica*, 92(1): 29–60.
- Hodgson, Charles.** 2024. "Information Externalities, Free Riding, and Optimal Exploration in the UK Oil Industry." *NBER Working Paper Series*. Available at: https://www.nber.org/system/files/working_papers/w33067/w33067.pdf.
- Interagency Working Group on the Social Cost of Greenhouse Gases.** 2021. "Technical Support Document: Social Cost of Carbon, Methane, and Nitrous Oxide Interim Estimates under Executive Order 13990." https://web.archive.org/web/20250116092806/https://www.whitehouse.gov/wp-content/uploads/2021/02/TechnicalSupportDocument_SocialCostofCarbonMethaneNitrousOxide.pdf, Accessed: 2025-06-13.
- Jordà, Òscar.** 2005. "Estimation and Inference of Impulse Responses by Local Projections." *American Economic Review*, 95(1): 161–182.
- Karion, Anna, Subhomoy Ghosh, Israel Lopez-Coto, Kimberly Mueller, Sharon Gourdji, Joseph Pitt, and James Whetstone.** 2023. "Methane Emissions Show Recent Decline but Strong Seasonality in Two US Northeastern Cities." *Environmental Science & Technology*, 57(48): 19565–19574. Publisher: American Chemical Society.
- Kellogg, Ryan.** 2011. "Learning by Drilling: Interfirm Learning and Relationship Persistence in the Texas Oilpatch." *The Quarterly Journal of Economics*, 126(4): 1961–2004.
- Kellogg, Ryan.** 2014. "The Effect of Uncertainty on Investment: Evidence from Texas Oil Drilling." *American Economic Review*, 104(6): 1698–1734.
- Kinder Morgan, Inc.** 2019. "Gulf Coast Express Pipeline Project." https://pipeline2.kindermorgan.com/Documents/GCX/GCX_CI_Cpny_Overview.pdf, Accessed: 2025-06-12.
- Kinder Morgan, Inc.** 2021. "Permian Highway Pipeline Project." https://pipeline2.kindermorgan.com/Documents/PHP/PHP_CI_Cpny_Overview.pdf, Accessed: 2025-06-12.
- Kinder Morgan, Inc.** 2024. "Form 10-K: Annual Report for the Fiscal Year Ended December 31, 2023." https://s24.q4cdn.com/126708163/files/doc_financials/2023/ar/KMI-2023-10K-Final-wo-Exhibits.pdf, Accessed: 2025-06-12.
- Kolesár, Michal, and Mikkel Plagborg-Møller.** 2025. "Dynamic Causal Effects in a Nonlinear World: the Good, the Bad, and the Ugly." Available at: <https://www.princeton.edu/~mkolesar/papers/dynamic.pdf>.
- Labandeira, Xavier, José M Labeaga, and Xiral López-Otero.** 2017. "A meta-analysis on the price elasticity of energy demand." *Energy Policy*, 102: 549–568.
- Lade, Gabriel E., and Ivan Rudik.** 2020. "Costs of inefficient regulation: Evidence from the Bakken." *Journal of Environmental Economics and Management*, 102: 102336.
- Lewis, Eric K, Jiayang Wang, and Arvind P Ravikumar.** 2025. "Incentives and information in methane leak detection and repair." *Journal of the Association of Environmental and Resource Economists*, 12(3): 637–662.
- Lu, Xiao, Daniel J. Jacob, Yuzhong Zhang, Lu Shen, Melissa P. Sulprizio, Joannes D. Maasakkers, Daniel J. Varon, Zhen Qu, Zichong Chen, Benjamin Hmiel, Robert J. Parker, Hartmut Boesch, Haolin Wang, Cheng He, and Shaojia Fan.** 2023. "Observation-derived 2010–2019 trends in methane emissions and intensities from US oil and gas fields tied to activity metrics." *Proceedings of the National Academy of Sciences*, 120(17): e2217900120.

- Lyon, David R., Benjamin Hmiel, Ritesh Gautam, Mark Omara, Katherine A. Roberts, Zachary R. Barkley, Kenneth J. Davis, Natasha L. Miles, Vanessa C. Monteiro, Scott J. Richardson, Stephen Conley, Mackenzie L. Smith, Daniel J. Jacob, Lu Shen, Daniel J. Varon, Aijun Deng, Xander Rudelis, Nikhil Sharma, Kyle T. Story, Adam R. Brandt, Mary Kang, Eric A. Kort, Anthony J. Marchese, and Steven P. Hamburg.** 2021. "Concurrent variation in oil and gas methane emissions and oil price during the COVID-19 pandemic." *Atmospheric Chemistry and Physics*, 21(9): 6605–6626. Publisher: Copernicus GmbH.
- Marks, Levi.** 2022. "The Abatement Cost of Methane Emissions from Natural Gas Production." *Journal of the Association of Environmental and Resource Economists*, 9(2): 165–198.
- McDonough, Richard.** 2025. "North Dakota's Bakken Basin Set for Midstream Comeback, Experts Say." <https://www.pgjonline.com/magazine/2025/may-2025-vol-252-no-5/features/north-dakota-s-bakken-basin-set-for-midstream-comeback-experts-say>. Accessed: 2025-06-12.
- Mercatus Energy.** 2019. "Basis - An Often Overlooked Aspect of Natural Gas Hedging." <https://www.mercatusenergy.com/blog/basis-an-often-overlooked-aspect-of-natural-gas-hedging>, Accessed: 2025-08-04.
- Newell, Richard G., and Brian C. Prest.** 2019. "The Unconventional Oil Supply Boom: Aggregate Price Response from Microdata." *The Energy Journal*, 40(3): 1–30.
- Newell, Richard G., Brian C. Prest, and Ashley B. Vissing.** 2019. "Trophy Hunting versus Manufacturing Energy: The Price Responsiveness of Shale Gas." *Journal of the Association of Environmental and Resource Economists*, 6(2): 391–431.
- Newman, Chris.** 2025. "Shrinking Spare Natural Gas Takeaway Capacity Could Indicate 'Grimmer' Outlook for Permian Prices." <https://naturalgasintel.com/news/shrinking-spare-natural-gas-takeaway-capacity-could-indicate-grimmer-outlook-for-permian-prices/>. Accessed: 2025-06-12.
- Oliver, Matthew E., Charles F. Mason, and David Finnoff.** 2014. "Pipeline congestion and basis differentials." *Journal of Regulatory Economics*, 46(3): 261–291.
- Omara, Mark, Daniel Zavala-Araiza, David R. Lyon, Benjamin Hmiel, Katherine A. Roberts, and Steven P. Hamburg.** 2022. "Methane emissions from US low production oil and natural gas well sites." *Nature Communications*, 13(1): 2085. Number: 1 Publisher: Nature Publishing Group.
- Omara, Mark, Naomi Zimmerman, Melissa R. Sullivan, Xiang Li, Aja Ellis, Rebecca Cesa, R. Subramanian, Albert A. Presto, and Allen L. Robinson.** 2018. "Methane Emissions from Natural Gas Production Sites in the United States: Data Synthesis and National Estimate." *Environmental Science & Technology*, 52(21): 12915–12925. Publisher: American Chemical Society.
- Plant, Genevieve, Eric A. Kort, Adam R. Brandt, Yuanlei Chen, Graham Fordice, Alan M. Gorchov Negron, Stefan Schwietzke, Mackenzie Smith, and Daniel Zavala-Araiza.** 2022. "Inefficient and unlit natural gas flares both emit large quantities of methane." *Science*, 377(6614): 1566–1571. Publisher: American Association for the Advancement of Science.
- Prest, Brian C.** 2025. "Where Does the Marginal Methane Molecule Come From? Implications of LNG Exports for US Natural Gas Supply and Methane Emissions." Resources for the Future Working Paper 25-05.
- Railroad Commission of Texas.** 2023. "Production Data Query Dump." Available at: <https://www.rrc.texas.gov/resource-center/research/data-sets-available-for-download/>, Accessed: 2023-11-13.
- Rambachan, Ashesh, and Neil Shephard.** 2025. "When Do Common Time Series Estimands Have Nonparametric Causal Meaning?" *arXiv:1903.01637*, Accessed: 2025-09-05.
- Sargent, Maryann R., Cody Floerchinger, Kathryn McKain, John Budney, Elaine W. Gottlieb, Lucy R. Hutyra, Joseph Rudek, and Steven C. Wofsy.** 2021. "Majority of US urban natural gas emissions unaccounted for in inventories." *Proceedings of the National Academy of Sciences*, 118(44): e2105804118. Publisher: Proceedings of the National Academy of Sciences.

- Sherwin, Evan D., Jeffrey S. Rutherford, Zhan Zhang, Yuanlei Chen, Erin B. Wetherley, Petr V. Yakovlev, Elena S. F. Berman, Brian B. Jones, Daniel H. Cusworth, Andrew K. Thorpe, Alana K. Ayasse, Riley M. Duren, and Adam R. Brandt.** 2024. "US oil and gas system emissions from nearly one million aerial site measurements." *Nature*, 627(8003): 328–334. Publisher: Nature Publishing Group.
- S&P Capital IQ.** 2024. "Commodity Charting." Available at: <https://www.capitaliq.spglobal.com/web/client?auth=inherit#markets/commoditiesChart>, Accessed: 2024-12-23.
- Stock, James H., and Matthew Zaragoza-Watkins.** 2024. "The Market and Climate Implications of U.S. LNG Exports." *NBER Working Paper Series*. <https://www.nber.org/papers/w32228>.
- The World Bank.** n.d.. "Methane from Oil and Gas Production Explained." <https://www.worldbank.org/en/programs/gasflaringreduction/methane-explained>, Accessed: 2025-12-18.
- U.S. Department of Energy.** 2022. "North American LNG Export Terminals." https://www.energy.gov/sites/default/files/2022-03/FERC%20N.%20American%20LNG%20export%20terminals_0.pdf, Accessed: 2025-08-05.
- Varon, Daniel J., Daniel J. Jacob, Benjamin Hmiel, Ritesh Gautam, David R. Lyon, Mark Omara, Melissa Sulprizio, Lu Shen, Drew Pendergrass, Hannah Nesser, Zhen Qu, Zachary R. Barkley, Natasha L. Miles, Scott J. Richardson, Kenneth J. Davis, Sudhanshu Pandey, Xiao Lu, Alba Lorente, Tobias Borsdorff, Joannes D. Maasakkers, and Ilse Aben.** 2023. "Continuous weekly monitoring of methane emissions from the Permian Basin by inversion of TROPOMI satellite observations." *Atmospheric Chemistry and Physics*, 23: 7503–7520.
- Varon, Daniel J., Daniel J. Jacob, Lucas A. Estrada, Nicholas Balasus, James D. East, Drew C. Pendergrass, Zichong Chen, Melissa Sulprizio, Mark Omara, Ritesh Gautam, Zachary R. Barkley, Felipe J. Cardoso Saldaña, Emily K. Reidy, Harshil Kamdar, Evan D. Sherwin, Sébastien C. Biraud, Dylan Jervis, Sudhanshu Pandey, John R. Worden, Kevin W. Bowman, Joannes D. Maasakkers, and Robert L. Kleinberg.** 2026. "Seasonality and Declining Intensity of Methane Emissions from the Permian and Nearby US Oil and Gas Basins." *Environmental Science & Technology*, 60(1): 425–435. Publisher: American Chemical Society.
- Williams, James P., Mark Omara, Anthony Himmelberger, Daniel Zavala-Araiza, Katlyn MacKay, Joshua Benmergui, Maryann Sargent, Steven C. Wofsy, Steven P. Hamburg, and Ritesh Gautam.** 2025. "Small emission sources in aggregate disproportionately account for a large majority of total methane emissions from the US oil and gas sector." *Atmospheric Chemistry and Physics*, 25(3): 1513–1532. Publisher: Copernicus GmbH.
- Zou, Eric Yongchen.** 2021. "Unwatched Pollution: The Effect of Intermittent Monitoring on Air Quality." *American Economic Review*, 111(7): 2101–2126.